

**ELUCIDATION OF MOLECULAR MECHANISMS UNDERLYING  
REGULATION OF CHOLESTEROL SYNTHESIS**

APPROVED BY SUPERVISORY COMMITTEE

Russell A. DeBoseBoyd, Ph.D. (Supervisor) \_\_\_\_\_

Sandra L. Hofmann, M.D., Ph.D. (Chair) \_\_\_\_\_

George N. DeMartino, Ph.D. \_\_\_\_\_

David J. Mangelsdorf, Ph.D. \_\_\_\_\_

To my Parents  
Kyung Shik Lee, Hyea Ja Park  
&  
my wife  
Ji Yeon  
&  
my son  
Kyu-chan

**ELUCIDATION OF MOLECULAR MECHANISMS UNDERLYING  
REGULATION OF CHOLESTEROL SYNTHESIS**

by

Peter Chang-Whan Lee

DISSERTATION

Presented to the Faculty of the Graduate School of Biomedical Sciences

The University of Texas Southwestern Medical Center at Dallas

In Partial Fulfillment of the Requirements

For the Degree of

DOCTOR OF PHILOSOPHY

The University of Texas Southwestern Medical Center at Dallas

Dallas, Texas

April, 2007

Copyright

by

Peter Chang Whan Lee, 2007

All Rights Reserved

## ACKNOWLEDGEMENTS

This is the most important and precious part of my thesis where I will have a chance to acknowledge all the people that made this work possible. It may not be long enough to express how indebted I am but I will try not to omit any people.

I am deeply grateful to Russell DeBose-Boyd not only science but also my life. He offers guidance, inspiration, perspective, and confidence. He was always available when I need him and care for my development as an individual scientist. He is the most generous people I have known and I will always feel very fortunate for the opportunity to work with him.

Furthermore, I would like to express my appreciation to Mike brown and Joe Godstein for their endless supports and continuous encouragements. It has been a tremendous experience to work with two Nobel laureates. They both share their useful insights, thoughtful critiques through lab meeting which will serve me well in the future.

I greatly appreciate the time and effort of members of my thesis committee, Sandra Hofmann, George DeMartino, and David Mangelsdorf. They were always available for counsel and very supportive.

I am also grateful to all my other colleagues in the Department of Molecular Genetics. Specially, Navdar Sever for initiated the project and mentored me during the first couple of months; Rob Rawson shares his precious knowledge and experience with somatic cell genetics and cell fusions; Jin Ye for his critiques and comments.

I am particularly thank to our BIPS members, Arun Radhakrishnan, Rodney Infante, Tom Lagace, Andy Nguyen, Lina Abi Moslesh, Mathew Francis, Yukio Ikeda, Joon Lee, and Amit Kunte for being a constant source of discussion, laughter, and friendship.

It would be impossible to accomplish any of this work without the technical staff of Molecular Genetics. Lisa Beatty, Angela Carroll, and Marissa Hodgkin spent many hours to set up cells and maintain cultures. Tammy Dinh, and Kristi Garland provided critical technical assistance throughout my project.

Finally, this work is dedicated to my parents and my wife. They always support my decision and encourage my future. They have sacrificed and done for me, I am forever grateful and indebted to them.

**ELUCIDATION OF MOLECULAR MECHANISMS UNDERLYING  
REGULATION OF CHOLESTEROL SYNTHESIS**

Peter Chang-Whan Lee, Ph.D.

The University of Texas Southwestern Medical Center at Dallas, 2007

Supervising Professor: Russell A. DeBose-Boyd, Ph.D.

Insig-1 and Insig-2, a pair of ER membrane proteins, mediate feedback control of cholesterol synthesis through their sterol-dependent binding to two polytopic ER membrane proteins: SCAP and HMG CoA reductase. Sterol-induced binding of Insigs to SCAP prevents the proteolytic processing of SREBPs, membrane-bound transcription factors that enhance the synthesis of cholesterol, by retaining complexes between SCAP and SREBP in the ER. Sterol-induced binding of Insigs to reductase leads to the ubiquitination and ER-associated degradation of the enzyme, thereby slowing a rate-controlling step in cholesterol synthesis. The successful application of somatic cell genetics in unraveling the SREBP

pathway, merits its use in the dissection of mechanisms for Insig-mediated, sterol-accelerated degradation of reductase or ER retention of SCAP.

I have designed a genetic screen to isolate mutants of CHO cells that cannot degrade reductase when presented with sterols. CHO cells were mutagenized and selected for growth in cholesterol-free medium containing the SR-12813. SR-12813 blocks cholesterol synthesis by mimicking the action of sterols in accelerating reductase degradation. Using this screen I have isolated the following mutant cell lines. 1) SRD-14 cells, which do not produce Insig-1 mRNA and protein due to a partial deletion of the Insig-1 gene. Sterols fail to promote reductase ubiquitination/degradation and the rate at which sterols suppress SREBP processing is significantly slower in SRD-14 than wild type cells; 2) SRD-15 cells which are deficient in both Insig-1 and Insig-2. Sterols neither inhibit SREBP processing nor promote reductase ubiquitination/degradation in SRD-15 even upon prolonged treatment; 3) SRD-16, -17, and -18 cells contain a point mutation in one reductase allele. Sterols failed to promote ubiquitination and degradation of these reductase mutants, owing to their decreased affinity for Insigs; 4) SRD-19 cells have amplified the number of copies of the gene encoding SCAP, leading to the overproduction of SCAP mRNA and protein. Sterols fail to suppress processing of SREBPs, even though the cells express normal levels of Insig-2.

These studies demonstrate 1) absolute requirement for Insig proteins in the regulatory system that mediates lipid homeostasis in animal cells; 2) the importance of interactions between Insigs and the membrane domain of reductase in feedback control of a rate-determining step in cholesterol synthesis; 3) the importance of Insig-SCAP ratios in the normal regulation of SREBP processing.



# TABLE OF CONTENTS

ACKNOWLEDGEMENTS.....	v
TABLE OF CONTENTS.....	ix
PRIOR PUBLICATIONS.....	xi
LIST OF FIGURES AND TABLES.....	xiii
ABBREVIATIONS .....	xvi
INTRODUCTION .....	1
EXPERIMENTAL PROCEDURES.....	11
CHAPTER 1    ISOLATION OF MUTANT CELLS LACKING INSIG-1 THROUGH SELECTION WITH SR-12813, AN AGENT THAT STIMULATES DEGRADATION OF HMG-COA REDUCTASE.....	24
RESULTS .....	25
DISCUSSION .....	44
CHAPTER 2    ISOLATION OF STEROL-RESISTANT CHINESE HAMSTER OVARY CELLS WITH GENETIC DEFICIENCIES IN BOTH INSIG-1 AND INSIG-2.....	48
RESULTS .....	49
DISCUSSION .....	68
CHAPTER 3    MUTATIONS WITHIN THE MEMBRANE DOMAIN OF HMG-COA REDUCTASE CONFER RESISTANCE TO STEROL-ACCELERATED DEGRADATION .....	72
RESULTS .....	73

DISCUSSION .....	89
CHAPTER 4    AMPLIFICATION OF THE GENE FOR <i>SCAP</i> , COUPLED WITH INSIG- 1 DEFICIENCY, CONFERS STEROL RESISTANCE IN MUTANT CHINESE HAMSTER OVARY CELLS .....	91
RESULTS .....	92
DISCUSSION .....	113
CONCLUSION AND PERSPECTIVE .....	117
BIBLIOGRAPHY .....	123
VITAE.....	134

## PRIOR PUBLICATIONS

### PRESENT WORK:

**Lee, P.C.W.**, Liu, P., Li, W., and DeBose-Boyd, R.A. (2007). Amplification of gene for SCAP, coupled with Insig-1 deficiency, confers sterol resistance in mutant Chinese Hamster Ovary Cells (Submitted).

**Lee, P.C.W.**, Nguyen, A., and DeBose-Boyd, R.A. (2007). Mutations within the membrane domain of HMG-CoA reductase confer resistance to sterol-accelerated degradation. *J. Lipid Res.* 48, 318-327.

Gong, Y., Lee, J.N., **Lee, P.C.W.**, Goldstein, J.L., Brown, M.S., and Ye, J. (2006). Sterol-regulated ubiquitination and degradation of Insig-1 creates a convergent mechanism for feedback control of cholesterol synthesis and uptake. *Cell Metab.* 3, 15-24.

**Lee, P.C.W.**, Sever, N., and DeBose-Boyd, R.A. (2005). Isolation of sterol-resistant Chinese hamster ovary cells with genetic deficiencies in both Insig-1 and Insig-2. *J. Biol. Chem.* 280, 25242-25249.

Sever, N., **Lee, P.C.W.**, Song, B.L., Rawson, R.B., and DeBose-Boyd, R.A. (2004). Isolation of cells lacking Insig-1 through selection with SR-12813, an agent that stimulates degradation of 3-hydroxy-3-methylglutaryl coenzyme A reductase. *J. Biol. Chem.* 279, 43136-43147.

### PREVIOUS WORK:

Kang, S.H., Cho, K.K., Bok, J.D., Kim, S.C., Cho, J.S., **Lee, P.C.W.**, Kang, S.K., Lee, H.G., Woo, J.H., Lee, H.J., Lee, S.C., and Choi, Y.J. (2006) Cloning, sequencing and characterization of a novel phosphatase gene, *pho I*, from soil bacterium *Enterobacter* sp. 4. *Current Microbiology* 52, 243-248

Cho, J.S., **Lee, C.W.**, Kang, S.H., Lee, J.C., Lee, H.G., Bok, J.D., Woo, J.H., Moon, Y.S., and Choi, Y.J. (2005) Molecular cloning of a phytase gene (phy M) from *Pseudomonas syringae* MOK1. *Current Microbiology* 51, 11-15

Cho, J.S., **Lee, C.W.**, Kang, S.H., Lee, J.C., Bok, J.D., Moon, Y.S., Lee, H.G., Kim, S.C., and Choi, Y.J. (2003) Purification and characterization of a phytase from *Pseudomonas syringae* MOK1. *Current Microbiology* 47, 290-294

# LIST OF FIGURES AND TABLES

## INTRODUCTION

FIGURE 1:	The mevalonate pathway .....	8
FIGURE 2:	The SREBP pathway.....	9
FIGURE 3:	Growth pattern of sterol-resistant (A) and -requiring (B) mutant cells .....	10

## EXPERIMENTAL PROCEDURES

TABLE I:	Cell lines for this study .....	23
----------	---------------------------------	----

## CHAPTER 1

FIGURE 1-1:	SR-12813 mimics sterols in promoting Insig-dependent ubiquitination and degradation of HMG CoA reductase and cannot accelerate degradation-resistant forms of the enzyme .....	33
FIGURE 1-2:	SR-12813 mediated killing of CHO cells is prevented by cholesterol .....	35
FIGURE 1-3:	Comparison of growth, HMG CoA reductase degradation/ ubiquitination, and SREBP processing in parental CHO cells and SRD-14 cells treated with sterols and SR-12813 .....	37
FIGURE 1-4:	Immunoblot analysis and molecular characterization of Insig-1 mRNA in parental CHO and mutant SRD-14 cells.....	39
FIGURE 1-5:	Kinetics of sterol-mediated suppression of nuclear SREBP-2 and SREBP-target gene expression in parental CHO and mutant SRD-14 cells .....	41
FIGURE 1-6:	Stable transfection of SRD-14 cells with pCMV-Insig-1-Myc or pCMV-Insig-2-Myc restores regulation of HMG CoA reductase degradation/ ubiquitination and SREBP2 processing mediated by sterols and SR-12813 .....	43

## CHAPTER 2

FIGURE 2-1:	Growth of parental and mutant cells in the absence and presence of 25-HC .....	57
-------------	--	----

FIGURE 2-2: Proteolytic processing of SREBPs is refractory to sterol regulation in SRD-15 cells .....	59
FIGURE 2-3: Comparison of HMG CoA reductase synthesis and sterol-regulated turnover in CHO-7 and SRD-15 cells.....	61
FIGURE 2-4: Molecular characterization of Insig-2 mRNA and genomic DNA in CHO, SRD-14, and SRD-15 cells .....	63
FIGURE 2-5: Stable transfection of SRD-15 cells with pCMV-Insig-1-Myc or pCMV-Insig-2-Myc restores regulation of SREBP-2 processing mediated by sterols .....	65
FIGURE 2-6: Stable transfection of SRD-15 cells with pCMV-Insig-1-Myc or pCMV-Insig-2-Myc restores sterol regulation of HMG-CoA reductase ubiquitination and degradation .....	67

### CHAPTER 3

FIGURE 3-1: Characterization of mutant CHO cells resistant to SR-12813 .....	80
FIGURE 3-2: Localization and conservation of amino acid residues in HMG CoA reductase membrane domain.....	82
FIGURE 3-3: Ubiquitination of S60N, G87R, and A333P versions of HMG CoA reductase .....	84
FIGURE 3-4: Properties of S60N, G87R, and A333P HMG CoA reductase in transfected cells .....	86
FIGURE 3-5: Introduction of the G87R mutation into membrane domain of HMG CoA reductase impairs binding to Insig-1 in the presence of 25-HC.....	88

### CHAPTER 4

TABLE II: Incorporation of [ <sup>14</sup> C] acetate into [ <sup>14</sup> C] cholesterol and <sup>14</sup> C-labeled fatty acids in parental cells and mutant cells resistant to 25-HC .....	98
FIGURE 4-1: Growth of parental and mutant cells in the absence and presence of 25-HC .....	100

FIGURE 4-2: Sterol content of wild type CHO-7 and mutant SRD-14, SRD-15, and SRD -19 cells .....	102
FIGURE 4-3: Accumulation of neutral lipids in CHO-7, SRD-14, SRD-15, and SRD-19 cells as revealed by Oil Red O .....	104
FIGURE 4-4: Analysis of lipid isolated from parental CHO-7 and mutant SRD-14, SRD-15, and SRD-19 cells .....	106
FIGURE 4-5: Sterol regulation of SREBP processing in wild type and mutant cells.....	108
FIGURE 4-6: Molecular characterization of SCAP mRNA and genomic DNA in parental CHO-7 and mutant SRD-19 cells.....	110
FIGURE 4-7: Stable transfection of pCMV-Insig-1-Myc or pCMV-Insig-2-Myc restores sterol-mediated suppression of SREBP-2 processing in SRD-19 cells .....	112

## **CONCLUSION AND PERSPECTIVE**

FIGURE 4: Gene Trap Vector.....	122
---------------------------------	-----

## **ABBREVIATIONS**

ALLN – N-acetyl-leucinal-leucinal-norleucinal

CHO – Chinese hamster ovary

CMV – cytomegalovirus

DMEM – Dulbecco's modified Eagle's medium

EMS – Ethylmethane sulfonate

ER – endoplasmic reticulum

ERAD – ER-associated degradation

FCS – fetal calf serum

GAPDH – glyceraldehyde-3-phosphate dehydrogenase

HMG CoA – 3-hydroxy-3-methylglutaryl Coenzyme A

HPCD – hydroxypropyl- $\beta$ -cyclodextrin

LDL – low density lipoprotein

LPDS – lipoprotein-deficient serum

MCD – Methyl- $\beta$ -cyclodextrin

PBS – Phosphate-buffered saline

RNAi – RNA interference

SCAP – SREBP cleavage-activating protein

SRD – sterol regulatory defective

SRE – Sterol regulatory element

SREBP – SRE binding protein

25-HC – 25-hydroxycholesterol



## INTRODUCTION

The 27-carbon tetracyclic cholesterol is essential for mammalian life as a structural component of cell membranes. In addition, cholesterol is a precursor of steroid hormones, bile acids, vitamin D, sex hormones, and lipoproteins (Ikonen, 2006; Russell, 1999). However, an excess of cholesterol can be toxic not only because it can form crystals that kills cells but because excess cholesterol promotes atheroma formation in the walls of arteries. This condition is known as atherosclerosis, the primary cause of coronary heart disease and other forms of cardiovascular disease in humans (Ikonen, 2006; Libby et al., 2000). Thus, levels of cholesterol must be properly maintained owing to its key role in cellular and whole-body physiology. Cholesterol homeostasis is controlled by a feedback regulatory system that balances of cholesterol-rich low density lipoproteins (LDL) from the plasma via LDL receptor-mediated endocytosis and *de novo* synthesis of cholesterol. Cholesterol is synthesized through the mevalonate pathway and the rate-limiting step is 3-hydroxy-3-methylglutaryl coenzyme A (HMG CoA) reductase which catalyzes reduction of HMG CoA to mevalonate. In addition to cholesterol, nonsterol isoprenoids, which include prenyl groups that are attached to several proteins, are produced via the mevalonate pathway (Fig. 1). The synthesis and uptake of cholesterol are coordinately regulated such that excess cellular cholesterol suppresses expression of cholesterol biosynthetic enzymes and the LDL receptor. Statins, competitive inhibitors of HMG CoA reductase, trigger reactions that relieve the negative feedback repression giving rise to an increase in LDL receptors. The increase in LDL receptors leads to a decrease in the LDL-cholesterol in the blood and to a reduction in the occurrence of heart attacks (Brown and Goldstein, 1996). However, the effects of statins

are limited because of the HMG CoA reductase regulatory system that comes into play when the enzyme is inhibited. Operating at transcriptional, and post-transcriptional levels, this regulatory system leads to a major increase in the amount of reductase enzyme that becomes progressively harder to inhibit. This invokes the need for higher levels of statins to maintain their cholesterol-lowering effects. A complete understanding of this regulatory system is essential; not only for scientific reasons, but also because it is at the center of clinical medicine.

### **Regulation of the Mevalonate Pathway**

HMG CoA reductase catalyzes the two-step reduction of HMG CoA to mevalonate, a rate-determining reaction in synthesis of cholesterol and nonsterol isoprenoids (reviewed in Goldstein and Brown, 1990). HMG CoA reductase, a resident glycoprotein of the endoplasmic reticulum (ER), is integrated into membranes through a hydrophobic NH<sub>2</sub>-terminal domain that contains eight membrane-spanning segments separated by short loops (Roitelman et al., 1992). The membrane domain of reductase precedes a hydrophilic COOH-terminal domain that projects into the cytosol and contains all enzymatic activity (Gil et al., 1985; Liscum et al., 1985). Sterol and nonsterol end-products of mevalonate metabolism exert stringent feedback control on reductase through multivalent negative feedback regulation (Brown and Goldstein, 1980; Nakanishi et al., 1988; Roitelman and Simoni, 1992). 1) The coordinate regulation of cholesterol biosynthetic enzymes and LDL receptor is mediated by sterol-regulated transcription. 2) HMG CoA reductase is also regulated at the level of its translation and its half-life (Nakanishi et al., 1988). The translational regulation of

HMG CoA reductase is controlled by nonsterol products of mevalonate pathway through an unknown mechanism thought to be mediated by the complex 5' untranslated region of the reductase. 3) The half-life of reductase is regulated by both sterol and nonsterol products and requires the membrane domain. The central event in this degradation is sterol-induced binding of reductase to ER membrane proteins called Insig-1 and Insig-2 (Sever et al., 2003a; Sever et al., 2003b). In sterol-depleted cells, the reductase protein is stable with a half-life of more than 12 h. The accumulation of sterols in ER membranes triggers binding of reductase to Insigs, carriers of a membrane-anchored ubiquitin ligase called gp78 that initiates reductase ubiquitination (Song et al., 2005b). This ubiquitination marks reductase for rapid, proteasome-mediated degradation with a half-life of less than 1 h and halts production of mevalonate, hence blunting the rate of cholesterol synthesis. Altogether, these modes of regulation give rise to a practically all-or-none change in HMG CoA reductase activity. Another control mechanism is the reversible phosphorylation of HMG CoA reductase catalytic domain by AMP-dependent kinase, which inactivates the enzyme. AMP-dependent kinase senses cellular energy levels and inhibits cholesterol synthesis under conditions of low ATP. This phosphorylation event is not part of the end-product mediated negative feedback regulation and does not affect the half-life of HMG CoA reductase under any condition (Sato et al., 1993).

### **Control of Cholesterol homeostasis**

Cholesterol and fatty acids synthesis are controlled by a family of membrane-bound transcription factors called sterol regulatory element-binding proteins (SREBPs). These were

purified from nuclear extracts of human HeLa cells by virtue of their ability to bind SRE sequences (Wang et al., 1993). Subsequently, cDNA cloning revealed that mammalian cells express three closely related isoforms of SREBP, known as SREBP-1a, SREBP-1c, and SREBP-2. SREBP-1a and -1c are produced from the same gene through the use of different promoters and alternative splicing. All three SREBPs belong to the basic helix-loop-helix leucine zipper (bHLH-Zip) family of transcription factors. However, unlike other bHLH-Zip members, SREBPs are intrinsic membrane proteins of the ER, and share a tripartite structure that is composed of: 1) an NH<sub>2</sub>-terminal transcription factor domain of ~480 amino acids; 2) a membrane anchoring domain of ~80 amino acids that comprises two transmembrane segments; and 3) a COOH-terminal regulatory domain of ~590 amino acids. Both the NH<sub>2</sub>- and COOH- termini domains face the cytosol where these domains are separated by two membrane-spanning helices of SREBPs project into the ER lumen (Brown and Goldstein, 1997; Goldstein et al., 2006). Newly synthesized SREBPs are translated as inactive precursors that are immediately inserted into the ER membrane where they constitutively bind SREBP cleavage activating protein (SCAP).

SCAP is a polytopic ER protein of 1276 amino acids, which can be divided broadly into two domains (Nohturfft et al., 1998): a hydrophobic NH<sub>2</sub>-terminal domain with eight membrane-spanning segments that anchor the proteins to ER membranes; and a large hydrophilic COOH-terminal domain that projects into the cytosol and mediates complex formation with the SREBP family of transcription factors (Nohturfft et al., 1998). In sterol deprived cells, SCAP facilitates the translocation of membrane-bound SREBPs from the ER to the Golgi through COPII budding vesicle, where NH<sub>2</sub>-terminal transcription factor domain

of SREBPs is released from membranes through two sequential cleavages in a process called Regulated Intermembrane Proteolysis (RIP). From the cytosol, processed SREBPs rapidly migrate into the nucleus to enhance the transcription of genes encoding reductase and other cholesterol biosynthetic enzymes. When cells are treated with cholesterol or oxysterols, SCAP-SREBP complexes are trapped in the ER and SREBP processing is abolished; rates of SREBP target gene transcription and cholesterol synthesis decline (Hua et al., 1996; Sun et al., 2005; Yang et al., 2002). The block in ER-to-Golgi transport occurs through sterol-induced binding of SCAP to Insigs (Yabe et al., 2002a; Yang et al., 2002). This binding is mediated by a segment of ~170 amino acids in SCAP that constitute transmembrane helices 2–6, which is known as the sterol-sensing domain (Brown and Goldstein, 1999; Kuwabara and Labouesse, 2002). Point mutations within the sterol-sensing domains of SCAP prevent their association with Insigs, thereby abolishing the sterol-mediated ER retention of SCAP-SREBP complexes (Yabe et al., 2002b).

Insig-1 and Insig-2, a pair of ER membrane proteins, mediate feedback control of cholesterol synthesis through their sterol-dependent binding to SCAP and HMG CoA reductase. Sterol-induced binding of Insigs to SCAP prevents proteolytic processing of SREBP by retaining SCAP-SREBP complexes in the ER. Sterol-induced binding of Insigs to reductase leads to the ubiquitination and ER-associated degradation of the enzyme, thereby slowing the rate-controlling step in cholesterol synthesis (Fig. 2). Insig-1 and Insig-2 are 59% identical over their lengths of 277 and 225 amino acids, respectively. Even though they seem functionally redundant in transfection studies, they are differentially regulated. *INSIG-1* (insulin induced gene-1) is an SREBP target gene giving rise to an apparent paradox,

whereby Insig-1 is suppressed by sterols, exactly when it is supposed to exert its action. Insig-2 has two alternative splice forms, Insig-2a and Insig-2b, which produce identical proteins (Yabe et al., 2002a). Insig-2a is the liver-specific isoform and is repressed by insulin whereas Insig-2b is constitutive and the only form expressed in cultured cells.

Gp78 is a 643 amino acid protein with four identifiable domains (Fang et al., 2001; Shimizu et al., 1999): (1) an NH<sub>2</sub>-terminal membrane attachment region of 298 amino acids that binds Insigs; (2) RING finger domain conferring E3 ubiquitin ligase activity; (3) Cue1p homologous sequence, an ER membrane protein in yeast that serves as a membrane anchor for Ubc7p, a cytosolic ubiquitin-carrying E2 protein (Ponting, 2000); and (4) VCP (Valosin-containing protein, also known as p97), an ATPase implicated in the postubiquitination steps of ER-associated protein degradation (Zhong et al., 2004). The central event in this HMG CoA reductase degradation is the sterol-induced binding of reductase to Insigs. Formation of the reductase-Insig complex is mediated by the membrane domain of reductase and results in the recruitment of gp78. This sterol-induced ubiquitination is an obligatory reaction for the proteasome-mediated degradation of reductase. Gp78 also served as an E3 ligase of Insig-1. In sterol-depleted cells, a fraction of gp78 is associated with Insig-1, which leads to the ubiquitination and subsequent proteasomal degradation of Insig-1. When sterol-dependent stabilization of Insig-1 occurs, Insig-1 and Scap forms a complex, which in turn displaces gp78, thereby preventing ubiquitination and subsequent degradation of Insig-1.

## Somatic Cell Genetics

Somatic cell genetics has been invaluable in illuminating the complex pathway of lipid homeostasis that is controlled by the SREBP pathway (Goldstein *et al.*, 2002). The identity and function of the following proteins has been in some way revealed by somatic cell genetics through studies using mutant Chinese hamster ovary cells; HMG CoA reductase, HMG CoA synthase, SCAP, SREBP, ACAT, S1P, S2P and others (Chang *et al.*, 1993a; Chin *et al.*, 1982; Hua *et al.*, 1996; Luskey *et al.*, 1983; Rawson *et al.*, 1999; Rawson *et al.*, 1997; Sakai *et al.*, 1998). To date, two classes of sterol mutants have been isolated (Fig. 3). Cells in the first class are cholesterol auxotrophs and isolated by the use of amphotericin B, a polyene antibiotic that kills the cell by binding to cholesterol and forming pores in the plasma membrane. These cells cannot process SREBP; therefore, they do not express the cholesterol biosynthetic enzymes, explaining their survival against a transient treatment with amphotericin B. The other class is sterol-resistant cells, which fail to properly regulate the processing of SREBP in response to sterols. They were isolated using the oxysterol:25-HC, which can suppress SREBP processing but cannot replace cholesterol in the plasma membrane. Wild type cells die with a chronic treatment of 25-HC due to cholesterol depletion. Two types of mutations have been observed in sterol-resistant cells. Type 1 mutations occur in the SREBP-2 gene, producing truncated SREBP-2 that terminates before the first transmembrane segment and constitutively migrates to the nucleus. Type 2 mutations are point mutations, Y298C, L315F and D443N, which are in the SSD (sterol-sensing domain) of SCAP and render SCAP insensitive to sterols. These SCAP mutants cannot bind to Insig-1 or Insig-2; thus, they escort SREBP to the Golgi even in the presence of sterols

explaining the constitutive processing of SREBPs in cells expressing these mutants (Yabe *et al.*, 2002b).

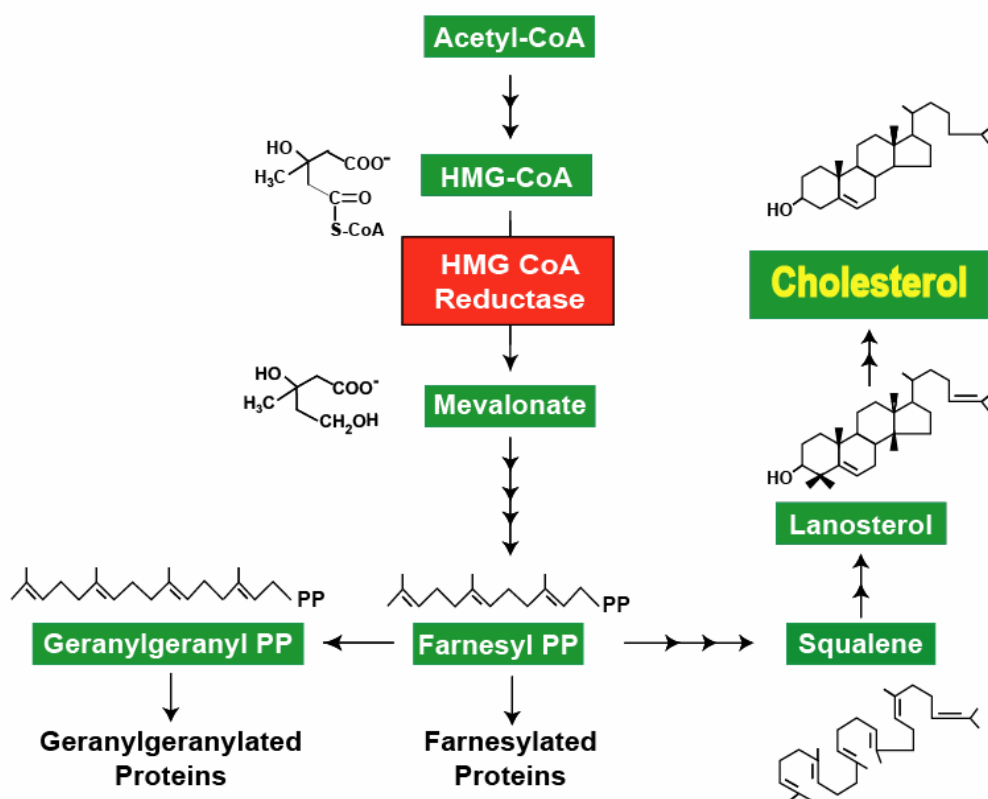


**FIGURE 1: The mevalonate pathway.** Adapted from Goldstein and Brown (1990).



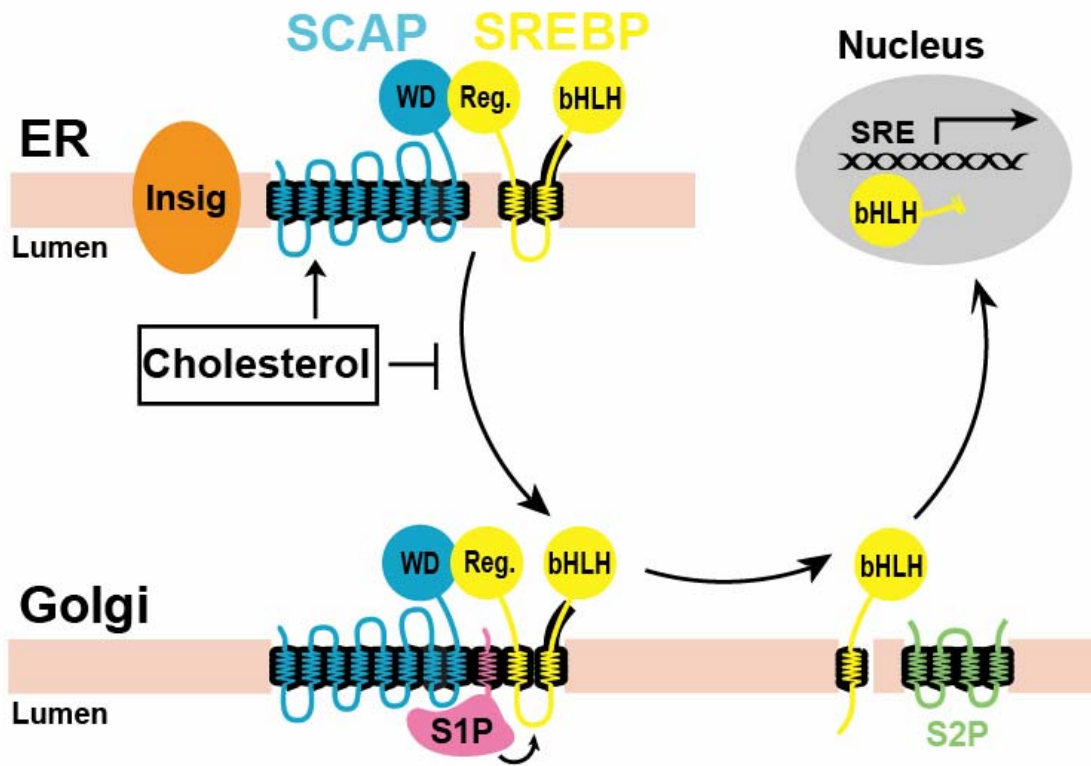


**FIGURE 2: The SREBP pathway.** Reprinted from Goldstein et al., Copyright (2002), with permission from Elsevier.

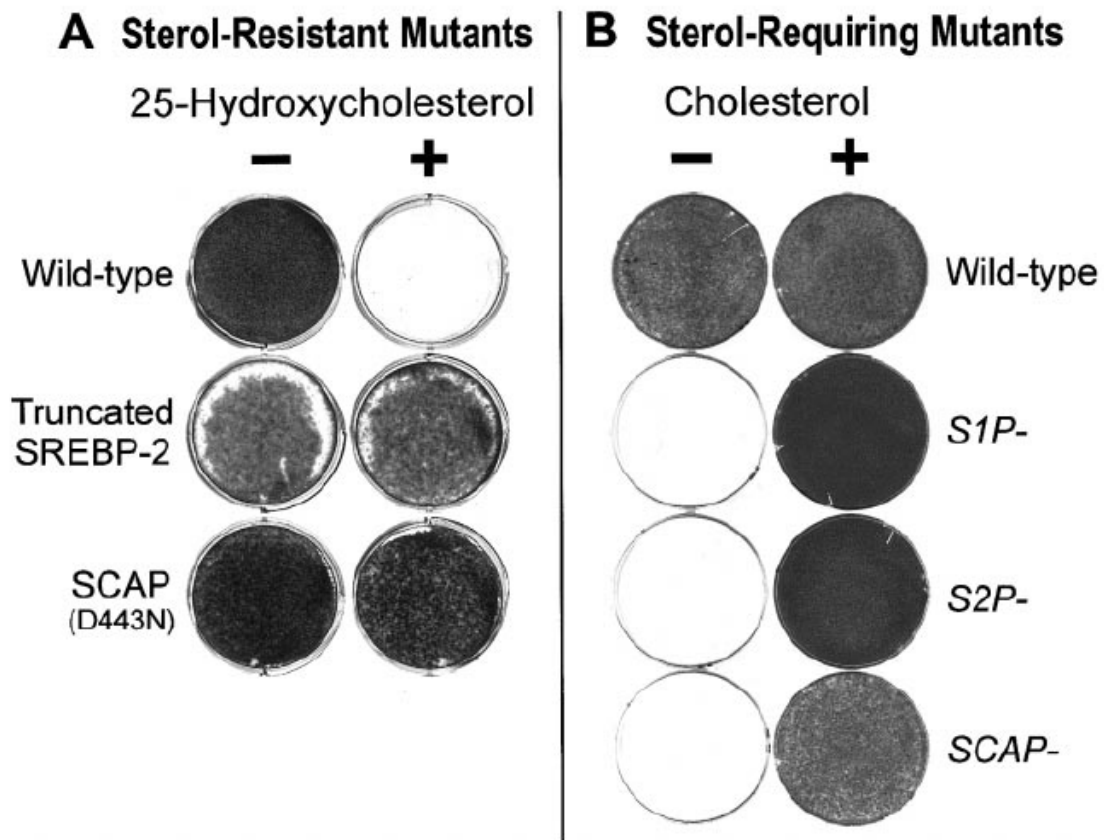


**FIGURE 3: Growth pattern of sterol-resistant (A) and -requiring (B) mutant cells.**

Reprinted from Goldstein et al., Copyright (2002), with permission from Elsevier.

## EXPERIMENTAL PROCEDURES

**Materials.** I obtained MG-132 from Calbiochem, horseradish peroxidase-conjugated, donkey anti-mouse and anti-rabbit IgGs from Jackson ImmunoResearch, SR-12813 from GlaxoSmithKline (Research Triangle Park, NC) or Core Medicinal Chemistry Laboratory, Department of Biochemistry, University of Texas Southwestern Medical Center, and sterols (25-HC and cholesterol) from Steraloids, Inc. (Newport, RI). MCD and HPCD were from Cyclodextrin Technologies Development, Inc. DECA template- $\beta$ -actin-mouse was from Ambion. EMS, Mouse monoclonal anti-HA IgG were from Sigma. Rabbit polyclonal anti-T7-Tag IgG was from Bethyl Laboratories. Mouse monoclonal anti-HA IgG was from Sigma. [ $^{14}\text{C}$ ] acetate and [ $^{14}\text{C}$ ] oleate were from American Radiolabeled Chemicals, Inc. (St. Louis, MO). All other reagents were obtained from previously described sources (DeBose-Boyd et al., 1999; Rawson et al., 1999; Yabe et al., 2002a; Yang et al., 2002).

**Cell Culture.** Cells were maintained in monolayer culture at 37 °C in an 8-9%  $\text{CO}_2$  incubator. CHO-7 cells were maintained in medium A (1:1 mixture of Ham's F12 medium and DMEM containing 100 units/ml penicillin and 100  $\mu\text{g/ml}$  streptomycin sulfate) supplemented with 5% LPDS. SRD-1 cells were maintained in medium A supplemented with 5% LPDS and 2.5  $\mu\text{M}$  25-HC. SRD-14, SRD-16, SRD-17, SRD-18 cells were grown in medium A supplemented with 5% LPDS and 10  $\mu\text{M}$  SR-12813. SRD-15, SRD-19 grown in medium A containing 5% LPDS and 2.5  $\mu\text{M}$  25-HC. SRD-13A, CHO-7/pInsig-2 cells were

maintained in medium A supplemented with 5% FCS, 1 mM mevalonate, 20  $\mu$ M sodium oleate, 5  $\mu$ g/ml cholesterol, and 500  $\mu$ g/ml G418.

Monolayers of SV-589 cells, an immortalized line of human fibroblasts expressing the SV40 large T antigen (Yamamoto *et al.*, 1984), were grown at 37 °C in 5% CO<sub>2</sub>. Stock cultures of SV-589 cells were maintained in medium B (DMEM containing 100 units/ml penicillin and 100  $\mu$ g/ml streptomycin sulfate) supplemented with 10% FCS.

**Antibodies.** Mouse monoclonal anti-T7-Tag (IgG<sub>2b</sub>) (Novagen); mouse monoclonal anti-Myc (IgG fraction) from the culture medium of hybridoma clone 9E10 (American Type Culture Collection); IgG-A9, a mouse monoclonal antibody against the catalytic domain of hamster HMG CoA reductase (amino acids 450-887) (Liscum *et al.*, 1983); IgG-1D2, a mouse monoclonal antibody against the NH<sub>2</sub>-terminus of human SREBP-2 (amino acids 48-403) (Yabe *et al.*, 2002a); IgG-7D4, a mouse monoclonal antibody against the NH<sub>2</sub> terminus of hamster SREBP-2 (Yang *et al.*, 1995); anti-Insig-1, a rabbit polyclonal antibody against full-length mouse Insig-1 (Engelking *et al.*, 2004); R-139, a rabbit polyclonal antibody against amino acids 54-207 and 540-707 of hamster SCAP (Sakai *et al.*, 1997); and IgG-P4D1, a mouse monoclonal antibody against bovine ubiquitin (Santa Cruz Biotechnology). Mouse monoclonal antibody IgG-9D5 against hamster SCAP has been described (Sakai *et al.*, 1997).

**Plasmids.** The following recombinant plasmids were previously described in the indicated reference: pCMV-Insig-1-Myc, encoding amino acids 1-277 of human Insig-1 followed by

six tandem copies of a c-Myc epitope tag under control of the cytomegalovirus (CMV) promoter (Yang *et al.*, 2002); pCMV-Insig-2-Myc, encoding amino acids 1-225 of human Insig-2 followed by six tandem copies of a c-Myc epitope tag under control of the CMV promoter (Yabe *et al.*, 2002a); pCMV-HMG-Red-T7, encoding amino acids 1-887 of hamster HMG CoA reductase followed by three tandem copies of the T7 epitope tag under control of the CMV promoter (Sever *et al.*, 2003a); and pCMV-HMG-Red-T7 (TM 1-8), encoding amino acids 1-346 of hamster HMG CoA reductase followed by three tandem copies of the T7 epitope tag under control of the CMV promoter (Sever *et al.*, 2003b). The S60N, G87R, and A333P mutations were introduced into pCMV-HMG-Red-T7 and pCMV-HMG-Red-T7 (TM1-8) by site-directed mutagenesis using the QuikChange XL kit (Stratagene) and the following primer pairs:

S60N	5'-GAGGAGGATGTATTGAGCAATGACATCATCATCC-3'
	5'-GGATGATGATGTCATTGCTCAATACATCCTCCTC-3'
G87R	5'-CCAGAACTTACGTCAGCTTAGGTCTGAAGTATATTTTAGG-3'
	5'-CCTAAAATATACTTCGACCTAAGCTGACGTAAGTTCTGG-3'
A333P	5'-GCTTAGCTTTTCTGTTGCCTGTCAAGTACATTTTCTTTG-3'
	5'-CAAAGAAAATGTACTTGACAGGCAACAGAAAAGCTAAGC-3'

The integrity of each plasmid was confirmed by DNA sequencing.

**Transient Transfection.** Transfections were performed as described (Rawson *et al.*, 1999) with minor modifications. CHO-7 cells were transfected with 3 µg of DNA per 60-mm dish. For each transfection, FuGENE-6 DNA transfection reagent (Roche Diagnostics) was added to 0.2 ml of medium B at a ratio of 3 µl of FuGENE-6 per 1 µg DNA. Conditions of the

incubations are described in the figure legends. At the end of the incubations, triplicate dishes of cells for each variable were harvested and pooled for analysis.

**Cell Fractionation and Immunoblot Analysis.** The pooled cell pellets from triplicate dishes of cells were used to isolate  $2 \times 10^4$ -g membrane fractions and/or nuclear extract fractions as previously described (Sever *et al.*, 2003a) with a minor modification. The nuclear extract fractions (300  $\mu$ l) were precipitated with 1.5 ml acetone for 16 h at  $-20^\circ\text{C}$ . Precipitated material was collected by centrifugation at  $2 \times 10^4$ -g for 15 min and solubilized in 100  $\mu$ l of buffer containing 10 mM Tris-HCl (pH 6.8), 1% (w/v) sodium dodecyl sulfate, 100 mM NaCl, 1 mM EDTA, and 1 mM EGTA, mixed with 25  $\mu$ l of 5X SDS loading buffer, and boiled for 5 min. Aliquots of nuclear extract and membrane fractions were subjected to 8% SDS-PAGE and immunoblot analysis was carried out as described (Sever *et al.*, 2003a).

**Ubiquitination of Endogenous HMG CoA Reductase.** Conditions of incubations are described in the figure legends. At the end of the incubations, the cells were harvested, lysed in detergent-containing buffer, and immunoprecipitation of reductase from the detergent lysates was carried out with polyclonal antibodies against the 60-kDa COOH-terminal domain of human reductase as previously described (Sato *et al.*, 1993; Sever *et al.*, 2003a; Sever *et al.*, 2003b). Aliquots of the immunoprecipitates were subjected to SDS-PAGE on 6% gels, transferred to nylon membranes, and subjected to immunoblot analysis.

**Ubiquitination Exogenous HMG CoA Reductase.** Conditions of incubations are described in the figure legends. At the end of the incubations, the cells were harvested, lysed in detergent-containing buffer and immunoprecipitations were carried out with either polyclonal antibodies against the catalytic domain of human reductase or monoclonal anti-T7 IgG-coupled agarose beads (Novagen) against transfected reductase as described previously (Sever *et al.*, 2003a).

**RNA Interference.** Duplexes of small-interfering RNA targeting human Insig-1, human Insig-2, and an irrelevant control gene, vesicular stomatitis virus glycoprotein (VSV-G) were synthesized by Dharmacon Research (Lafayette, CO), and RNA interference (RNAi) experiments were carried out as described previously (Sever *et al.*, 2003a).

**Mutagenesis and Isolation of SR-12813-resistant Cells Deficient in Insig-1.** On day 0,  $2.5 \times 10^7$  CHO-7 cells were subjected to  $\gamma$ -irradiation as previously described (Rawson *et al.*, 1998). The cells were immediately plated at  $5 \times 10^5$  cells/100-mm dish in medium B supplemented with 5% LPDS. On day 1, the medium was replaced with medium B containing 5% LPDS and 10  $\mu$ M SR-12813. Fresh medium was added to the cells every 2 days until colonies formed. On day 29, the surviving colonies were isolated with cloning cylinders and allowed to proliferate. Of the 50 original dishes, 14 contained SR-12813-resistant colonies and it was determined that 8 of the colonies lacked expression of Insig-1 mRNA. The most vigorous colony was cloned by limiting dilution and designated SRD-14 cells.

**Mutagenesis and Isolation of 25-HC-resistant SRD-15, and SRD-19 cells.** SRD-14 cells were subjected to  $\gamma$ -irradiation and select with medium A supplemented with 5% LPDS and 1.25  $\mu$ M 25-HC. Of the 50 original dishes, 20 contained 25-HC-resistant colonies, and it was determined that 19 of the colonies exhibited reduced expression of Insig-2 mRNA as determined by Northern blot analysis and real time PCR. The most vigorous colony was cloned by limiting dilution and designated SRD-15 cells. The remaining colony (expressing normal levels of Insig-2) was cloned by limiting dilution and designated SRD-19.

**Mutagenesis and Isolation of SR-12813-Resistant SRD-16, -17-, and -18 Cells.** CHO-7 or CHO-7/pInsig-2 cells were plated on day 0 at  $1 \times 10^6$  cells/100-mm dish in medium A supplemented with 5% LPDS. On day 1, cells were refed the identical medium containing 0.3 mg/ml EMS. Following incubation for 16 h at 37 °C, cells were washed twice with PBS, trypsinized, and split 1:10 in medium A containing 5% LPDS. After 3 days (to allow expression of altered phenotypes), the cells were washed and refed medium A containing 5% LPDS and 10  $\mu$ M SR-12813. The most vigorous SR-12813-resistant colonies were cloned by limiting dilution and designated SRD-16, -17-, and -18.

**Stable cell lines.** SRD-14/pInsig-1 and SRD-14/pInsig-2 cells, derivatives of SRD-14 cells stably expressing Insig-1-Myc or Insig-2-Myc, respectively, were generated as follows. On day 0, SRD-14 cells were set up at  $5 \times 10^5$  cells per 60-mm dish in medium A supplemented with 5% LPDS. On day 1, the cells were transfected with 1  $\mu$ g of pCMV-Insig-1-Myc or



pCMV-Insig-2-Myc using the FuGENE 6 transfection reagent as described above. On day 2, cells were switched to medium A supplemented with 5% LPDS and 700 µg/ml G418. Fresh medium was added every 2-3 days until colonies formed after about 2 weeks. Individual colonies were isolated with cloning cylinders, and Insig-1 or Insig-2 expression was assessed by immunoblot analysis with anti-Myc. Cells from a single colony were cloned by limiting dilution and maintained in medium A containing 5% LPDS and 500 µg/ml G418 at 37 °C, 8-9% CO<sub>2</sub>. SRD-15/pInsig-1, SRD-15/pInsig-2, SRD-19/pInsig-1 and SRD-19/pInsig-2 cells were generated and maintaining in medium A supplemented with 5% FCS, 5 µg/ml cholesterol, 1 mM mevalonate, and 20 µM sodium oleate and 500 µg/ml G418.

**Real-Time PCR, Southern, and Northern Blot Analysis.** The protocol for real-time PCR was identical to that described by Liang et al (Liang *et al.*, 2002). Total RNA was isolated from CHO-7 and mutant cells using the RNeasy Kit (Qiagen) according to the manufacturer's instructions and subjected to reverse transcription. Triplicate samples of reverse-transcribed total RNA were subjected to real-time PCR quantification using forward and reverse primers for hamster HMG CoA reductase, HMG CoA synthase, LDL receptor, Insig-1, Insig-2, GAPDH, and β-actin (invariant control). Relative amounts of mRNAs were calculated using the comparative C<sub>T</sub> method.

Probes were prepared by PCR amplification of reverse-transcribed total RNA isolated from wild type CHO-7 cells using the following forward and reverse primers. In addition, the PCR products of the Insig-2 reaction were digested with *KpnI* and the resulting two fragments (corresponding to nucleotides 1-216 and 217-678 of the Insig-2 cDNA,

respectively) were used as probes in Southern blot analyses. The resulting PCR products were radiolabeled with [ $\alpha$ - $^{32}$ P]dCTP using the Megaprime DNA Labeling System (Amersham Pharmacia Biotech). Total RNA and restriction enzyme-digested genomic DNA was subjected to electrophoresis and transferred to Hybond N<sup>+</sup> membranes (Amersham Pharmacia Biotech), and filters were hybridized at 60-65 °C with radiolabeled probe using the ExpressHyb Hybridization Solution (CLONTECH) according to the manufacturer's instructions. Filters were exposed to film with intensifying screens for the indicated time at -80 °C.

Hamster Insig-1	5'-CCAAGGATCCATGCCCAGGCTGCACGACCAC-3'
	5'-CCAAGCGGCCGCTCAGTCACTGTGAGGCTTTTCCGG-3'
Hamster Insig-2	5'-CCAAGGATCCATGCCCAGGCTGCACGACCAC-3'
	5'-CCAAGCGGCCGCTCAGTCACTGTGAGGCTTTTCCGG-3'
Hamster SCAP	5'-GATGTCCATTGTCTTTGGTATCC-3'
	5'-AGACCGTCCTCTTCCTTGTG-3'
Hamster SREBP-2	5'-ATGGACGAGAGCAGCGAGCTGGGCGG-3'
	5'-ACAGGAGGAGAGTCTGGTTCATC-3'

**Synthesis and Pulse-Chase Analysis of HMG CoA Reductase.** Cells were pulse-labeled in methionine/cysteine-free medium A, and pulse-chase analysis was carried out as described (Sever *et al.*, 2003a). Immunoprecipitation of labeled reductase from detergent lysates was carried out with polyclonal antibodies against the 60-kDa COOH-terminal domain of human reductase as described previously (Sato *et al.*, 1993; Sever *et al.*, 2003a).

Immunoprecipitates were subjected to SDS-PAGE and transferred to Hybond C-extra nitrocellulose filters. Dried filters were exposed to an imaging plate at room temperature and scanned in a Molecular Dynamics Storm 820 Phosphorimager (Amersham Biosciences).

**PCR amplification and cloning of HMG CoA Reductase cDNA from SRD-16, -17-, and -18 Cells.** Total RNA was isolated from CHO-7, CHO-7/pInsig-2, and SRD cells using the RNeasy kit (Qiagen) and subjected to reverse transcription reactions. First-strand cDNA was used to obtain PCR-amplified fragments containing nucleotides 4-823, 599-1597, 871-2418, and 2353-2661 of the reductase cDNA with the following forward and reverse primers, respectively: 5'-TTGTCACGACTTTTCCGTATG-3' and 5'-CTATCCATCGACTGTGAGCAT-3'; 5'-CTGTGCTTGCCAACTACTTCGTGT-3' and 5'-TATATCCGATCACATTCTCACAG-3'; 5'-TTGGGACTGGATGAAGATGTGT-3' and 5'-ACCACCCACAGTTCCTATCTCTAT-3'; and 5'-TGCAGCAAACATCGTCA-3' and 5'-CCATCAAAGGAGCCCCGTAAAT-3'. PCR-amplified fragments (corresponding to nucleotides 124-327 and 817-1120 of the reductase cDNA) were generated from genomic DNA isolated from the same cell lines using the following sets of forward and reverse primers: 5'-AAGATCTGTGGTTGGAATTACGAGTGC-3' and 5'-GACTGTACTAAAGACAAAAGTGAG-3'; 5'-TTGGGACTGGATGAAGATGTG T-3' and 5'-GAGGCTCCCGTCTACAACAGT. The resulting PCR products were subcloned into the pCRII vector (Invitrogen), and 10-30 individual clones were subjected to DNA sequencing to identify potential mutations in the reductase.

**Blue Native-PAGE.** SRD-13A cells were set up for experiments and transfected as described in the legend to Figure 3-5, after which they were harvested for preparation of a  $1 \times 10^5$  g membrane pellet. The membrane pellet was then solubilized in buffer containing 1% (w/v) digitonin and subjected to centrifugation at  $20,000 \times g$ . One aliquot of the resulting supernatant was mixed with a 6-amino-*n*-hexanoic acid containing buffer and subjected to electrophoresis on a 4–16% blue native gel as described (Sever *et al.*, 2003a). A second aliquot of the supernatant was mixed with SDS-containing buffer and subjected to 8% SDS-PAGE.

**Neutral Lipid Staining of Cells with Oil Red O.** On day 0, CHO-7, SRD-14, SRD-15, and SRD-19 cells were set up for experiments on coverslips as described in the figure legends. On day 3, the cells were fixed with 10% formalin in PBS for 1 h at room temperature. After washing three times with deionized water, the cells were processed for Oil red O staining using the dye at a concentration of 4  $\mu\text{g/ml}$  in isopropyl alcohol. Finally, each coverslip was washed 10 min with deionized water, stained for 5 min with 17  $\mu\text{g/ml}$  DAPI, and subjected to another 10 min wash with deionized water. Coverslips were then mounted onto glass slide and analyzed on a microscope.

**Metabolic Assays.** CHO-7, SRD-14, SRD-15, and SRD-19 cells were set up for experiments as described in the figure legends. The incorporation of [ $^{14}\text{C}$ ]-acetate into cellular cholesterol and fatty acids and that of [ $^{14}\text{C}$ ]-oleate into cellular cholesteryl esters and triglycerides was measured in cell monolayers as previously described (Brown *et al.*, 1978;

Goldstein *et al.*, 1983). The protein content of cell extracts was determined using the BCA Protein Assay Reagent (Pierce) according to the manufacturer's instructions.

**Analysis of Lipid Droplets Isolated from Wild type and Mutant CHO Cells.** On day 0, CHO-7, SRD-14, SRD-15, and SRD-19 cells were set up for experiments as described in the figure legends. On day 1, the cells were labeled with 100  $\mu\text{Ci}$  [ $^{14}\text{C}$ ] acetate for 2 days and collected by scraping in ice-cold phosphate-buffered saline (PBS) containing a protease inhibitor cocktail. Lipid droplet fractions were then purified using a previously described method (Liu *et al.*, 2004). Total lipids were extracted from purified droplet fractions using a 2:1 (v/v) mixture of acetone and  $\text{CHCl}_3$ , after which an aliquot of the extracted lipids was subjected to scintillation counting. The remaining samples (normalized for equal counts loaded per lane) were separated by thin layer chromatography on Si gel G60 plates (Whatman) that were developed in a solvent system consisting of 80:20:1 (v/v) hexane/diethyl ether/ acetic acid. The migration of radiolabeled phospholipids, fatty acids, triglycerides, ether lipids, and cholesterol were determined by visualizing unlabeled standards with iodine vapor. The region corresponding to the various lipids were then collected by scraping and subjected to scintillation counting.

**Determination of Cellular Sterol Composition.** CHO-7, SRD-14, -15, and -19 cells were set up for experiments on day 0 as described in the figure legends. On day 3, cell monolayers were washed with buffer containing 5 mM Tris-HCl (pH 7.4), 150 mM NaCl, and 0.2% BSA, followed by an additional wash in the identical buffer containing no BSA.

Subsequently, 1 ml of wash buffer containing no BSA was added to each dish; the cells were harvested by scraping, transferred to a 1.5 ml eppendorf tube, and subjected to centrifugation for 5 min at 4,000 rpm at 4°C. After removal of the supernatant, the cell pellets were resuspended in 1 ml of 0.1 M NaOH and vortexed at room temperature for 30 min. An aliquot of the resulting cell lysates was used to determine protein concentration as described above. An ethanolic solution containing the internal standards 5 $\alpha$ -cholestane (50  $\mu$ g) and epicoprostanol (2.5  $\mu$ g) was added to 200  $\mu$ l of the remaining cell lysates, and sterols were hydrolyzed by heating (to 100 °C) in ethanolic KOH (100 mM) for 2 h. Lipids were extracted in petroleum ether, dried under nitrogen, and derivatized with hexamethyldisilazane-trimethylchlorosilane. Gas chromatography-mass spectroscopy (GC-MS) analysis was performed by using a 6890N gas chromatograph coupled to a 5973 mass selective detector (Agilent Technologies, Palo Alto, CA). Trimethylsilyl-derived sterols were separated on an HP-5MS 5%-phenyl methyl polysiloxane capillary column (30-m x 0.25-mm inside diameter x 0.25- $\mu$ m film) with carrier gas helium at the rate of 1 ml/min. The temperature program was 150 °C for 2 min, followed by increasing the temperature by 20 °C per min up to 280 °C and holding it for 13 min. The injector was operated in the splitless mode and was kept at 280 °C. The mass spectrometer was operated in selective ion monitoring mode. The extracted ions were 458.4 (cholesterol), 343.3 (desmosterol), 458.4 (lathosterol), 441.4 (zymosterol), 393.4 (lanosterol), and 350.4 (7-dehydrocholesterol).

**TABLE I. Cell lines for this study**

Cell line	Description	Source
CHO-K1	Parental cells for all lines used in this study	ATCC No. CRL-9618
CHO-7	Subline of CHO-K1 cells selected for growth in lipoprotein-deficient serum	(Metherall et al., 1989)
SRD-1	Mutant CHO-7 cells that express constitutively active SREBP-2 resulting from genomic rearrangements of the <i>SREBP-2</i> gene	(Yang et al., 1994)
SRD-13A	Mutant CHO/pS2P cells deficient in SCAP. Auxotrophic for cholesterol, mevalonate, and unsaturated fatty acids	(Rawson et al., 1999)
SRD-14	Mutant CHO-7 cells lacking Insig-1	(Sever et al., 2004)
SRD-15	Mutant CHO-7 cells lacking Insig-1, and Insig-2	(Lee et al., 2005)
SRD-16	Mutant CHO/pS2P cells has point mutation in HMG CoA reductase (S60N)	(Lee et al., 2007)
SRD-17	Mutant CHO-7 cells has point mutation in HMG CoA reductase (G87R)	(Lee et al., 2007)
SRD-18	Mutant CHO-7 cells has point mutation in HMG CoA reductase (A333P)	(Lee et al., 2007)
SRD-19	Mutant CHO-7 cells lacking Insig-1, and amplified <i>SCAP</i> gene	Chapter 5.

**CHAPTER 1    ISOLATION OF MUTANT CELLS LACKING  
INSIG-1 THROUGH SELECTION WITH SR-  
12813, AN AGENT THAT STIMULATES  
DEGRADATION OF HMG-COA REDUCTASE**



## RESULTS

The experiments shown in Fig. 1-1 were designed to determine whether SR-12813 utilizes mechanisms distinct from those of sterols to accelerate degradation of reductase. SV-589 cells, a line of transformed human fibroblasts, were depleted of sterols by incubation for 16 h in medium containing LPDS, the reductase inhibitor, compactin (Brown *et al.*, 1978), and a low level of mevalonate (50  $\mu$ M), which is the lowest level that assures viability (Fig. 1-1A). Cells were then treated for an additional 5 h with various combinations of SR-12813, a high level of mevalonate (10 mM), and 30  $\mu$ M geranylgeraniol (the alcohol derivative of geranylgeranyl pyrophosphate). Following treatments, the cells were harvested and separated into membrane and nuclear extract fractions. Aliquots of the fractions were subsequently subjected to SDS-PAGE and immunoblotted with anti-reductase and anti-SREBP-2 monoclonal antibodies. In untreated cells, we observed a full-length band of reductase that remained unchanged upon treatment of the cells with SR-12813 alone (*top panel, lanes 1 and 2*). However, when cells were treated with the combination of SR-12813 and mevalonate or geranylgeraniol, reductase degradation was accelerated as indicated by the dramatic decrease in the reductase band (*top panel, lanes 4 and 6, respectively*). These results indicate that nonsterol mevalonate-derived products or geranylgeraniol can synergize with SR-12813 to accelerate degradation of reductase. Similarly, we and others have observed that these nonsterol products of mevalonate metabolism also significantly contribute to sterol-accelerated degradation of reductase (Nakanishi *et al.*, 1988; Roitelman and Simoni, 1992; Sever *et al.*, 2003a). In contrast to its effects on the degradation of reductase, SR-12813 did not alter SCAP activity, as indicated by the persistence of nuclear

SREBP-2, regardless of treatment conditions (*bottom panel, lanes 1-6*). These results indicate that SR-12813 can replace sterols to promote accelerated degradation of reductase, but the drug can not substitute for sterols in mediating ER retention of the SCAP/SREBP-2 complex. It should be noted that in this and subsequent experiments in this report, regulation of nuclear SREBP-1 mirrored that of nuclear SREBP-2 (data not shown).

In previous studies, we used RNA interference (RNAi) to demonstrate that sterol-dependent degradation and ubiquitination of endogenous reductase requires either Insig-1 or Insig-2 (Sever *et al.*, 2003a). To determine whether Insigs are required for SR-12813-dependent degradation and ubiquitination of reductase, SV-589 cells were transfected with duplexes of small interfering RNA (siRNA) targeting the control gene, vesicular stomatitis virus glycoprotein, which is not expressed in the cells, or the combination of Insig-1 and Insig-2. For degradation experiments (Fig. 1-1B), cells were treated for 5 h with 10 mM mevalonate and either sterols or SR-12813. In control transfected cells, sterols and SR-12813 accelerated the degradation of reductase (*lanes 1-3*), yet when siRNAs targeting Insig-1 and Insig-2 were introduced into the cells, both sterol- and SR-12813-dependent degradation of reductase was severely blunted (*lanes 4-6*). Similar results were obtained for reductase ubiquitination (Fig. 1-1C). For ubiquitination experiments, the cells were treated for 1 h with 10 mM mevalonate, the proteasome inhibitor MG-132, and either sterols or SR-12813. Following the incubation, the cells were harvested, lysed in detergent-containing buffer, and subjected to immunoprecipitation with polyclonal anti-reductase antibodies. Sterols and SR-12813 stimulated ubiquitination of reductase to similar levels in the control transfected cells, as indicated by the appearance of high molecular weight smears in anti-

ubiquitin immunoblots of the reductase immunoprecipitates (*lanes 1-3*). Ubiquitination of reductase was ablated when the cells received Insig-1 and Insig-2 siRNAs (*lanes 4-6*). Together, the results of Figs. 1-1*B* and *C* demonstrate that sterols and SR-12813 promote ubiquitination and degradation of reductase through a shared, Insig-dependent mechanism.

Considering that SR-12813 effectively replaces sterols for Insig-dependent regulation of reductase degradation, but not ER retention of SCAP (see Fig. 1-1), we reasoned the specificity of SR-12813 could be exploited to isolate mutant cells which no longer accelerate degradation of reductase. The experiment of Fig. 1-2, which shows a series of stained Petri dishes, was designed to determine the effects of SR-12813 on the growth of CHO-7 cells. The growth of CHO-7 cells tolerated supplementation of LPDS-containing medium with as much as 2  $\mu$ M SR-12813. However, the cells failed to proliferate when challenged with 4-10  $\mu$ M SR-12813, and growth could be restored by the addition of cholesterol (5  $\mu$ g/ml) to the culture medium. This indicates that toxicity of SR-12813 is attributable to its ability to accelerate degradation of reductase, thereby inhibiting cholesterol synthesis, and ultimately leading to cell death as a result of cholesterol depletion.

Approximately  $2.5 \times 10^7$  CHO-7 cells were mutagenized with  $\gamma$ -irradiation, and subjected to selection in 10  $\mu$ M SR-12813. The most vigorous clone was isolated, expanded, and designated SRD-14 cells. The growth assay in Fig. 1-3A shows that SRD-14 cells were resistant to growth in 10  $\mu$ M SR-12813 and up to 0.1  $\mu$ g/ml 25-HC. In contrast, the parental CHO-7 cells were effectively killed by SR-12813 and their growth exhibited a greater sensitivity (about 3-fold) to 25-HC than that of SRD-14 cells. The resistance of SRD-14 cells to SR-12813 and 25-HC indicates that in these cells, reductase is refractory to

accelerated degradation. We tested this hypothesis directly by comparing the effects of sterols and SR-12813 on reductase degradation and SREBP-2 processing in CHO-7 and SRD-14 cells (Figs. 1-3*B* and 3*C*). As shown in Fig. 1-3*B*, sterols and SR-12813 promoted the rapid degradation of reductase in parental CHO-7 cells (*top panel, lanes 2 and 3*), while the disappearance of nuclear SREBP-2 was only observed upon sterol treatment (*bottom panel, lane 2*). However, both SR-12813 and sterols failed to promote degradation of reductase and sterols did not suppress nuclear SREBP-2 in the mutant SRD-14 cells (*top and bottom panels, lanes 4-6*). SCAP appeared to be produced at approximately equivalent levels in the CHO-7 and SRD-14 cells (*second panel, lanes 1-6*). Consistent with their inability to promote reductase degradation in the mutant cells, sterols also failed to promote ubiquitination of reductase to appreciable levels (Fig. 1-3*C*, compare *lanes 1 and 2* with *3 and 4*). Thus, the inability of SRD-14 cells to carry out reductase ubiquitination and degradation explains their resistance to the growth inhibitory effects of SR-12813.

The failure of sterols to promote reductase degradation and inhibit processing of SREBP-2 indicated that SRD-14 cells are defective in a common component required for sterol-regulation of both SCAP and reductase. We reasoned that this defective component was most likely one of the Insig proteins, considering their participation in sterol regulation of both proteins. Hence, membranes from CHO-7 and SRD-14 cells were isolated and subjected to immunoblot analysis with polyclonal anti-Insig-1 antibodies (Fig. 1-4*A*). To ensure maximal expression of Insig-1, which is a target gene of SREBP-2 (Yabe *et al.*, 2002a; Yang *et al.*, 2002), the cells were incubated in sterol-depleting medium for 16 h and treated for an additional 5 h in the absence or presence of sterols prior to harvesting. Some

of the dishes of cells also received MG-132 to inhibit the activity of proteasomes. In the absence of MG-132, Insig-1 was barely detectable in the anti-Insig-1 immunoblots, regardless of the absence or presence of sterols (*lanes 1 and 2*). However, treatment of the cells with MG-132 led to the appearance of two bands at 28 kDa and 25 kDa (*lanes 3 and 4*), which likely results from the use of two start sites for translation, as has been reported for the human Insig-1 protein (Yang *et al.*, 2002). The stabilization of Insig-1 by MG-132 indicates that the protein is rapidly degraded by proteasomes. In contrast to those from CHO-7 cells, membranes from the SRD-14 cells lacked detectable Insig-1 when incubated in the absence or presence of sterols and/or MG-132 (*lanes 5-8*).

We next conducted a series of experiments designed to assess the nature of the genetic defect that leads to the absence of Insig-1 protein in SRD-14 cells. Fig. 1-4B shows a Northern blot, comparing the amounts of Insig-1 mRNA in CHO-7 and SRD-14 cells. Insig-1 mRNA was present in the parental cells when they were incubated in the absence of sterols (*lane 1*), and it declined when the cells were treated with sterols (*lane 2*), a result of the sterol-dependent suppression of nuclear SREBP-2. In contrast, Insig-1 mRNA failed to be detected in SRD-14 cells, regardless of the absence or presence of sterols (*lanes 3 and 4*). The absence of detectable Insig-1 mRNA and protein in SRD-14 cells is caused by the a partial deletion of the Insig-1 gene (data not shown). In previously identified mutant cell lines, the persistence of nuclear SREBP-2 upon 25-HC treatment was indicative of the ability of the cells to survive chronic treatment with the oxysterol (Dawson *et al.*, 1991; Hua *et al.*, 1996; Yabe *et al.*, 2002b; Yang *et al.*, 1995; Yang *et al.*, 1994). However, in the experiment of Fig. 1-3 we observed that despite their resistance to sterol-mediated suppression of nuclear

SREBP-2 (Fig. 1-3B), SRD-14 cells were only partially resistant to growth in 25-HC (Fig. 1-3A). Considering that, in Fig. 1-3B, the extent to which sterols influenced SREBP-2 processing was assessed after treating cells for 5 h, we designed an experiment to compare the kinetics of sterol-dependent suppression of SREBP-2 processing in CHO-7 and SRD-14 cells (Fig. 1-5A). In the wild type cells, we noticed that sterols suppressed nuclear SREBP-2 in 2 h (*bottom panel, lane 2*), whereas sterol treatments for 8-16 h was required to block SREBP-2 processing in SRD-14 cells (*bottom panel, lanes 13 and 14*). In parallel experiments, we measured the amounts of mRNAs encoding Insig-1, Insig-2, and three SREBP-2 target genes; HMG CoA synthase, HMG CoA reductase, and the LDL-receptor, by quantitative real-time PCR analysis and the results are presented graphically in Fig. 1-5B-F. The mRNAs encoding SREBP-2 target genes in CHO-7 cells declined with sterol treatment at rates which mirrored those of nuclear SREBP-2 suppression and again, we found the sterol response of the SRD-14 cells was markedly delayed. As expected, Insig-1mRNA was not detected in the mutant cells and exhibited a similar response to sterols as the other SREBP-2 target genes in wild type cells (Fig. 1-5B). Insig-2 mRNA was present at similar levels in CHO-7 and SRD-14 cells and remained constant throughout the time course in both cell lines (Fig. 1-5C).

We sought next to determine whether overexpression of Insig-1 or Insig-2 would restore sterol regulation of reductase ubiquitination/degradation and SREBP-2 processing after 5 h. SRD-14 cells were transfected with pCMV-Insig-1-Myc and pCMV-Insig-2-Myc, expression plasmids encoding full-length human Insig-1 and Insig-2 followed by six tandem copies of the c-Myc epitope, and clones that expressed equivalent levels of the Insig proteins

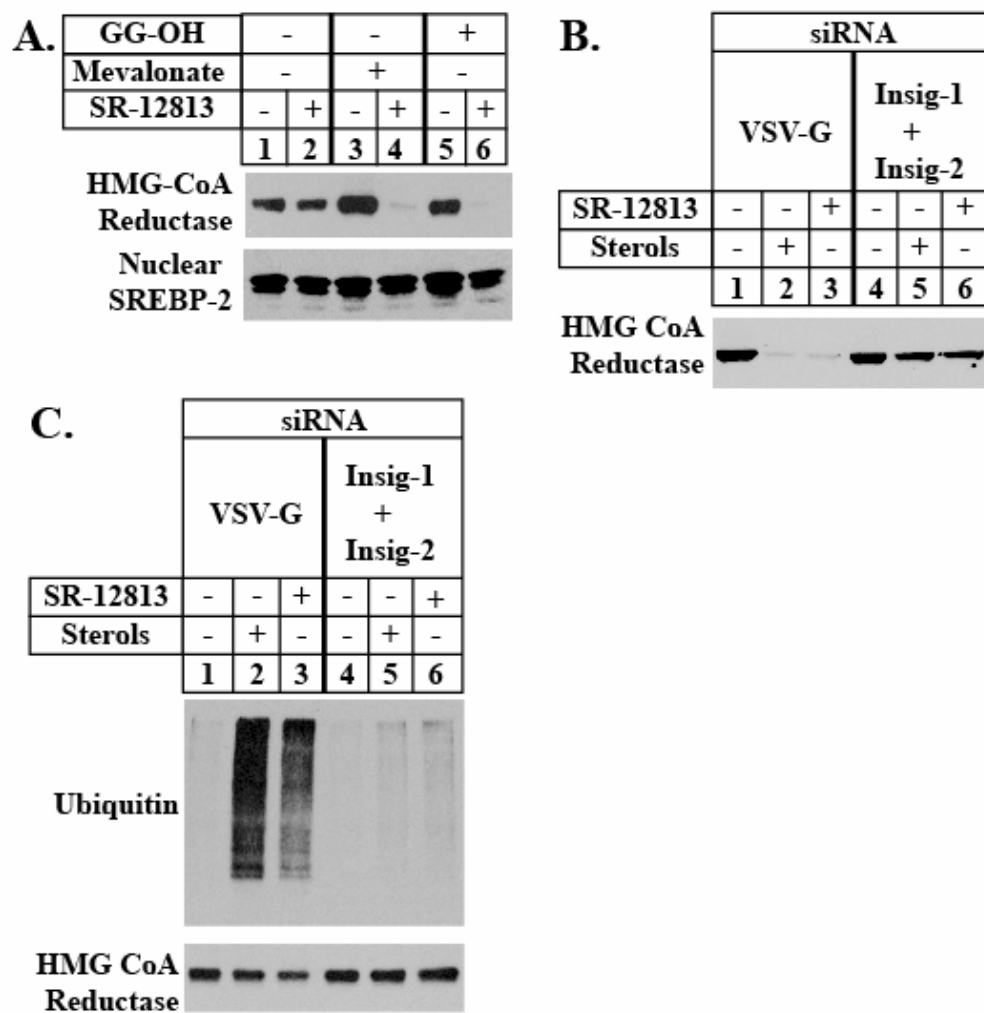
were isolated (Fig. 1-6, *bottom panel, lanes 7-12*). Fig. 1-6A shows that in CHO-7 cells, sterols and SR-12813 promoted complete degradation of reductase (*top panel, lanes 2 and 3*) and sterols fully suppressed nuclear SREBP-2 (*third panel, lane 2*). The SRD-14 cells, as expected, were resistant to both reagents (*top and third panel, lanes 4-6*). In the SRD-14 cells stably overexpressing Insig-1-Myc or Insig-2-Myc, regulated degradation of reductase and suppression of nuclear SREBP-2 was completely restored (*top three panels, lanes 7-12*). Finally, regulated ubiquitination of reductase was fully restored in the SRD-14 cells upon overexpression of Insig-1 or Insig-2 (Fig. 1-6B). Considered together, these results demonstrate that the regulatory defects exhibited by SRD-14 cells can be completely restored upon stable transfection of either Insig-1-Myc or Insig-2-Myc.

**FIGURE 1-1: SR-12813 mimics sterols in promoting Insig-dependent ubiquitination and degradation of HMG CoA Reductase.**

*A*, SV-589 cells were set up in medium B containing 10% FCS. On day 2, the cells were washed with PBS and refed medium B supplemented with 10% LPDS, 50  $\mu$ M compactin, and 50  $\mu$ M mevalonate. After 16 h at 37 °C, cells were switched to medium B containing 10% LPDS and 50  $\mu$ M compactin in the absence or presence of 10  $\mu$ M SR-12813, 10 mM mevalonate, and 30  $\mu$ M geranylgeraniol as indicated. After incubation at 37 °C for 5 h, the cells were subjected to fractionation. Aliquots of the membrane (3  $\mu$ g *protein/lane*) and nuclear extract (30  $\mu$ g *protein/lane*) were subjected to SDS-PAGE immunoblotted with IgG-A9 (Reductase) or IgG-1D2 (SREBP-2). *B* and *C*, SV-589 cells were set up in medium B with 10% FCS. On days 1 and 3, cells were transfected with 400 pmol/dish of VSV-G siRNA (*lanes 1-3*) or Insig-1 and Insig-2 siRNA (*lanes 4-6*). After the second transfection on day 3, cells were incubated for 16 h at 37 °C in medium B containing 10% LPDS, 50  $\mu$ M compactin, and 50  $\mu$ M mevalonate. On day 4, the cells were switched to medium A containing 10% LPDS, 50  $\mu$ M compactin, and 10 mM mevalonate in the absence or presence of sterols (1  $\mu$ g/ml 25-HC and 10  $\mu$ g/ml cholesterol) or 10  $\mu$ M SR-12813, as indicated. In *C*, the medium also contained 10  $\mu$ M MG-132. *B*, after 5 h at 37 °C, the cells were harvested, cell fractionation, subjected to SDS-PAGE and immunoblot analysis as in *A*. *C*, after 1 h at 37 °C, cells were harvested, lysed, and subjected to immunoprecipitation with polyclonal anti-reductase. Aliquots of immunoprecipitates were subjected to SDS-PAGE, and immunoblotted with IgG-A9 (Reductase) or IgG-P4D1 (Ubiquitin).

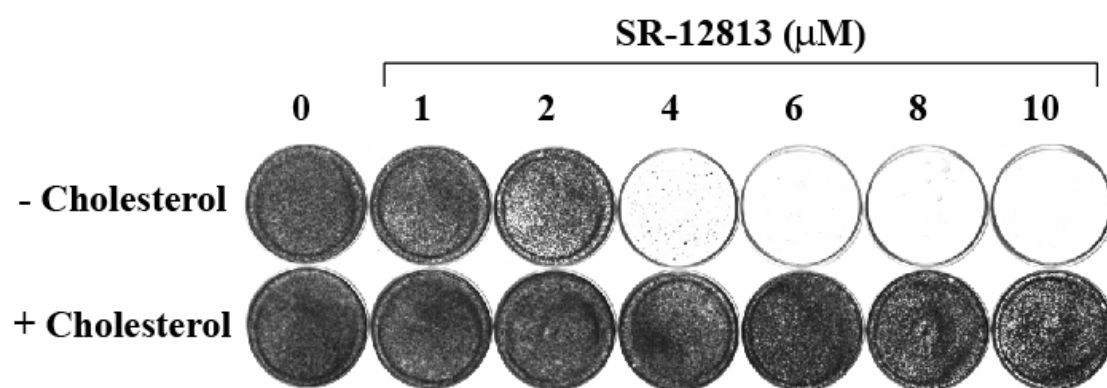


FIGURE 1-1



**FIGURE 1-2: SR-12813 mediated killing of CHO cells is prevented by cholesterol.**

CHO-7 cells were set up on day 0 at  $4 \times 10^4$  cells per 60-mm dish in medium A containing 5% LPDS. On day 1, the cells were refed medium B supplemented with 5% LPDS and the indicated concentration of SR-12813 in the absence or presence of 5  $\mu$ g/ml cholesterol. Cells were refed every 2-3 days. On day 14, the cells were washed with phosphate-buffered saline, fixed in 95% ethanol, and stained with crystal violet.

**FIGURE 1-2**

**FIGURE 1-3: Comparison of growth, HMG CoA Reductase degradation/ubiquitination, and SREBP processing in parental CHO cells and SRD-14 cells treated with sterols and SR-12813.**

*A*, CHO-7 and SRD-14 cells were set up in medium A containing 5% LPDS. On day 1, the cells were refed medium A supplemented with 5% LPDS and 10  $\mu$ M SR-12813 or the indicated concentration of 25-HC. Cells were refed every 2-3 days. On day 14, the cells were washed, fixed in 95% ethanol, and stained with crystal violet. *B* and *C*, On day 2, the cells were refed medium B supplemented with 5% LPDS, 10  $\mu$ M compactin, and 50  $\mu$ M mevalonate. *B*, after 16 h at 37 °C, cells were switched to medium A containing 5% LPDS and 50  $\mu$ M compactin in the absence or presence of either sterols (1  $\mu$ g/ml 25-HC and 10  $\mu$ g/ml cholesterol) or 10  $\mu$ M SR-12813 plus 10 mM mevalonate as indicated. After incubation at 37 °C for 5 h, the cells were harvested and subjected to cell fractionation. Aliquots of the membrane (5-32  $\mu$ g *protein/lane*) and nuclear extract fractions (33  $\mu$ g *protein/lane*) were subjected to SDS-PAGE, and immunoblot analysis with IgG-A9 (Reductase), IgG-R139 (SCAP), or IgG-7D4 (SREBP-2). *C*, after 16 h at 37 °C, cells were switched to medium A containing 5% LPDS, 50  $\mu$ M compactin, and 10  $\mu$ M MG-132 in the absence or presence of sterols (1  $\mu$ g/ml 25-HC and 10  $\mu$ g/ml cholesterol) plus 10 mM mevalonate as indicated. After 2 h, the cells were harvested, lysed, and subjected sequentially to immunoprecipitation and immunoblot analysis with IgG-A9 (Reductase) or IgG-P4D1 (Ubiquitin).

FIGURE 1-3

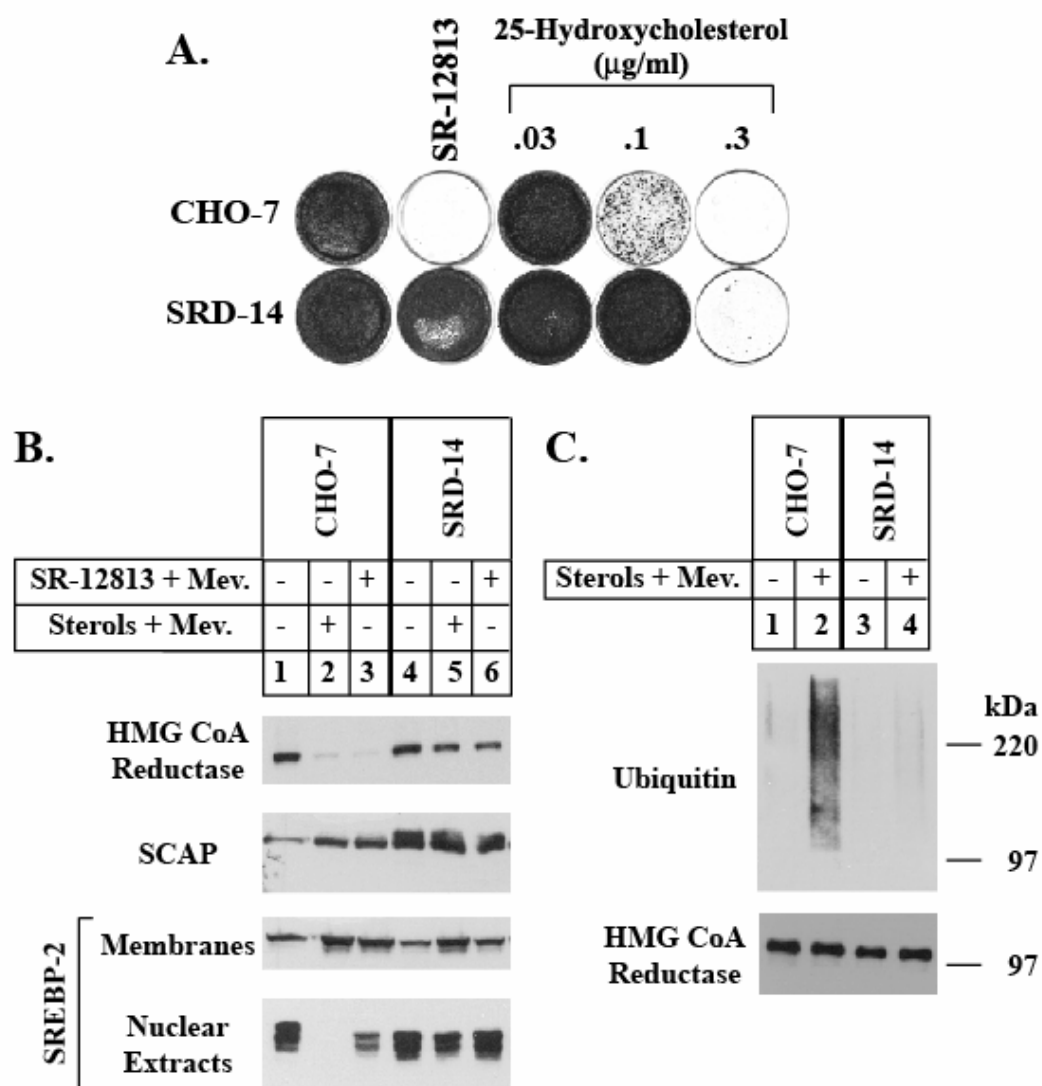


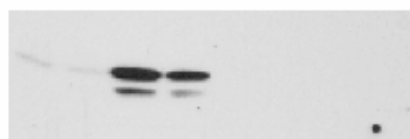
**FIGURE 1-4: Immunoblot analysis and molecular characterization of Insig-1 mRNA in parental CHO and mutant SRD-14 cells.**

*A* and *B*, CHO-7 and SRD-14 cells were set up in medium A containing 5% LPDS. On day 2, the cells were refed medium A supplemented with 5% LPDS, 10  $\mu$ M compactin, and 50  $\mu$ M mevalonate. After 16 h at 37 °C, cells were switched to medium A containing 5% LPDS and 50  $\mu$ M compactin in the absence or presence of sterols (1  $\mu$ g/ml 25-HC and 10  $\mu$ g/ml cholesterol) as indicated. After incubation at 37 °C for 5 h, the cells were harvested, subjected to cell fractionation, and aliquots of the membrane fraction (30  $\mu$ g *protein/lane*) were subjected to SDS-PAGE and immunoblot analysis with a 1:1000 dilution of polyclonal anti-Insig-1. *B*, following incubation at 37 °C for 5 h, the cells were harvested and total RNA was isolated. Aliquots of total RNA (20  $\mu$ g/*lane*) were subjected to electrophoresis in a denaturing (formaldehyde) gel and transferred to a nylon filter by capillary blotting. The filter was hybridized with a 796-bp  $^{32}$ P-labeled probe encoding the open reading frame of Insig-1. The filter was exposed to film at -80 °C for 16 h.

FIGURE 1-4

**A. Western Blot**

		CHO-7				SRD-14			
MG-132		-		+		-		+	
Sterols		-	+	-	+	-	+	-	+
		1	2	3	4	5	6	7	8

**B. Northern Blot**

		CHO-7		SRD-14	
Sterols + Mev.		-	+	-	+
		1	2	3	4

Insig-1

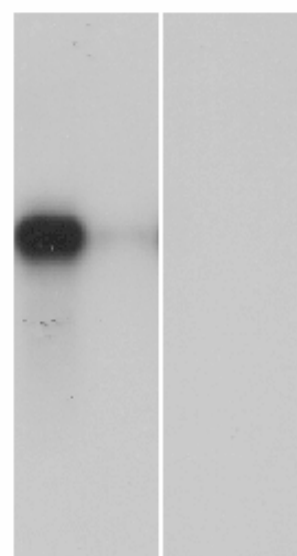
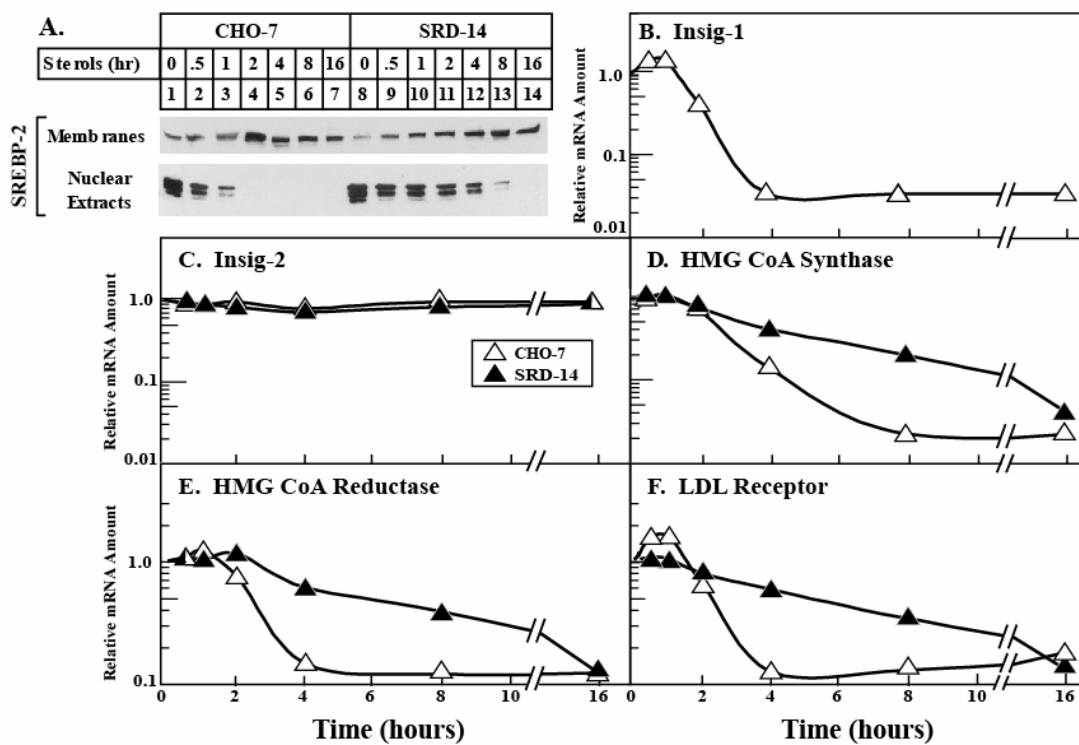


**FIGURE 1-5: Kinetics of sterol-mediated suppression of nuclear SREBP-2 and SREBP-target gene expression in parental CHO and mutant SRD-14 cells.**

CHO-7 and SRD-14 cells were set up in medium A containing 5% LPDS. On day 2, the cells were refed medium B supplemented with 5% LPDS, 50  $\mu$ M compactin, and 50  $\mu$ M mevalonate. Some of the cells were refed the same media supplemented with a mixture of 25-HC (1  $\mu$ g/ml) and cholesterol (10  $\mu$ g/ml) for the indicated period of time. Sterols were added in a staggered fashion, such that all of the cells could be harvested together. *A*, after incubation, the cells were harvested, subjected to cell fractionation and aliquots of the membrane (34  $\mu$ g *protein/lane*) and nuclear extract (13  $\mu$ g *protein/lane*) fractions were subjected to SDS-PAGE. Immunoblot analysis was subsequently carried out as described in the legend to Fig. 1-3. *B-F*, following incubations, the cells were harvested and total RNA was isolated and subjected to reverse transcription. Aliquots of reverse-transcribed total RNA were then subjected to real-time PCR analysis using primers specific for the indicated SREBP-2 target gene. Each value for cells incubated with sterols for the indicated time represents the amount of target gene expression relative to that in control cells harvested at time 0. The values for Insig-2 mRNA in the cells represent its expression relative to that in wild type cells harvested at time 0.

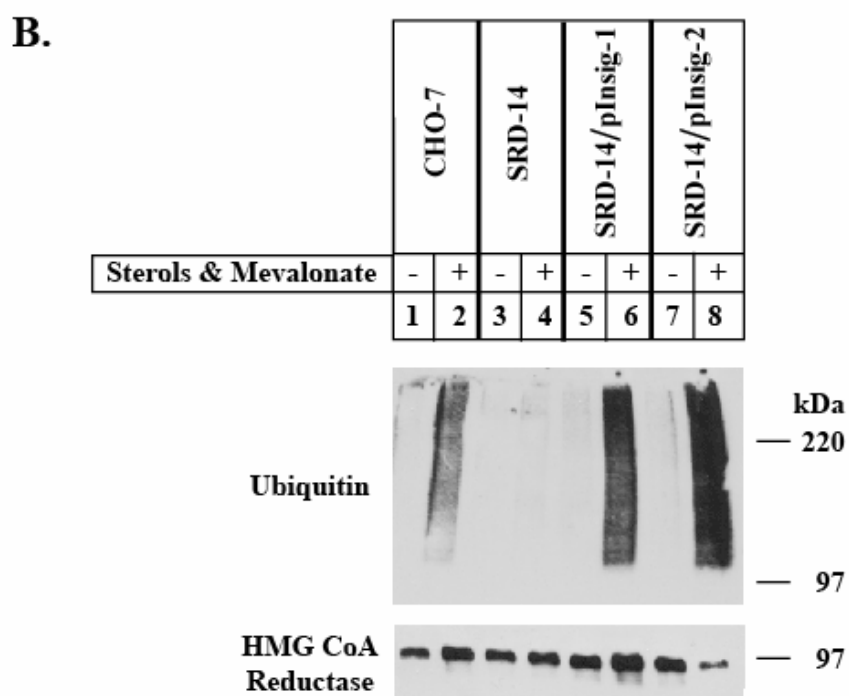
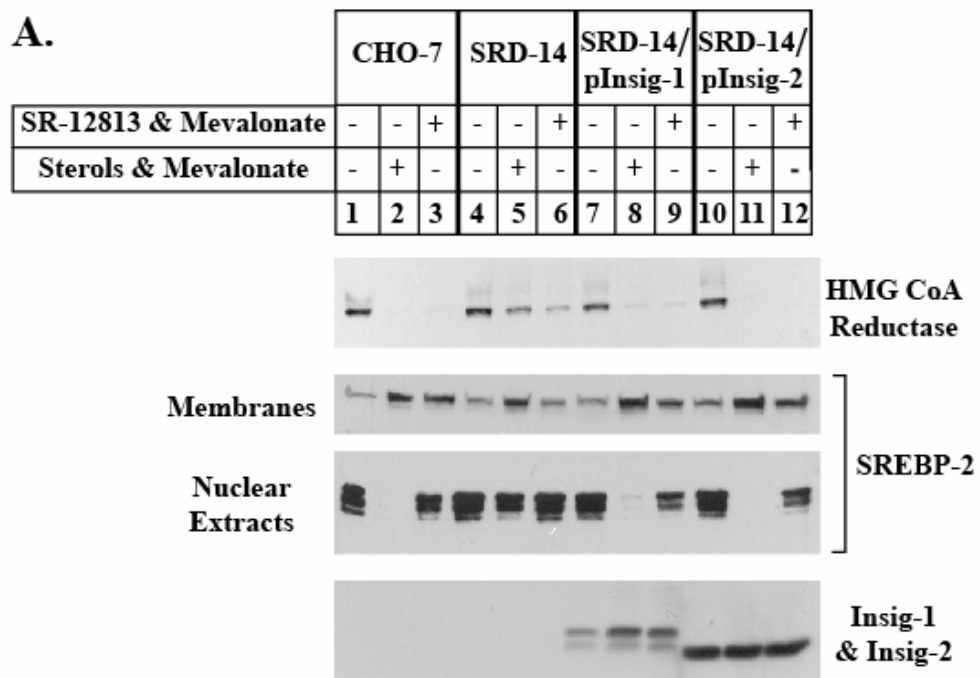


FIGURE 1-5



**FIGURE 1-6: Stable transfection of SRD-14 cells with pCMV-Insig-1-Myc or pCMV-Insig-2-Myc restores regulation of HMG CoA Reductase degradation/ ubiquitination and SREBP-2 processing mediated by sterols and SR-12813.**

CHO-7, SRD-14, SRD-14/pInsig-1, and SRD-14/pInsig-2 cells were set up in medium A containing 5% LPDS. On day 2, the cells were switched to medium B supplemented with 5% LPDS, 10  $\mu$ M compactin, and 50  $\mu$ M mevalonate. *A*, after 16 h at 37 °C, the cells were switched to medium B containing 5% LPDS and 50  $\mu$ M compactin in the absence or presence of sterols (1  $\mu$ g/ml 25-HC and 10  $\mu$ g/ml cholesterol) or 10  $\mu$ M SR-12813 plus 10 mM mevalonate, as indicated. In *C*, the medium also contained 10  $\mu$ M MG-132. Following incubation at 37 °C for 5 h, the cells were harvested, subjected to cell fractionation and aliquots of the membrane (4-50  $\mu$ g *protein/lane*) and nuclear extract (11-27  $\mu$ g *protein/lane*) fractions were subjected to SDS-PAGE. Immunoblot analysis with IgG-A9 (Reductase), IgG-7D4 (SREBP-2), and IgG-Myc (Insig-1 and Insig-2). *B*, after incubation for 2 h at 37 °C, cells were harvested, lysed, and sequentially subjected to immunoprecipitation, SDS-PAGE, and immunoblot analysis with IgG-A9 (Reductase) or IgG-P4D1 (Ubiquitin).

**FIGURE 1-6**

## DISCUSSION

The data presented in the current chapter describe the isolation and characterization of a new line of mutant CHO cells, designated SRD-14, resistant to chronic selection with the 1,1-bisphosphonate ester, SR-12813. We chose to select mutagenized CHO-7 cells with SR-12813 for several reasons. 1) SR-12813 replaced sterols in promoting Insig-dependent degradation and ubiquitination of reductase, but not ER retention of the SCAP/SREBP-2 complex (Fig. 1-1). 2) CHO-7 cells failed to grow in the presence of SR-12813, and this was overcome by the addition of exogenous cholesterol to the growth medium (Fig. 1-2A). 3) SR-12813 did not influence the stability of degradation-resistant mutant forms of reductase and consequently, the drug failed to kill cells that expressed the mutant, but not the wild type form of full-length reductase (data not shown). The mutant cells that survived SR-12813 selection did so because they failed to accelerate degradation of reductase (Fig. 1-3B and C), owing to the absence of Insig-1 mRNA and protein that resulted from a partial deletion of the Insig-1 gene (data not shown). SRD-14 and 7 other lines of Insig-1-deficient cells were produced from a single round of mutagenesis of approximately  $2.5 \times 10^7$  CHO-7 cells, followed by selection in SR-12813. The repeated isolation of Insig-1-deficient cells in our experiments indicates that CHO-7 cells may only have one functional copy of the Insig-1 gene, thus a single mutagenic event can destroy the single copy of the Insig-1 gene, leading to Insig-1 deficiency. The failure of SRD-14 cells to degrade reductase in response to SR-12813 or sterols appears to result from their deficiency in total Insig. This is indicated by the restoration of regulated ubiquitination and degradation of reductase upon overexpression of either Insig-1-Myc or Insig-2-Myc in the SRD-14 cells (Fig. 1-6).

The growth of SRD-14 cells in SR-12813 indicates that Insig-2 alone cannot carry out reductase degradation, whereas their inability to grow in the presence of 25-HC suggests that regulation of SREBP processing must be intact upon prolonged sterol treatment (Fig. 1-3A). Thus, we compared the kinetics of sterol-dependent suppression of SREBP-2 processing in parental CHO-7 and mutant SRD-14 cells (Figs. 1-5). In the parental cells, sterols rapidly suppressed SREBP-2 processing and mRNAs encoding Insig-1 and other SREBP-2 target genes fell accordingly. In the absence of sterols, we approximate that Insig-1 expression exceeds that of Insig-2 by 10-fold in CHO cells, thus 90% of total Insig is susceptible to sterol-dependent suppression. As expected, Insig-2 alone mediated sterol suppression of SREBP-2 processing in SRD-14 cells, although at a slower rate than wild type cells. Thus, it appears that cells require their total complement of Insigs to carry out sterol-accelerated degradation of reductase, whereas sterol suppression of SREBP processing can occur at lower Insig levels. These results are consistent with those we obtained with RNAi experiments, where transient knockdown of Insig-1 and Insig-2 blocked sterol-accelerated degradation of reductase, but sterol-mediated suppression of SREBP processing remained intact (data not shown). This disparity may reflect differences in the affinities of reductase and SCAP for sterols and/or Insigs. Finally, stable overexpression of Insig-1 or Insig-2 in SRD-14 cells restored the rapid suppression of SREBP processing (Fig. 1-6), thus reflecting the redundant role of the two proteins in mediating sterol regulation of SREBP as well as reductase.

Taken together, the current results provide compelling genetic evidence for the important role Insig-1 plays in mediating two distinct sterol-regulated reactions: ER

retention of SCAP and accelerated degradation of reductase. In addition, these data substantiate previous reasoning for the existence of two Insig isoforms (Yabe *et al.*, 2002a). In wild type, sterol-deprived cells, SCAP readily enters budding vesicles, en route to carrying SREBP to the Golgi for proteolytic processing, and reductase is stable and produces mevalonate. In the nucleus, the processed SREBPs activate transcription of genes encoding cholesterol biosynthetic enzymes (including reductase), resulting in a rise in the synthesis of sterols. The combination of sterols and Insig-1 prevents translocation of SCAP to the Golgi, resulting in the decline of SREBP processing, and promotes accelerated degradation of reductase. In the absence of nuclear SREBPs, Insig-1 levels diminish and over time, the level of SCAP should eventually exceed that of Insig-1, permitting its escape from the ER to activate processing of SREBPs.

The analysis of SREBP processing in SRD-14 cells indicates that because of its constitutive, SREBP-independent expression, Insig-2 prevents the escape of SCAP from the ER in cells replete with sterols. We reason that sterols synthesized prior to the fall of Insig-1 sensitize the system such that Insig-2 is sufficient to block SCAP transport and maintain suppression of SREBP processing as long as intracellular sterols remain high. Considering that under conditions of sterol-deprivation Insig-1 accounts for 90% of total Insigs, the ability of SREBPs to modulate levels of its inhibitor provides a reset mechanism which permits cells to rapidly modulate SREBP processing according to their demands for sterols. When cellular sterols are high, Insig-2 is the only form of Insig present, thus the cells can respond rapidly to cholesterol depletion. On the other hand, when SREBPs are actively processed, the Insig-1

gene is activated, and the increase in total Insigs primes the cells for rapid suppression when sterol levels rise.

In conclusion, the analysis of regulated SREBP processing and accelerated degradation of reductase in the Insig-1-deficient SRD-14 cells has revealed an interesting circuitry underlying sterol regulation; however, the complete resolution of this unique regulatory system requires the availability of Insig-2 deficient cells, as well as cells lacking both Insig-1 and Insig-2.

**CHAPTER 2    ISOLATION    OF    STEROL-RESISTANT  
CHINESE HAMSTER OVARY CELLS WITH  
GENETIC DEFICIENCIES IN BOTH INSIG-1  
AND INSIG-2**



## RESULTS

The oxysterol 25-HC blocks cholesterol synthesis through its potent ability to simultaneously inhibit SREBP processing and stimulate the ubiquitination and degradation of reductase. In the absence of exogenous cholesterol, the continual culture of normal cells in 25-HC is toxic because the oxysterol blocks the synthesis of cholesterol, but cannot replace the structural function of cholesterol in cellular membranes. Thus, to isolate mutant cells deficient in both Insig-1 and Insig-2, we began by mutagenizing approximately  $2.5 \times 10^7$  Insig-1-deficient SRD-14 cells with  $\gamma$ -irradiation and subjecting them to chronic selection in 25-HC. The most vigorous clone of mutagenized cells proliferated in 1.25  $\mu$ M 25-HC, a concentration previously determined to completely inhibit growth of SRD-14 cells as well as wild-type cells (Sever *et al.*, 2004). The resistant clone was isolated, expanded, and designated SRD-15 cells. Fig. 2-1 shows an experiment in which we compared the growth of wild-type and mutant cells in medium supplemented with lipoprotein-deficient serum and various concentrations of 25-HC. Wild-type cells were efficiently killed in medium containing 0.25  $\mu$ M 25-HC, whereas higher concentrations (0.75  $\mu$ M) of the oxysterol were required to block growth of the SRD-14 cells. In contrast, SRD-15 cells were resistant to culture in 25-HC at concentrations as high as 2.5  $\mu$ M. Considering that growth of cells in medium containing lipoprotein-deficient serum renders them dependent upon endogenous cholesterol synthesis for survival (Metherall *et al.*, 1989), the resistance of SRD-15 cells to culture in 25-HC indicates that the cells do not suppress cholesterol synthesis in response to oxysterol treatment.

In Chapter 1, we found that sterols blocked the accumulation of nuclear SREBPs in SRD-14 cells only after prolonged treatment (up to 16 h) (Sever *et al.*, 2004). In light of this, we compared the sterol regulation of SREBP processing in wild-type CHO-7, Insig-1-deficient SRD-14, and SRD-15 cells (Fig. 2-2). We depleted the cells of sterols by incubating them in medium containing lipoprotein-deficient serum, the reductase inhibitor compactin (Brown *et al.*, 1978), and the lowest level of mevalonate (50  $\mu$ M) that ensures viability. Some of the cells also received various concentrations of 25-HC. After 5 h or 16 h, the cells were harvested, separated into membrane and nuclear extract fractions, and aliquots of the fractions were subjected to SDS-PAGE. Subsequently, immunoblot analysis of the fractions was carried out with anti-SREBP-1 (Fig. 2-2A, *top panel*) and anti-SREBP-2 (Fig. 2-2A, *bottom panel*) antibodies. In untreated cells, bands corresponding to the processed, nuclear forms of SREBP-1 and SREBP-2 were observed at the 5 h and 16 h time points (*top and bottom panels, lanes 1, 5, 9, 13, 17, and 21*). In CHO-7 cells, 25-HC caused the disappearance of both nuclear SREBP-1 and SREBP-2 in a dose-dependent manner after 5 h and 16 h of treatment (*top and bottom panels, lanes 2-4 and 14-16*). After 5 h of treatment, 25-HC did not appreciably reduce nuclear SREBP-1 and SREBP-2 levels in either SRD-14 or SRD-15 cells (*top and bottom panels, lanes 6-8; 10-12*). At the 16 h time point, 25-HC completely blocked processing of both SREBPs in CHO-7 and SRD-14 cells (*lanes 14-16; 18-20*), whereas SREBP processing in the SRD-15 cells was fully resistant to oxysterol-mediated suppression (*top and bottom panels, lanes 22-24*).

In addition to inhibition by 25-HC, SREBP processing is inhibited by high concentrations of cholesterol added in MCD (Adams *et al.*, 2004). The experiment of Fig. 2-

2B shows that SRD-15 cells are resistant to cholesterol as well as 25-HC. When delivered to CHO-7 cells as complexes with MCD, 25-HC at 2.5  $\mu$ M and cholesterol at 25  $\mu$ M inhibited accumulation of nuclear SREBP-2 (*lanes 3, 4, and 7*), whereas no such effect was seen in SRD-15 cells (*lanes 10, 11, and 14*).

We next compared the steady state levels of endogenous reductase and nuclear SREBP-2 in CHO-7 and SRD-15 cells incubated in LPDS with or without compactin supplementation for 16 h. Immunoblotting membranes with anti-reductase revealed that in the absence of compactin, the steady state level of reductase was low in wild-type CHO-7 cells (Fig. 2-3A, *top panel, lane a*), and this rose with compactin treatment in a dose-dependent fashion (*lanes b-d*). This finding is consistent with previous observations which demonstrated that blocking mevalonate metabolism reduces regulatory molecules that normally govern the reductase regulatory system, resulting in a compensatory increase of the enzyme in ER membranes (Kita *et al.*, 1980). In untreated SRD-15 cells, the steady-state levels of reductase were equal to that of compactin-treated CHO-7 cells (compare *lanes d* and *e*) and failed to be increased by compactin (*lanes f-h*). Nuclear SREBP-2 followed a similar pattern to that of reductase (*bottom panel*). Compactin treatment led to an increased nuclear accumulation of SREBP-2 in the wild-type cells (*lanes a-d*), whereas the drug had no effect on the elevated levels of nuclear SREBP-2 in SRD-15 cells (*lanes e-h*). In parallel experiments, we isolated total RNA from the treated cells and measured the levels of mRNAs for SCAP, reductase, HMG CoA synthase, and the LDL-receptor by quantitative real-time PCR. As expected, SCAP mRNA was constant in CHO-7 and SRD-15 cells, regardless of the absence or presence of compactin. In CHO-7 cells, compactin treatment led to a dose-

dependent increase in the expression reductase, HMG CoA synthase, and LDL-receptor mRNAs. These mRNAs were somewhat elevated to varying degrees in SRD-15 cells, but compactin had no effect on their expression.

In the experiment of Fig. 2-3B, we compared the rate of reductase synthesis in CHO-7 and SRD-15 cells. Following incubation for 16 h in the absence or presence of compactin, the cells were pulse-labeled with a mixture of  $^{35}\text{S}$ -methionine plus cysteine for increasing periods of time, after which they were harvested, lysed in detergent-containing buffer, and immunoprecipitated with polyclonal antibodies against reductase. CHO-7 (*lanes a-e; k-o*) and SRD-15 (*lanes f-j; p-t*) cells incorporated  $^{35}\text{S}$ -radioactivity into reductase protein in a similar manner that increased with time. Notably, quantification of the gels revealed that the rate of reductase synthesis was marginally higher in the SRD-15 cells than in CHO-7 cells.

The experiment of Fig. 2-3C was designed to compare the rate of sterol-regulated turnover of reductase in CHO-7 and SRD-15 cells. Cells were depleted of sterols for 16 h by incubating them in LPDS containing compactin. Subsequently, the cells were pulse-labeled for 30 min with  $^{35}\text{S}$ -methionine, after which they were washed and switched to medium containing an excess of unlabeled methionine and cysteine in the absence of sterols plus high levels (10 mM) of mevalonate (Sever *et al.*, 2003a). In the absence of sterols, the amount of  $^{35}\text{S}$ -labeled reductase in CHO-7 cells declined during the 6 h chase period (*lanes b, d, and f*), and this decline was accelerated by the addition of sterols plus mevalonate to the chase medium (*lanes c, e, and g*). In contrast, accelerated degradation of reductase was refractory to sterol regulation in SRD-15 cells, as indicated by the identical rate of decline in radiolabeled reductase in the absence or presence of sterols plus mevalonate (*lanes i-n*).

The failure of SRD-15 cells to respond to 25-HC and cholesterol suggested that these cells were deficient in Insig-2 as well as Insig-1. To test this hypothesis, we pretreated CHO-7, SRD-14, and SRD-15 cells in the absence and presence of sterols for 16 h (Fig. 2-4A) and isolated total RNA. Northern blotting with a radiolabeled Insig-1 cDNA probe revealed the presence of Insig-1 mRNA in untreated CHO-7 cells (*top panel, lane 1*) which declined when the cells were treated with sterols (*lane 2*), a result of the sterol-dependent reduction in nuclear SREBPs. As expected, Insig-1 was not detected in SRD-14 and SRD-15 cells (*lanes 3-6*). CHO-7 and SRD-14 cells expressed approximately equivalent levels of Insig-2 mRNA, regardless of sterol treatment (*middle panel, lanes 1-4*). However, the level of Insig-2 mRNA in SRD-15 cells was markedly reduced in comparison to that in the parental SRD-14 and wild-type CHO-7 cells (*lanes 5-6*). To quantify the amount of Insig-2 mRNA remaining in SRD-15 cells, we subjected total RNA to reverse transcription reactions and quantitative real-time PCR analysis (Fig. 2-4B). Consistent with the observation in Fig. 2-4A, Insig-1 mRNA was only detected in wild-type CHO-7 cells and its level was suppressed by sterols. The mRNAs encoding reductase, HMG CoA synthase, and LDL-receptor were similarly suppressed by sterols in CHO-7 and SRD-14 cells, but not in the SRD-15 cells. Insig-2 mRNA was present in the CHO-7 and SRD-14 cells at approximately equivalent levels. However, in the SRD-15 cells, Insig-2 mRNA was reduced to less than 20% of that in CHO-7 and SRD-14 cells. The Insig-2 mRNA that remained in the SRD-15 cells had a normal sequence as shown by cDNA cloning and sequencing. We also observed an 80% decrease of Insig-2 mRNA in 18 independent isolates from the mutagenesis experiment that yielded

SRD-15 cells. Moreover, this phenotype of the SRD-15 cells has been determined to be stable over a 6-month period.

The finding of some normal Insig-2 mRNA in SRD-15 cells indicates that at least one copy of the gene is intact. To determine whether the other copy of the Insig-2 gene is deleted or rearranged, we subjected genomic DNA isolated from SRD-14 and SRD-15 cells to Southern blot analysis (Fig. 2-4C). Restriction enzyme digested DNA from SRD-14 and SRD-15 cells was hybridized with four radiolabeled probes corresponding to: 1) the entire open reading frame of Insig-2 (nucleotides 1-678, *lanes 1-6*); 2) nucleotides 1-216 of the Insig-2 cDNA (*lanes 7-12*); 3) nucleotides 217-678 of the Insig-2 cDNA (*lanes 13-18*); and 4) nucleotides 1-697 of the SCAP cDNA (*lanes 19-24*) as a loading control. All of the bands observed in SRD-14 cells were also observed in SRD-15 cells and no novel bands appeared in the SRD-15 digests (*lanes 1-18*). However, the intensity of several bands was reduced in the SRD-15 digests in comparison to identical digests of SRD-14 genomic DNA, indicating that one copy of the Insig-2 gene has undergone a partial deletion. The other copy is presumably intact, but its transcription is somehow compromised. The net result is an 80% reduction in Insig-2 mRNA.

We sought next to determine whether overexpression of Insig-1 or Insig-2 would restore sterol regulation of SREBP-2 processing after 5 h and 16 h treatments (Fig. 2-5). SRD-15 cells were transfected with pCMV-Insig-1-Myc and pCMV-Insig-2-Myc, expression plasmids encoding full-length human Insig-1 and Insig-2 followed by six tandem copies of the c-Myc epitope. We isolated clones that expressed equivalent levels of the Insig proteins (*bottom panel, lanes 1-12*). As expected, processing of SREBP-2 in the SRD-15 cells was

fully resistant to sterols after 5 h or 16 h treatments (*top panel, lanes 1-2*). Overexpression of Insig-1 or Insig-2 in SRD-15 cells restored a full response to sterols at both time points (*lanes 3-6*). Overexpression of either Insig in SRD-15 cells also restored sterol-mediated suppression of SREBP-1 processing (data not shown).

We next determined whether sterol-dependent ubiquitination and degradation of reductase was restored by the overexpression of Insig-1 or Insig-2 in SRD-15 cells (Fig. 2-6). In the experiment of Fig. 2-6A, sterol-depleted cells were incubated for 5 h with sterols and 10 mM mevalonate, after which the cells were harvested, subjected to fractionation, and aliquots of the membrane fractions were immunoblotted with anti-reductase. In the SRD-15 cells, reductase was refractory to sterol-accelerated degradation (*top panel, lanes 1 and 2*). Overexpression of either Insig-1-Myc or Insig-2-Myc restored rapid degradation of the enzyme (*lanes 3-6*). To assay reductase ubiquitination, sterol-depleted cells were treated for 1 h with sterols and the proteasome inhibitor MG-132 to prevent degradation of ubiquitinated reductase. The cells were harvested, lysed, and subjected to immunoprecipitation with polyclonal anti-reductase antibodies. After electrophoresis of the immunoprecipitates, the membranes were blotted with antibodies against reductase or ubiquitin (Fig. 2-6B). Sterols stimulated ubiquitination of reductase in CHO-7 cells as indicated by the appearance of high molecular weight smears in the anti-ubiquitin immunoblots of the reductase immunoprecipitates (*top panel, compare lanes 1 and 2*). As expected, reductase ubiquitination was not stimulated by sterols in the SRD-14 or SRD-15 cells (*lanes 3-6*). Ubiquitination of reductase was restored in the SRD-15 cells when they overexpressed either Insig-1 or Insig-2 (*lanes 7-10*).

**FIGURE 2-1: Growth of parental and mutant cells in the absence and presence of 25-HC.**

CHO-7, SRD-14, SRD-1, and SRD-15 cells were set up medium A supplemented with 5% LPDS. On day 1, the cells were washed with PBS and refed medium A supplemented with 5% LPDS and the indicated concentration of 25-HC. Cells were refed every 2 days. On day 10, the cells were washed, fixed in 95% ethanol, and stained with crystal violet.



FIGURE 2-1

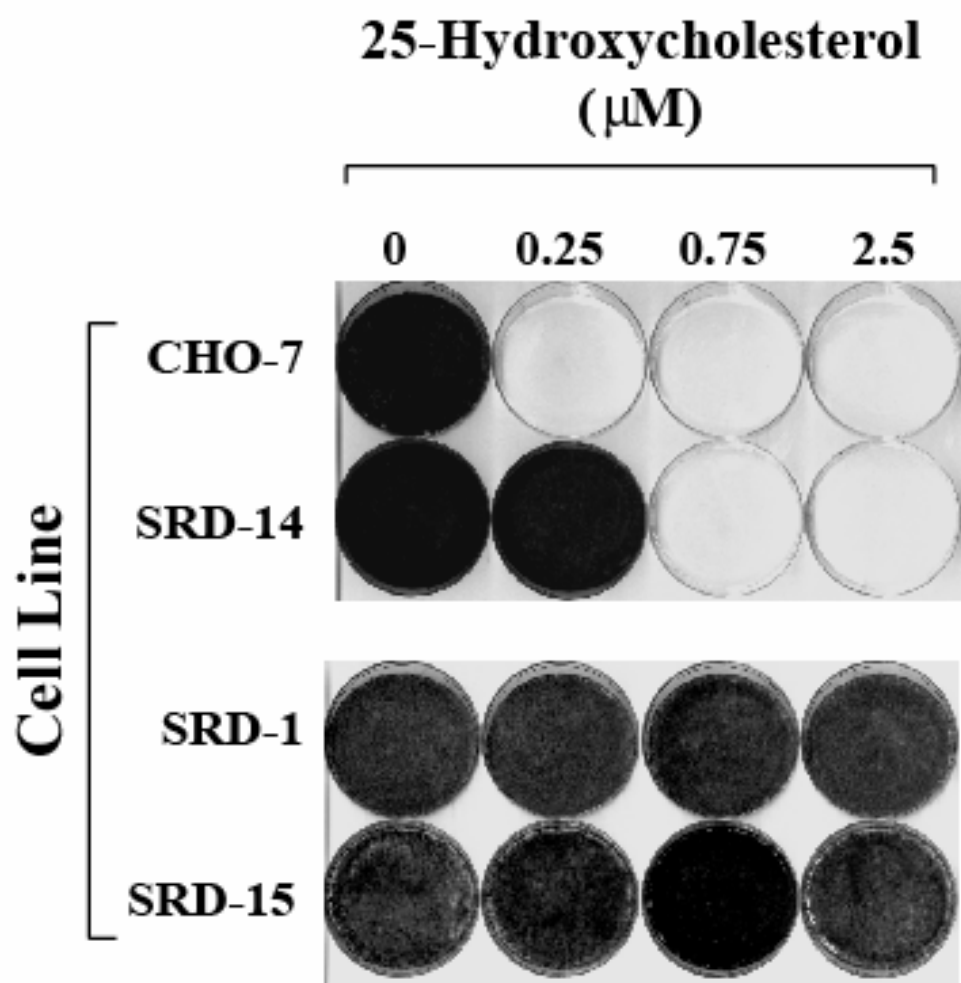


**FIGURE 2-2: Proteolytic processing of SREBPs is refractory to sterol regulation in SRD-15 cells.**

*A*, CHO-7, SRD-14, and SRD-15 cells were set up in medium A supplemented with 5% LPDS. On day 2, the cells were refed medium A containing 5% LPDS, 10  $\mu$ M sodium compactin, and 50  $\mu$ M sodium mevalonate. Some of the cells received the same medium supplemented with the indicated concentration of 25-HC. Sterols were added to the cells in a staggered fashion, such that all of the cells could be harvested together after incubations for 5 or 16 h at 37 °C. After the incubations, the cells were harvested and subjected to cell fractionation. Aliquots of the membrane (40  $\mu$ g protein/lane) and nuclear extract (32  $\mu$ g protein/lane) fractions were subjected to SDS-PAGE, and immunoblot analysis with IgG-2179 (SREBP-1) or IgG-7D4 (SREBP-2). *B*, CHO-7 and SRD-15 cells were set up and refed as in *A*. On day 3, the cells were incubated for 1 h in medium A supplemented with 5% LPDS, 50  $\mu$ M compactin, 50  $\mu$ M mevalonate, and 1% (w/v) HPCD. Subsequently, the cells were washed with PBS and subjected to an additional 6 h incubation at 37 °C in medium A containing 5% LPDS, 50  $\mu$ M compactin, 50  $\mu$ M mevalonate, and the indicated concentration of 25-HC (lanes 1–4, 8–11) or cholesterol (lanes 5–7, 12–14) complexed with MCD. Following the incubation, the cells were harvested and subjected to cell fractionation and immunoblot analysis as in *A*.

FIGURE 2-2

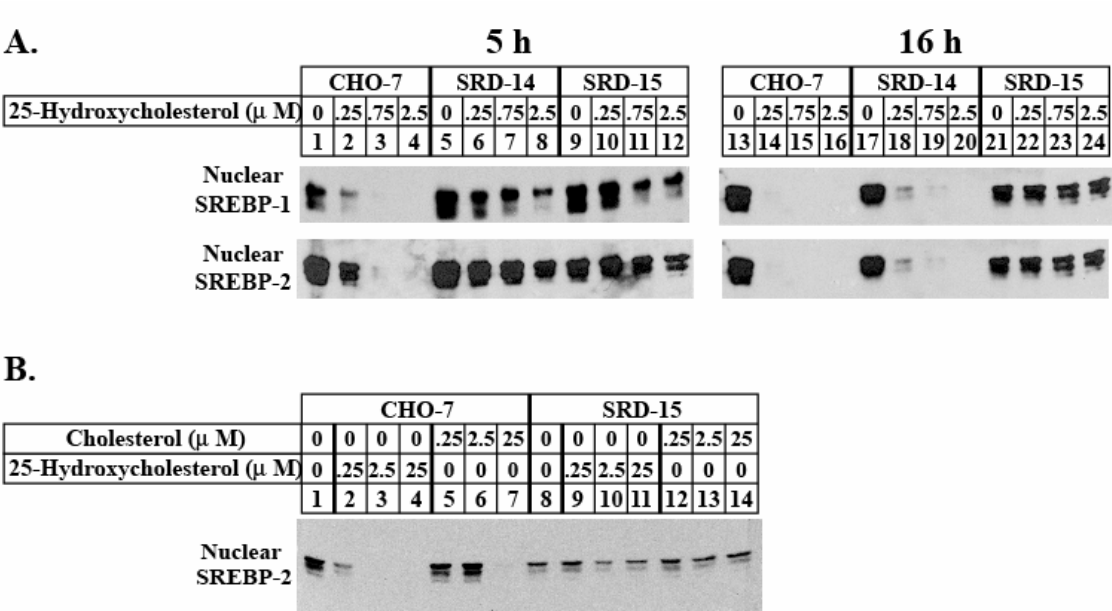
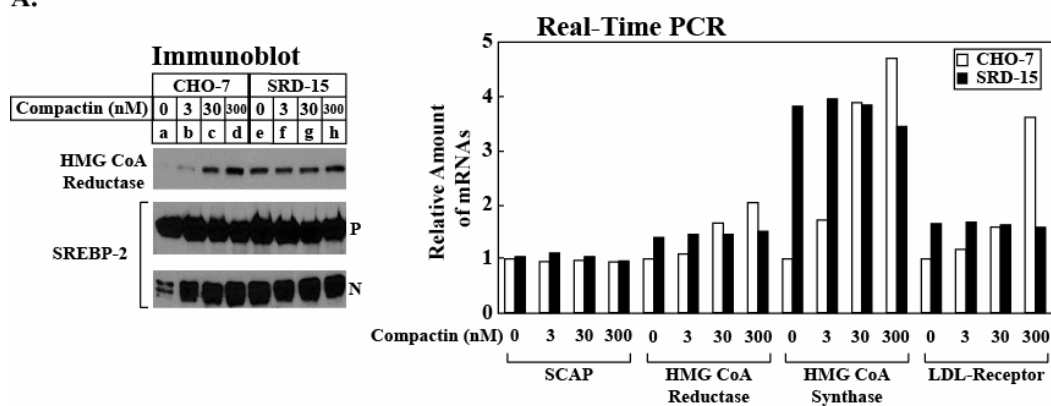


**FIGURE 2-3: Comparison of HMG CoA Reductase synthesis and sterol-regulated turnover in CHO-7 and SRD-15 cells.**

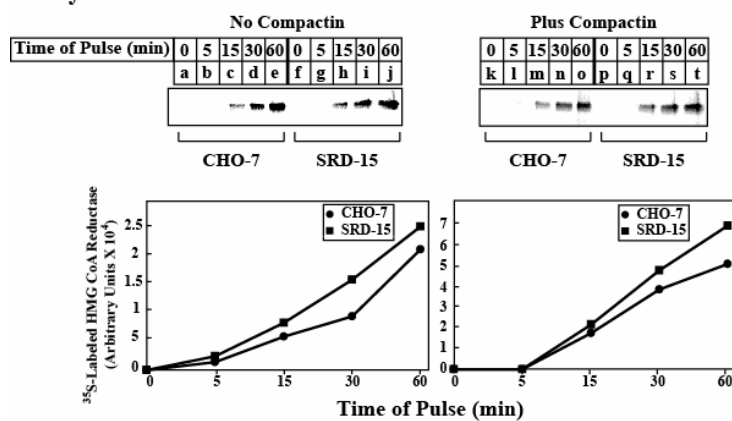
*A*, Cells were set up in medium A with 5% LPDS. On day 2, cells were refed medium A containing 5% LPDS and the indicated concentration of compactin. After 16 h at 37 °C, the cells were harvested for cell fractionation or total RNA. Aliquots of the membrane (10 µg protein/lane) and nuclear extract (40 µg protein/lane) were subjected to SDS-PAGE and immunoblots analysis was carried out with IgG-A9 (Reductase) and IgG-7D4 (SREBP-2). Reverse-transcribed total RNA were then subjected to quantitative real time PCR analysis. Each value represents the amount of the indicated mRNA relative to that of SCAP in CHO-7 cells incubated in the absence of compactin. *B* and *C*, on day 2, cells were switched to medium A containing 5% LPDS with or without 10 µM compactin and 50 µM mevalonate as indicated. In *B*, cells were incubated in medium supplemented with LPDS, 10 µM compactin, and 50 µM mevalonate. After 16 h, the cells were preincubated for 1 h in methionine/cysteine-free medium A supplemented with 5% LPDS and 10 µM compactin. Cells were pulse labeled with 100 µCi/ml <sup>35</sup>S-methionine in methionine/cysteine-free medium A supplemented with 5% LPDS and 10 µM compactin. *B*, following the indicated time of pulse, cells were harvested, and subjected to immunoprecipitation with polyclonal anti-reductase antibodies. Aliquots of immunoprecipitates (normalized for equal protein/lane) were subjected to SDS-PAGE and transferred to nylon membranes. *C*, after pulse labeling for 30 min at 37 °C, the cells were then chased in medium A supplemented with 5% LPDS, 10 µM compactin, 0.5 mM unlabeled methionine, and 1 mM unlabeled cysteine in the absence or presence of sterols (1 µg/ml 25-HC) plus 10 mM mevalonate. After the indicated time of chase, the cells were harvested, and subjected to immunoprecipitation and SDS-PAGE as described in *B*. Filters were exposed for 12 h to an imaging plate at room temperature and scanned in a Molecular Dynamics Storm 820 Phosphorimager, and the image photographed.

FIGURE 2-3

A.



B. HMG CoA Reductase Synthesis



C. HMG CoA Reductase Turnover

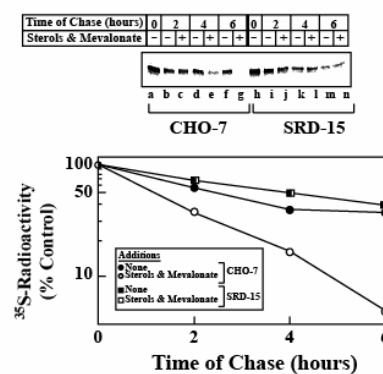


**FIGURE 2-4: Molecular characterization of Insig-2 mRNA and genomic DNA in CHO, SRD-14, and SRD-15 cells.**

*A* and *B*, CHO-7, SRD-14, and SRD-15 cells were set up in medium A supplemented with 5% LPDS. On day 2, the cells were switched to medium A containing 10  $\mu$ M compactin and 50  $\mu$ M mevalonate in the absence or presence of sterols (2.5  $\mu$ M 25-HC and 25  $\mu$ M cholesterol) as indicated. After incubation at 37 °C for 16 h, the cells were harvested and total RNA was isolated. *A*, aliquots of total RNA (15  $\mu$ g/lane) were subjected to electrophoresis in a denaturing gel and transferred to a nylon filter by capillary blotting. The filter was hybridized with indicated  $^{32}$ P-labeled probe and exposed to film at -80 °C for 6 h ( $\beta$ -actin) and 48 h (Insig-2). *B*, total RNA was subjected to reverse transcription reactions, after which aliquots of the resulting first-strand cDNA was subjected to quantitative real time PCR using specific primers for the indicated genes. The relative amount of mRNA in each condition was normalized to an internal control gene (GAPDH). *C*, aliquots of genomic DNA (20  $\mu$ g/lane) from SRD-14 and SRD-15 cells were digested with the indicated restriction enzyme, subjected to electrophoresis on 0.8% agarose gel, and transferred to nylon filters. Hybridizations were carried out with  $^{32}$ P-labeled cDNA probes corresponding to the full-length hamster Insig-2 cDNA (nucleotides 1-678, lanes 1-6) or 5'- (nucleotides 1-216, lanes 7-12) and 3'- (nucleotides 217-678, lanes 13-18) KpnI-restriction fragments of the Insig-2 cDNA as indicated. A fragment of the hamster SCAP cDNA, corresponding to nucleotides 1-697 (lanes 19-24), was utilized as a loading control. The filters were exposed to film at -80 °C for 16 h (Insig-1 and Insig-2 probes) and 6 h (SCAP probe).

FIGURE 2-4

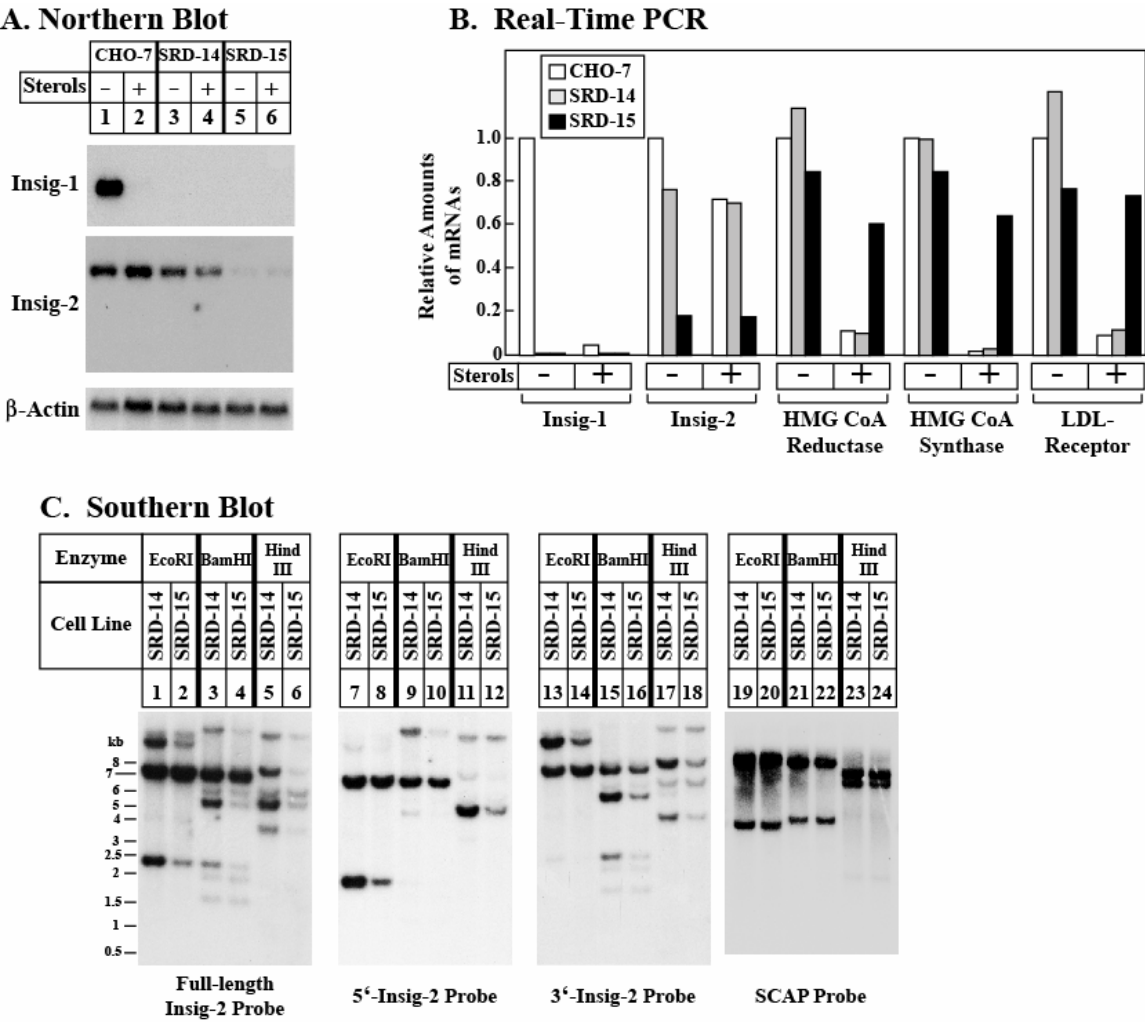
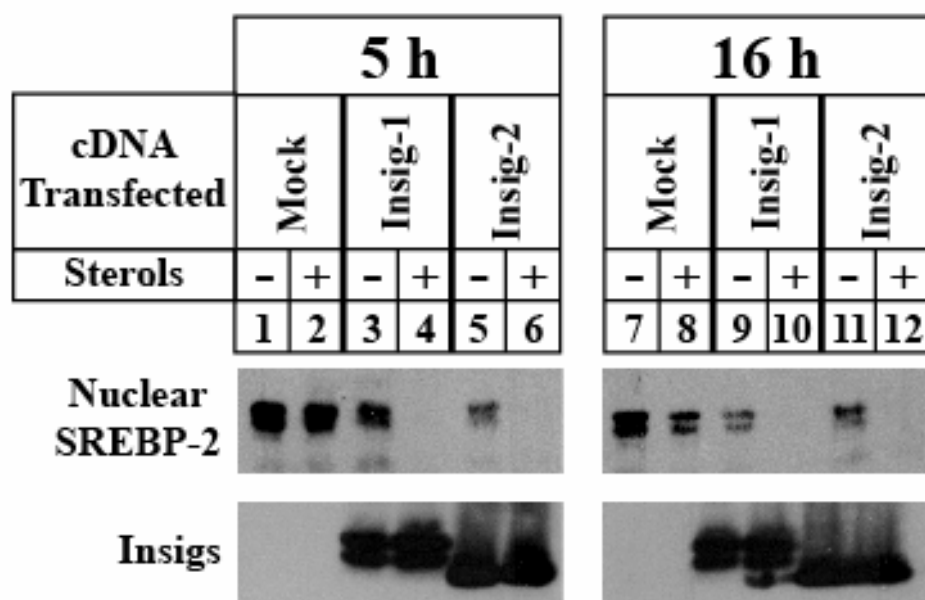


**FIGURE 2-5: Stable transfection of SRD-15 cells with pCMV-Insig-1-Myc or pCMV-Insig-2-Myc restores regulation of SREBP-2 processing mediated by sterols.**

Cells were set up in medium A supplemented with 5% LPDS. On day 2, the cells were switched to medium A containing 5% LPDS, 10  $\mu$ M compactin, and 50  $\mu$ M mevalonate. Some of the cells received the same medium supplemented with a mixture of 25-HC (2.5  $\mu$ M) and cholesterol (25  $\mu$ M) as indicated. Sterols were added to the cells in a staggered fashion, such that all of the cells could be harvested together after incubations for 5 or 16 h at 37 °C. Following the incubations, the cells were harvested, subjected to cell fractionation, and aliquots of the membrane (40  $\mu$ g protein/lane) and nuclear extract (32  $\mu$ g protein/lane) fractions were subjected to SDS-PAGE. Immunoblot analysis with IgG-7D4 (SREBP-2) or anti-Myc IgG (against Insig-1 and Insig-2).



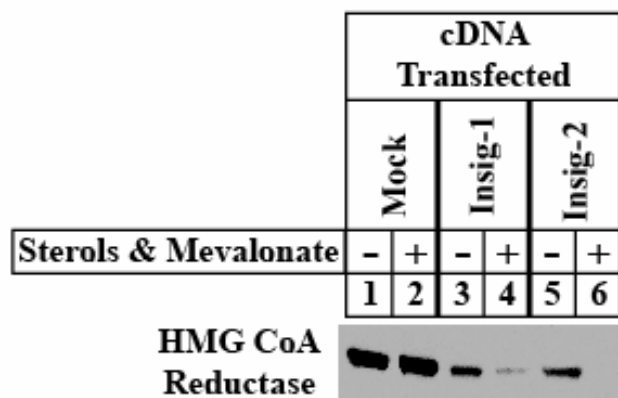
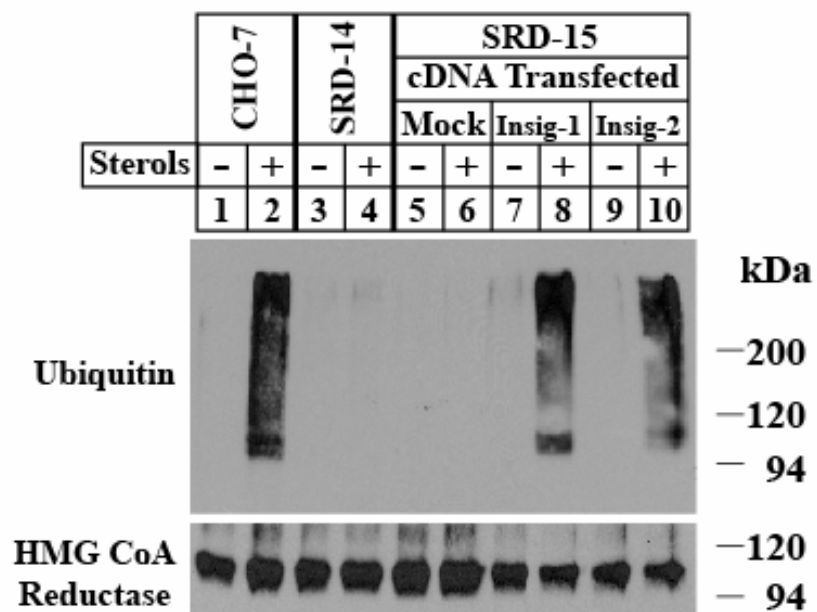
FIGURE 2-5



**FIGURE 2-6: Stable transfection of SRD-15 cells with pCMV-Insig-1-Myc or pCMV-Insig-2-Myc restores sterol regulation of HMG-CoA Reductase ubiquitination and degradation.**

*A*, Cells were set up in medium A supplemented with 5% LPDS. On day 2, the cells were switched to medium A containing 5% LPDS, 10  $\mu$ M compactin, and 50  $\mu$ M mevalonate. After 16 h at 37 °C, the cells were switched to medium A containing 50  $\mu$ M compactin in the absence or presence of sterols (2.5  $\mu$ M 25-HC and 25  $\mu$ M) plus 10 mM mevalonate, as indicated. In *B*, the medium also contained 10  $\mu$ M MG-132. *A*, Following incubation at 37 °C for 5 h, the cells were harvested, cell fractionation, subjected to SDS-PAGE and Immunoblot analysis with IgG-A9 (Reductase). *B*, following incubation for 1 h at 37 °C, the cells were harvested, lysed, and subjected to immunoprecipitation with polyclonal anti-reductase. Aliquots of the immunoprecipitates were subsequently subjected to SDS-PAGE, and immunoblotted with IgG-A9 (Reductase) or IgG-P4D1 (Ubiquitin).

FIGURE 2-6

**A. Immunoblot****B. Immunoprecipitation and Immunoblot**

## DISCUSSION

The data presented here provide compelling genetic evidence for a requirement of both Insigs in the normal regulation of cholesterol metabolism in cultured cells. This conclusion was drawn from the characterization of a new line of mutant CHO cells, designated SRD-15, with genetic deficiencies in both Insig-1 and Insig-2. SRD-15 cells were produced by mutagenesis of Insig-1-deficient SRD-14 cells, followed by selection for growth in the presence of 25-HC. It was previously determined that SREBP processing in SRD-14 cells remained sensitive to prolonged treatment with 25-HC, despite their Insig-1 deficiency. As a result, SRD-14 cells will not grow indefinitely in the presence of 25-HC. We reasoned that this residual sterol regulation was attributable to the remaining Insig-2 in SRD-14 cells and this hypothesis was substantiated in the current studies by two observations. First, SRD-15 cells grow in concentrations of 25-HC that kill SRD-14 cells (Fig. 2-1). Second, SREBP processing in the SRD-15 cells is completely refractory to sterol regulation, even after prolonged treatments (Fig. 2-2), and elevated in SRD-15 in comparison to CHO-7 cells (Fig. 2-3). Moreover, the steady-state levels of reductase were also increased in the mutant SRD-15 cells compared to their wild-type counterparts (Fig. 2-3). The sterol regulation of SREBP processing, as well as sterol-induced ubiquitination and degradation of reductase, was restored in SRD-15 cells by the overexpression of either Insig-1 or Insig-2 (Figs. 2-5 and 2-6). This indicates that the sterol-resistant phenotype of SRD-15 cells results from their deficiency in the amount of total Insig. This conclusion is supported by our failure to find mutations in any of the other genes known to participate in the SREBP pathway (SREBP-1, SREBP-2, and SCAP) as determined by cDNA cloning and sequencing (data not shown).

Considered together with previous observations in SRD-14 cells (Sever *et al.*, 2004), the current data have implications regarding the role of Insigs in regulating the processing of SREBPs and the degradation of reductase. First, it seems that the initial response of cells to sterols requires high levels of total Insig and is characterized by the rapid suppression of SREBP processing and the stimulation of reductase degradation. This follows from the observation that within 5 h of addition to sterol-depleted cells, sterols neither suppressed SREBP processing nor accelerated reductase degradation in Insig-1-deficient SRD-14 cells, even though the cells possess normal levels of Insig-2. This indicates that in wild-type cells, these rapid sterol-mediated reactions are primarily mediated by Insig-1, which we estimate accounts for 90% of total Insig. Moreover, the rapid response can be restored by the overexpression of either Insig-1 or Insig-2 in the SRD-14 cells.

Another implication relates to the delay in sterol-mediated inhibition of SREBP processing in SRD-14 cells (Fig. 2-2). This delay may indicate that the SCAP-SREBP complex binds with higher affinity to sterols and/or Insigs than reductase. When Insig-1 is present (as in sterol-depleted cells), SCAP-SREBP binding occurs rapidly upon sterol addition, and nuclear SREBP declines within 5 h. When Insig-1 is selectively absent (as in SRD-14 cells), the cells require a longer time in which to accumulate sufficient sterols to trigger binding to Insig-2. Hence, nuclear SREBP-2 does not disappear until 16 h after sterol addition. The conclusion that this delayed inhibition of SREBP cleavage is supported by the finding that the delayed response is abolished in SRD-15 cells, which have a severe reduction in Insig-2 as well as Insig-1. Since they lack both rapid and delayed responses, the SRD-15 cells (unlike the SRD-14 cells) are able to grow continuously in the presence of 25-HC (see

Fig. 2-1) and accumulate lipids when cultured in the absence of cholesterol-carrying lipoproteins (Fig. 2-2).

Until now, two types of mutant CHO cells have been classified as resistant to 25-HC in that they fail to suppress cholesterol synthesis under conditions of sterol overload and survive chronic oxysterol treatment (Goldstein *et al.*, 2002). Type 1 mutants express truncated forms of SREBP-2 that constitutively migrate to the nucleus and activate gene transcription, regardless of sterol treatment. Study of the Type 1 mutants revealed the central role of SREBP-2 in cholesterol homeostasis and provided genetic evidence for the regulated proteolytic pathway by which SREBP activation is controlled (Yang *et al.*, 1994). Type 2 sterol-resistant CHO cells harbor activating point mutations in the sterol-sensing domain of SCAP. These mutations render mutant SCAP refractory to sterol regulation; therefore it escorts SREBPs from the ER to the Golgi even when the cells are overloaded with sterols. Studies of the Type 2 mutants revealed the existence of SCAP and identified its activity as the target of sterol-mediated regulation of SREBP processing (Hua *et al.*, 1996). It should be noted that both Type 1 and Type 2 sterol-resistant mutants exhibit a dominant phenotype.

Data in the current paper demonstrate that the SRD-15 cells represent a new type of mutant CHO cells designated as Type 3 sterol-resistant mutants. The underlying defect that renders SRD-15 cells Type 3 sterol-resistant mutants has been traced to their deficiencies in Insig-1 and Insig-2 and the current studies establish an essential role for both Insig-1 and Insig-2 in the sterol regulation of SREBP processing and reductase degradation. However, unlike other sterol-resistant mutants, the phenotype of the Type 3 mutants is recessive due to their lack of both Insig-1 and Insig-2. Future studies with these cells may provide valuable

insights into other aspects of the cellular maintenance of lipid homeostasis. For example, the SRD-15 cells provide an ideal context in which to evaluate the possible participation of Insigs in the action of other sterol-sensing domain-containing proteins.

**CHAPTER 3    MUTATIONS WITHIN THE MEMBRANE  
DOMAIN OF HMG-COA REDUCTASE  
CONFER RESISTANCE TO STEROL-  
ACCELERATED DEGRADATION**



## RESULTS

CHO-7 and CHO-7/pInsig-2 cells (CHO-7 cells expressing multiple copies of an Insig-2 cDNA) were mutagenized with EMS and subjected to selection for 4 weeks in medium containing LPDS and 10  $\mu$ M SR-12813. Three SR-12813-resistant clones were isolated, expanded, and designated SRD-16, -17, and -18. SRD-16 cells were derived from CHO-7/pInsig-2 cells, while SRD-17 and -18 cells resulted from mutagenesis and selection of CHO-7 cells. Fig. 3-1A shows that growth of parental CHO-7 and CHO-7/pInsig-2 cells, but not that of the mutant cells, was prevented when LPDS-containing culture medium was supplemented with 10  $\mu$ M SR-12813. The addition of cholesterol restored growth of parental cells in SR-12813, indicating that cell death was caused by cholesterol depletion.

In the experiment of Fig. 3-1B, wild type and mutant cells were incubated for 16 h in medium containing LPDS, the reductase inhibitor compactin, and a low level of mevalonate, the product of reductase. The low level of mevalonate permits synthesis of nonsterol mevalonate-derived products, such as the prenyl groups that are found attached to many cellular proteins, but it is not sufficient to produce normal amounts of cholesterol (Brown and Goldstein, 1980). The resultant sterol-depleted cells were then subjected to 5 h treatments with SR-12813 or 25-HC, after which they were harvested and separated into membrane and nuclear extract fractions. Aliquots of each fraction were subjected to SDS-PAGE and immunoblotted with antibodies against reductase and SREBP-2, the SREBP family member that is most dedicated to cholesterol synthesis (Horton et al., 2002). Treatment of CHO-7/pInsig-2 and CHO-7 cells with either 25-HC or SR-12813 decreased the amount of reductase in membranes (*top panel, lanes 1-3; 7-9*), indicative of accelerated degradation of

the enzyme. In contrast, neither 25-HC nor SR-12813 stimulated degradation of the reductase in SRD-16, -17, or -18 cells (*lanes 4-6; 10-15*). Treatment with 25-HC caused the disappearance of nuclear SREBP-2 in parental and mutant cells (*bottom panel, lanes 2, 5, 8, 11, and 14*). On the other hand, SR-12813 failed to block SREBP-2 processing in any of the cell lines (*lanes 3, 6, 9, 12, and 15*).

The experiment of Fig. 3-1C was designed to determine the ubiquitination state of reductase in wild type and mutant cells treated with 25-HC. Sterol-depleted cells were subjected to 25-HC treatment in the presence of MG-132, a proteasome inhibitor that blocks degradation of ubiquitinated proteins. Following treatments, cells were harvested, detergent lysates were prepared, and subsequently immunoprecipitated with polyclonal antibodies against reductase. Immunoblotting with anti-ubiquitin revealed the accumulation of high molecular weight material in reductase immunoprecipitates from CHO-7/pInsig-2 and CHO-7 cells subjected to 25-HC treatment (*top panel, lanes 2 and 6*), indicating that reductase had become ubiquitinated. This 25-HC-dependent ubiquitination of reductase was markedly diminished in SRD cells (*lane 4, 8, and 10*), a result consistent with their inability to degrade reductase in the presence of the sterol (Fig. 3-1B).

Considering that reductase degradation, but not SREBP-2 processing, is resistant to 25-HC-mediated regulation in SRD cells and the propensity of EMS mutagenesis to generate point mutations, we hypothesized that this resistance was a consequence of mutation(s) in reductase. Thus, total RNA was isolated from SRD cells and used to synthesize first strand cDNA from which the cDNA encoding reductase was amplified by PCR. The resulting products were subcloned and 10-30 individual clones were subjected to DNA sequencing,

which revealed a G-to-A or -C substitution in reductase mRNAs from each cell line. These substitutions resulted in changes of Ser-60 (AGT) to Asn (AAT), Gly-87 (GGG) to Arg (AGG), and Ala-333 (GCT) to Pro (CCT) for SRD-16, -17, and -18 cells, respectively. The frequency of these changes in the randomly sequenced cDNA clones was close to 50% (8/16, SRD-16; 8/12, SRD-17; and 13/30, SRD-18). This strongly indicates that each of the SRD cell lines is heterozygous for their respective mutations. This 50% frequency was confirmed by sequencing multiple clones of PCR-amplified fragments from genomic DNA that included each codon (5/14, SRD-16; 6/10, SRD-17; and 5/10, SRD-18). As shown in Fig. 3-2A, Ser-60 and Ala-333 localize to transmembrane helices 2 and 8 of reductase, respectively; Gly-87 lies within the cytosolic loop that separates helices 2 and 3. The amino acid sequence alignment in Figure 2B shows that Ser-60, Gly-87, and Ala-333 are conserved between hamster, human, xenopus, zebrafish-1, and sea urchin reductase. Notably, Ser-60 is not conserved in zebrafish-2 reductase, one of two reductase isozymes expressed in zebrafish (Thorpe et al., 2004). Gly-87 is also present in the *Drosophila* reductase. Even though Ser-60 and Gly-87 localize to the sterol-sensing domain of reductase, neither amino acid is present in the corresponding region of SCAP's sterol-sensing domain.

Experiments were next designed to directly demonstrate that the S60N, G87R, and A333P mutations impart resistance of reductase to sterol-stimulated ubiquitination (Fig. 3-3) and degradation (Fig. 3-4A and B). CHO-7 cells were transfected with wild type or mutant versions (G87R, A333P, or S60N) of pCMV-HMG-Red-T7, an expression plasmid that encodes full-length reductase followed by three copies of a T7 epitope tag (Sever et al., 2003a). The sensitivity of ubiquitin detection was enhanced by the additional transfection of

pEFla-HA-ubiquitin, which encodes human ubiquitin with an NH<sub>2</sub>-terminal tag consisting of two copies of the HA epitope. Following sterol depletion, the cells were subjected to treatments with MG-132 and various concentrations of 25-HC. Transfected reductase was immunoprecipitated from detergent lysates using anti-T7 coupled agarose beads and the resulting precipitates were immunoblotted with antibodies against T7 and HA for reductase and ubiquitin, respectively. When transfected alone, wild type, S60N, G87R, and A333P reductase failed to become ubiquitinated in the presence of 2.5  $\mu$ M 25-HC (Fig. 3-3A-C, *top panel, lanes a and b; g and h*). Dose-dependent, 25-HC-induced ubiquitination of wild type reductase was restored upon the co-expression of pCMV-Insig-1-Myc, which encodes human Insig-1 followed by six copies of the c-Myc epitope (*lanes d-f*). Regulated ubiquitination was nearly absent for the G87R and A333P versions of reductase and S60N reductase only became ubiquitinated with the highest level (2.5  $\mu$ M) of 25-HC (*lanes j-l*).

Similar results were obtained for reductase degradation (Figs. 3-4A and B). In these experiments, sterol-depleted CHO-7 cells transfected with wild type or mutant reductase were incubated with various amounts of 25-HC (Fig. 3-4A) or lanosterol (Fig. 3-4B), a cholesterol synthesis intermediate that stimulates degradation of endogenous reductase (Song et al., 2005a). When transfected alone, degradation of wild type, S60N, G87R, or A333P reductase was not accelerated by 25-HC (*top panel, lanes a and b; g and h*) or lanosterol (*lanes m and n; s and t*). Co-expression of pCMV-Insig-1-Myc restored degradation of wild type reductase in the presence of 25-HC (*lanes d-f*) or lanosterol (*lanes p-r*), but G87R, A333P, and S60N reductase remained largely resistant to degradation (*lanes j-l and v-x*).

Fig. 3-4C shows a growth experiment designed to determine whether the S60N, G87R, and A333P mutations in reductase confer an SR-12813-resistant phenotype. CHO-7 cells were transfected with wild type or mutant versions of pCMV-HMG-Red-T7. The plasmids also encode *neo*, a gene that confers resistance to G418. Following transfection and selection of transformants with G418, the cells were grown for an additional 2 weeks in medium containing LPDS in the absence or presence of SR-12813. Transfection of the control plasmid or wild type reductase did not permit the cells to grow in medium containing SR-12813, whereas transfection of the mutant forms of reductase allowed cell growth in the presence of the drug.

In previous studies, blue native-polyacrylamide gel electrophoresis (BN-PAGE) was employed to visualize sterol-dependent complexes between Insig-1 and the membrane domain of reductase, which is necessary and sufficient for regulated degradation (Gil et al., 1985; Sever et al., 2003a; Skalnik et al., 1988). Considering the results of Figs. 3-3 and 3-4, which show Ser-60, Gly-87, and Ala-333 in reductase are essential for Insig-mediated ubiquitination and degradation, we used BN-PAGE to determine whether the most robust mutation (G87R) decreases binding between the membrane domain of reductase and Insig-1. In Fig. 3-5, SCAP-deficient SRD-13A cells were transfected with various combinations of pCMV-Insig-1-Myc and wild type or mutant versions of pCMV-HMG-Red-T7 (TM 1-8), which encodes a truncated reductase that contains the entire membrane domain (see Figure 3-2A), but lacks the catalytic domain. Following sterol depletion with hydroxypropyl- $\beta$ -cyclodextrin and pretreatment with MG-132, the cells were subjected to an additional incubation in the absence or presence of 25-HC. The cells were subsequently harvested;

membrane fractions were isolated and solubilized with digitonin. Soluble material was mixed with Coomassie Blue and 6-amino-n-hexanoic acid (to impart a negative charge and prevent precipitation of proteins), subjected to PAGE, and immunoblotted with antibodies against the T7 and Myc epitopes. The anti-T7 immunoblot of the native gel revealed that when transfected alone, the membrane domain of reductase appeared as a single band in the absence or presence of 25-HC (*top panel, lanes 3 and 4*). This band was designated unbound reductase. When Insig-1 was co-expressed, some of the reductase migrated more slowly (*lane 5*), and this band was designated as the reductase-Insig-1 complex. With 25-HC treatment, unbound reductase almost completely disappeared and the amount of reductase in complex with Insig-1 increased (*lanes 6 and 7*). In contrast, migration of the G87R version of the reductase membrane domain was not retarded in the presence of Insig-1 and sterols (*lanes 8-10*). A similar result was observed in the anti-Myc blots of the native gel (*second panel*). 25-HC caused a complete disappearance of unbound Insig-1 upon co-expression of wild type, but not the G87R mutant of the reductase membrane domain (*lanes 8-10*). Immunoblots of SDS-PAGE gels revealed constant expression of Insig-1, wild type reductase, and mutant G87R reductase, regardless of the absence or presence of 25-HC (*bottom two panels*). Taken together, these results indicate that the G87R mutation disrupts binding of reductase to Insigs, thereby rendering the enzyme resistant to sterol-regulated ubiquitination and degradation.

**FIGURE 3-1: Characterization of mutant CHO cells resistant to SR-12813.**

*A*, CHO-7, CHO-7/pInsig-2, SRD-16, -17, and -18 cells were set up in medium A supplemented with 5% LPDS. On day 1, cells were washed with PBS and refed medium A containing 5% LPDS in the absence or presence of 10  $\mu$ M SR-12813. Some of the SR-12813-treated cells also received 25  $\mu$ M cholesterol. Cells were refed fresh medium every 2 days. On day 10, cells were washed, fixed, and stained with crystal violet. *B*, CHO-7 cells were set up in medium A containing 5% LPDS. On day 2, cells were refed medium A supplemented with 5% LPDS, 10  $\mu$ M sodium compactin, and 50  $\mu$ M sodium mevalonate. After 16 h at 37 °C, cells were switched to medium A containing 5% LPDS and 10  $\mu$ M compactin in the absence or presence of either 25-HC or SR-12813 plus 10 mM mevalonate as indicated. After 5 h at 37 °C, the cells were harvested and subjected to subcellular fractionation. Aliquots of the membrane (13  $\mu$ g of protein/lane) and nuclear extract fractions (15  $\mu$ g of protein/lane) were subjected to SDS-PAGE and immunoblot analysis with IgG-A9 (Reductase) or IgG-7D4 (SREBP-2). *C*, Sterol-depleted cells were subsequently switched to medium A containing 5% LPDS, 10  $\mu$ M compactin, and 10  $\mu$ M MG-132 in the absence or presence of 2.5  $\mu$ M 25-HC plus 10 mM mevalonate as indicated. After 2 h, the cells were harvested, lysed, and subjected to immunoprecipitation with anti-reductase polyclonal antibodies. Immunoblot analysis with IgG-A9 (Reductase) or IgG-P4D1 (Ubiquitin).

FIGURE 3-1

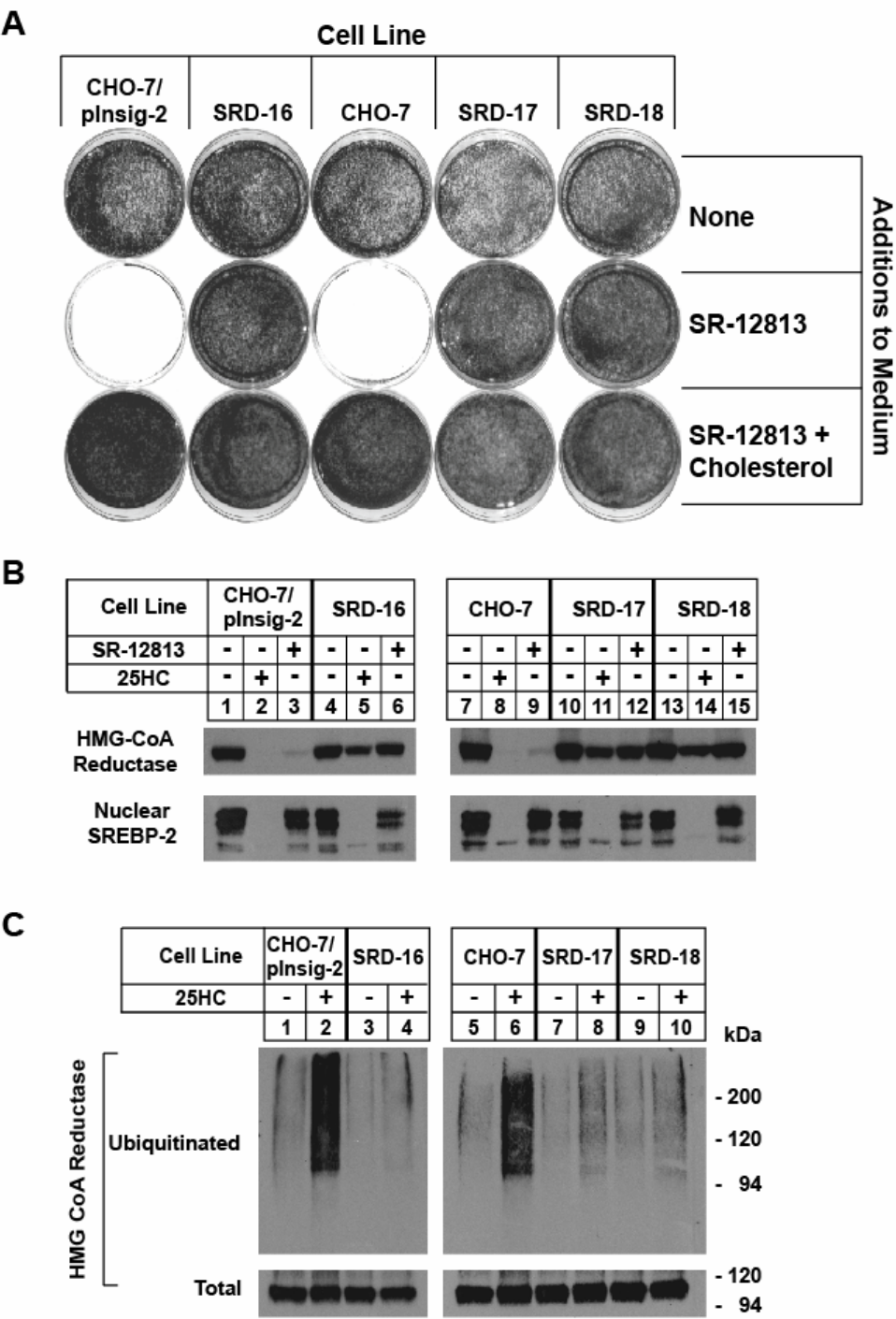




**FIGURE 3-2: Localization and conservation of amino acid residues in HMG CoA Reductase membrane domain.**

*A*, Amino acid sequence and topology of the membrane domain of hamster HMG CoA reductase. The amino acid residues that are mutated in SRD-16, -17-, and -18 cells are enlarged, shown in red, and denoted by arrows. *B*, comparison of amino acid residues in hamster, human, xenopus, zebrafish-1, zebrafish-2, sea urchin, and drosophila HMG CoA reductase surrounding Ser-60, Gly-87, and Ala-333 (shown in red). GenBank accession numbers are P00347, NP000850, P20715, XP684400, AI497311, NP999724, and P14773, respectively. Residues that are identical in all six proteins are highlighted in black.



**FIGURE 3-3: Ubiquitination of S60N, G87R, and A333P versions of HMG CoA Reductase.**

CHO-7 cells were set up in medium A containing 5% LPDS. On day 1, the cells were transfected with 1  $\mu$ g of wild type, S60N, G87R, or A333P versions of pCMV-HMG-Red-T7 together with 0.1  $\mu$ g pEF1a-HA-ubiquitin in 2 ml of medium A containing 5% LPDS. The total DNA in each dish was adjusted to 3  $\mu$ g by the addition of pcDNA3 mock vector. Six hours after transfection, the cells were depleted of sterols by the direct addition of 2 ml medium A containing 5% LPDS, 10  $\mu$ M compactin, and 50  $\mu$ M mevalonate (final concentrations). After 16 h at 37 °C, cells were switched to medium A containing 5% LPDS, 10  $\mu$ M compactin, 10  $\mu$ M MG-132, and the indicated concentration of 25-HC. Following incubation for 2 h at 37 °C, the cells were harvested, lysed, and subjected sequentially to immunoprecipitation with anti-T7 coupled agarose beads and SDS-PAGE. Immunoblot analysis with IgG-HA (Ubiquitin) or anti-T7 IgG (Reductase).

FIGURE 3-3

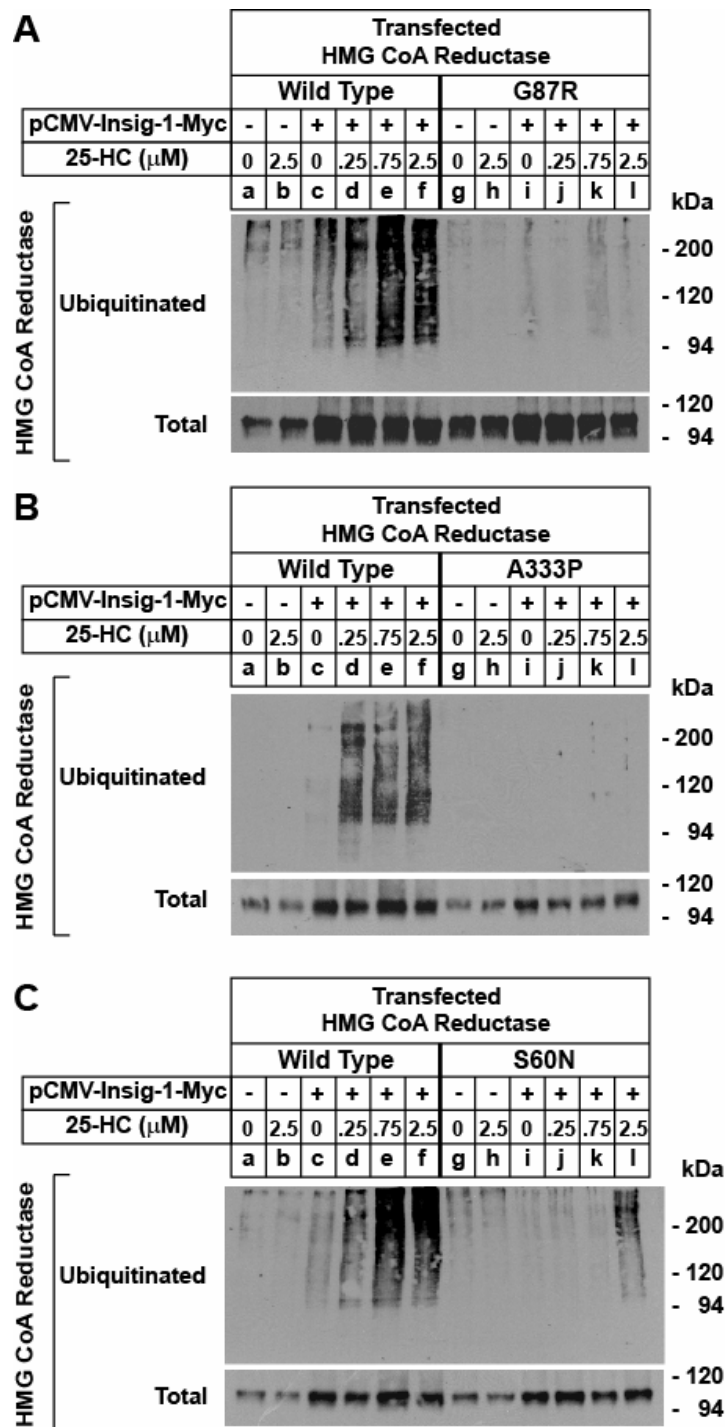


**FIGURE 3-4: Properties of S60N, G87R, and A333P HMG CoA Reductase in transfected cells.**

*A* and *B*, CHO-7 cells were set up and transfected with 1  $\mu$ g of wild type, S60N, G87R, or A333P versions of pCMV-HMG-Red-T7 in the absence or presence of 30 ng pCMV-Insig-1-Myc. After sterol depletion for 16 h at 37 °C, cells were switched to medium A containing 5% LPDS, 10  $\mu$ M compactin, and the indicated concentration of 25-HC (*B*) or lanosterol (*C*) plus 10 mM mevalonate. Following incubation for 5 h at 37 °C, cells were harvested, membrane fractions were prepared, and aliquots (3–6  $\mu$ g) were subjected to SDS-PAGE. Immunoblot analysis with anti-T7 IgG and IgG-9E10. *C*, CHO-7 cells were set up in medium A containing 5% LPDS. On day 1, the cells were transfected with 1  $\mu$ g of either pcDNA3 (Mock) or wild type, S60N, G87R, or A333P versions of pCMV-HMG-Red-T7. All of the plasmids contained the G418 resistance gene *neo*. On day 2, the cells were switched to medium A containing 5% LPDS and 0.7 mg/ml G418 and refed every 2 days. No cells survived in control dishes that did not receive any plasmid during transfection. On day 12, the surviving cells were trypsinized, pooled, and triplicate sets of dishes were set up in medium A containing 5% LPDS. On day 13, cells were switched to identical medium in the absence or presence of 10  $\mu$ M SR-12813. On day 22, cells were fixed and stained.

FIGURE 3-4

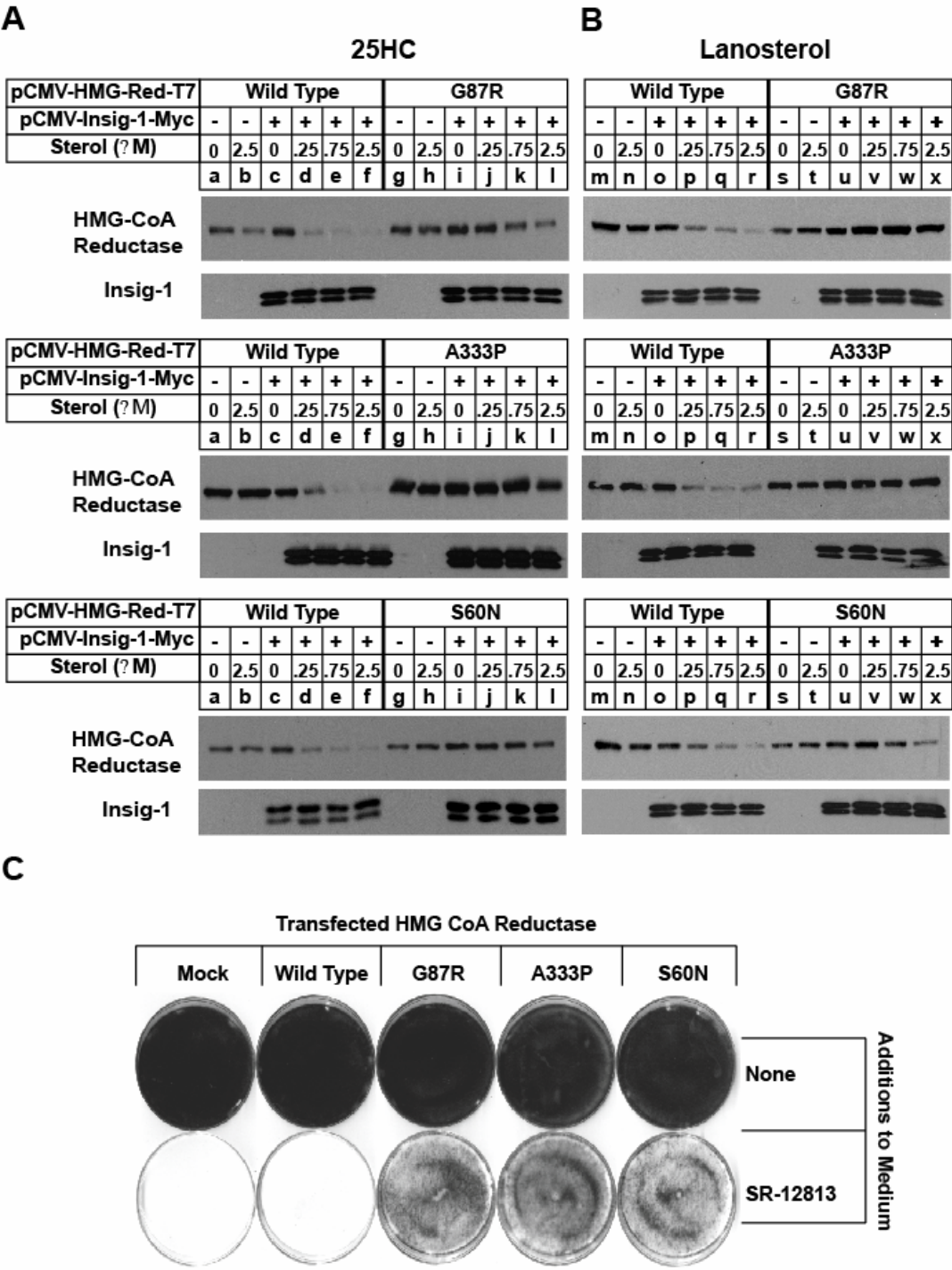
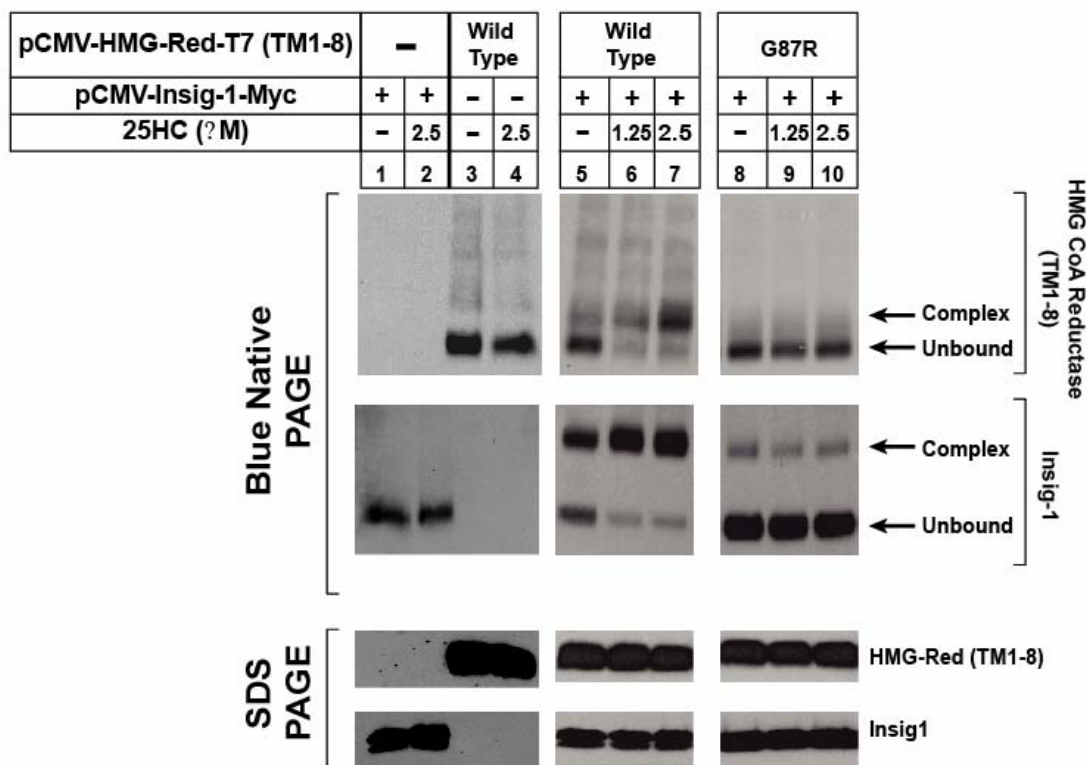


**FIGURE 3-5: Introduction of the G87R mutation into membrane domain of HMG CoA Reductase impairs binding to Insig-1 in the presence of 25-HC.**

SRD-13A cells were set up for experiments on day 0 at  $7 \times 10^5$  cells per 100-mm dish. On day 2, the cells were transfected in medium A containing 5% FCS as described in the legend to Fig. 3 with 60 ng of pCMV-Insig-1-Myc in the absence or presence of 4  $\mu$ g wild type or G87R versions of pCMV-HMG-Red-T7(TM1–8) as indicated. After incubation for 16 h at 37 °C, cells were switched to medium A containing 5% LPDS, 1% HPCD, and 10  $\mu$ M compactin and incubated for 1 h at 37 °C. The cells were then washed; switched to identical medium (without HPCD) supplemented with 10  $\mu$ M MG-132, and incubated for 1 h at 37 °C. This was followed by incubation for an additional 1 h in the same medium with or without 1  $\mu$ g/ml 25-HC plus 10 mM mevalonate as indicated. The cells were subsequently harvested and subjected to subcellular fractionation. Aliquots of the  $1 \times 10^5$  g membrane pellet were solubilized in 1% digitonin and subjected to BN- (*Upper two panels*) or SDS- (*Lower two panels*) PAGE. Immunoblot analysis with anti-T7 IgG (Reductase) and IgG-9E10 (Insig-1).

FIGURE 3-5





## DISCUSSION

The current data document the isolation of three independently derived lines of mutant CHO cells resistant to SR-12813, which inhibits cholesterol synthesis by stimulating Insig-dependent ubiquitination and degradation of HMG CoA reductase. Neither SR-12813 nor the oxysterol 25-HC stimulated degradation and ubiquitination of endogenous reductase in the mutant cells (Fig. 3-1*B* and *C*), which are designated SRD-16, -17, and -18. DNA sequencing revealed that SRD-16, -17, and -18 cells exhibit a G-to-A or -C substitution in codons 60, 87, and 333 of reductase, respectively, that result in changes of Ser-60 to Asn, Gly-87 to Arg, and Ala-333 to Pro. Transient transfection assays revealed that the S60N, G87R, and A333P mutations render reductase refractory to Insig-mediated, sterol-accelerated ubiquitination (Fig. 3-3) and degradation (Fig. 3-4*A* and *B*). Moreover, overexpression of a cDNA encoding full-length S60N, G87R, or A333P reductase allowed growth of wild type cells in SR-12813-supplemented medium (Fig. 3-4*C*). Considered together, these results identify Ser-60, Gly-87, and Ala-333 as key residues for regulated ubiquitination and degradation of reductase and demonstrate that their mutation confers a dominant, SR-12813-resistant phenotype.

The determining factor for degradation of reductase is sterol-induced binding of the enzyme to Insigs, which are carriers of the membrane-anchored gp78 ubiquitin ligase that facilitates reductase ubiquitination (Song et al., 2005b). Interactions between reductase and Insigs are mediated entirely by the membrane domain of reductase (Sever et al., 2003b), which may explain the high degree of conservation observed in the region across species (Fig. 3-2*B*). Indeed, sterol-regulated formation of the reductase-Insig complex is blocked by

mutation of a YIYF tetrapeptide sequence that is located in the second membrane-spanning region of reductase (Sever et al., 2003a). Similarly, Ser-60, Gly-87, and Ala-333 localize to the membrane domain of reductase (Fig. 3-2A), and introducing the G87 mutation into the membrane domain of reductase impaired sterol-regulated complex formation with Insig-1 (Fig. 3-5). It should be noted that native gels revealed that the A333P and S60N mutations in the membrane domain of reductase similarly disrupted reductase-Insig binding; however, the effect was not as pronounced as that observed with the G87R mutant.

The selection for SR-12813 resistance employed in the current study is unbiased. This selection produced three resistant cell lines with point mutations in the membrane domain of reductase, and all three mutations conferred resistance to sterol-stimulated, Insig-dependent ubiquitination. These findings provide strong and unbiased support for the conclusion that reductase degradation absolutely requires reductase-Insig interaction through the membrane domains of the two proteins. The predominance of reductase mutations found in the current study, and the isolation of Insig mutants in previous mutagenesis experiments (i.e., SRD-14 and SRD-15; (Lee *et al.*, 2005; Sever *et al.*, 2004)) strongly suggests that the number of other proteins required specifically for reductase degradation is limited and that our understanding of this process is relatively complete.

**CHAPTER 4    AMPLIFICATION OF THE GENE FOR *SCAP*,  
COUPLED WITH INSIG-1 DEFICIENCY,  
CONFERS STEROL RESISTANCE IN  
MUTANT CHINESE HAMSTER OVARY  
CELLS**

## RESULTS

SRD-14 are Insig-1 deficient cells derived from CHO-7 cells by mutagenesis with  $\gamma$ -irradiation and selection with SR-12813 (Sever et al., 2004). SRD-15 and SRD-19 cells were derived from SRD-14 cells by mutagenesis with  $\gamma$ -irradiation and selection with 1.25  $\mu$ M 25-HC. SRD-15 cells were previously shown to be deficient in Insig-2 as well as Insig-1 (Lee et al., 2006) and as a result, neither stimulate ubiquitination/degradation of reductase nor suppress processing of SREBPs in response to treatment with 25-HC. SRD-19 cells were not previously characterized. Fig. 4-1 shows the growth pattern of wild type and mutant cells in medium supplemented with lipoprotein-deficient serum and various concentrations of 25-HC. As expected, wild type CHO-7 cells were killed when cultured in medium containing 0.25  $\mu$ M 25-HC, whereas higher levels of the sterol (0.75  $\mu$ M) were required to kill SRD-14 cells. In contrast, SRD-15, SRD-19, and SRD-1 cells (which express constitutively active SREBP-2) were resistant to culture in medium containing up to 2.5  $\mu$ M 25-HC.

We next compared lipid synthesis in wild type and mutant cells by metabolically labeling them with [ $^{14}$ C]-acetate for 2 h and subsequently measuring incorporation of the radiolabel into cellular cholesterol and fatty acids. As shown in Table II, SRD-14 cells incorporated ~2.5-fold more [ $^{14}$ C]-acetate into cholesterol than wild type CHO-7 cells; the rate of [ $^{14}$ C]cholesterol synthesis was even more elevated in SRD-15 and SRD-19 cells (4.8 and 6.8-fold, respectively). In a similar manner, [ $^{14}$ C]-acetate labeling of fatty acids was elevated in SRD-14 (1.35-fold), SRD-15 (3.4-fold), and SRD-19 cells (4.6-fold) relative to that in CHO-7 cells.

The results of Table II led us to next compare the sterol composition of wild type CHO-7 and mutant SRD cells. The cells were cultured for 3 days in lipoprotein-deficient serum, after which they were harvested and lysed. The resulting cell lysates were mixed with internal standards and the sterols were hydrolyzed. Lipids were then extracted in petroleum ether and derivatized with trimethylsilane for gas chromatography-mass spectroscopy analysis, which revealed total sterol levels of 38, 70, 117, and 110  $\mu\text{g}/\text{mg}$  protein for CHO-7, SRD-14, SRD-15, and SRD-19 cells, respectively (Fig. 4-2A). As expected, cholesterol was the most abundant sterol in each cell line (>70% of total sterol content) and levels of the sterol were elevated 2-4 fold in the mutant cells (Fig. 4-2B). The cholesterol synthesis intermediate 7-dehydrocholesterol was similarly elevated in SRD-15 and SRD-19 cells, whereas lathosterol and zymosterol levels remained unchanged. Lanosterol, the first sterol in the cholesterol synthetic pathway, was dramatically elevated in SRD-15 cells (>10-fold) and to a lesser extent (~5-fold) in SRD-19 cells. The level of desmosterol was also elevated in SRD-15 cells, but not to the magnitude as that of lanosterol.

Lipid droplets, also termed lipid particles, lipid bodies, or adiposomes (Liu et al., 2004), are generally regarded as storage depots for neutral lipids, such as triglycerides and cholesterol esters. To determine whether the increase in cholesterol synthesis and total sterol content of SRD-14, SRD-15, and SRD-19 cells correlated with an increase in lipid droplet formation, cells were stained with the lipid-specific dye, Oil Red O. Fig. 4-3A shows that CHO-7 cells accumulated lipid droplets of varying size after 3 days of culture in lipoprotein-deficient serum. The number and size of lipid droplets markedly increased in SRD-14, SRD-15, and SRD-19 cells. Although the mutant cells accumulated roughly equivalent numbers

of lipid droplets, their size was significantly increased in SRD-15 and SRD-19 cells in comparison to SRD-14 cells (Fig. 4-3B).

We next conducted a compositional analysis of lipid droplet fractions isolated from CHO-7, SRD-14, SRD-15, and SRD-19 cells. The cells were labeled for 2 days with [ $^{14}\text{C}$ ]acetate, harvested, and the lipid droplet fractions were isolated using a standard procedure developed previously (Liu et al., 2004). Equal amounts of [ $^{14}\text{C}$ ]-labeled lipids extracted from the resulting fractions were then subjected to thin layer chromatography and incorporation of radiolabel into various lipids was determined by scintillation counting. Fig. 4-4A shows that >50% of [ $^{14}\text{C}$ ]acetate was incorporated into cholesterol esters in CHO-7 cells; about 30% of the radiolabel appeared in triglycerides. The percentage of [ $^{14}\text{C}$ ]acetate incorporation into cholesterol esters was elevated approximately 14%, 29%, and 11% in SRD-14, SRD-15, and SRD-19 cells, respectively. Conversely, incorporation of radiolabel into triglycerides was reduced 5-20% in the mutant cell lines. In Fig. 4-4B, we labeled CHO-7, SRD-14, SRD-15, and SRD-19 cells with [ $^{14}\text{C}$ ]oleate and subsequently measured formation of cholesteryl [ $^{14}\text{C}$ ]oleate and  $^{14}\text{C}$ -labeled triglycerides in the absence and presence of low-density lipoprotein (LDL) or 25-HC. SRD-15 and SRD-19 cells exhibited a slightly elevated level of basal cholesteryl [ $^{14}\text{C}$ ]oleate formation, which likely results from the increased levels of cholesterol in the cells (Fig. 4-2A). In all of the cell lines, LDL and 25-HC stimulated incorporation of [ $^{14}\text{C}$ ]oleate into cholesteryl [ $^{14}\text{C}$ ]oleate in a dose-dependent fashion. The incorporation of [ $^{14}\text{C}$ ]oleate into  $^{14}\text{C}$ -labeled triglycerides in CHO-7 cells was not responsive to the addition of LDL or 25-HC and the reaction was essentially normal in all of the mutant cell lines.

The resistance of SRD-19 cells to culture in 25-HC (Fig. 4-1), coupled with elevated cholesterol synthesis and overaccumulation of sterols (Table II and Fig. 4-2) indicates the cells do not suppress cholesterol synthesis in response to 25-HC treatment. Thus, we next compared sterol regulation of SREBP processing in CHO-7, SRD-14, SRD-15, SRD-19, and SRD-1 cells. In the experiment of Fig. 4-5, the cells were incubated in medium containing lipoprotein-deficient serum, the reductase inhibitor compactin, and 50  $\mu$ M mevalonate to assure cell viability. Some of the dishes also received 1.25  $\mu$ M 25-HC. After 16 h, the cells were harvested and separated into membrane and nuclear extract fractions. Immunoblot analysis of the fractions was subsequently carried out with antibodies against SREBP-1 (Fig. 4-5, *top panel*), SREBP-2 (*middle panel*), and SCAP (*bottom panel*). Bands corresponding to the processed forms of SREBP-1 and SREBP-2 were observed in nuclear extracts from untreated CHO-7, SRD-14, SRD-15, and SRD-19 cells (*top and bottom panels, lanes 1, 3, 5, and 7*). In CHO-7 and SRD-14 cells, 25-HC inhibited processing of both SREBPs after the 16 h incubation (*lanes 2 and 4*), whereas SREBP processing in SRD-15 and SRD-19 cells was fully resistant to oxysterol-mediated inhibition (*lanes 6 and 8*). A 25-HC resistant, truncated form of nuclear SREBP-2 was observed in the absence of nuclear SREBP-1 for SRD-1 cells (*lanes 9 and 10*). The absence of nuclear SREBP-1 in SRD-1 cells is attributable to the constitutively active SREBP-2 that stimulates overproduction of cholesterol, which in turn prevents SCAP-mediated processing of the membrane-bound SREBP-1 precursor (Yang et al., 2002).

The membrane fractions from CHO-7, SRD-14, SRD-15, and SRD-1 cells contained similar amounts of SCAP that were not affected by the absence or presence of 25-HC (Fig. 4-

5, *bottom panel*, lanes 1-6, 9, and 10). However, a marked increase in SCAP protein was observed in SRD-19 cells (*lanes 7 and 8*). These results led us to conduct a set of experiments to determine the molecular defect that leads to the accumulation of SCAP protein in SRD-19 membranes. Fig. 4-6A shows a Northern blot comparing the amount of SCAP mRNA in CHO-7, SRD-14, SRD-15, SRD-19, and SCAP-deficient SRD-13A cells. The amount of SCAP mRNA was elevated in SRD-19 cells in comparison to wild type CHO-7 and the other SRD cell lines; the levels of SCAP mRNA was not influenced by the presence of 25-HC. Quantitative real-time PCR revealed that SRD-19 cells express >4.5-fold more SCAP mRNA than their wild type CHO-7 counterparts and ~3-fold more than parental SRD-14 cells (Fig. 4-6B). In the experiment shown in Fig. 5-6C, restriction enzyme-digested genomic DNA from CHO-7 and SRD-19 cells was subjected to agarose gel electrophoresis, transferred to nylon membranes, and hybridized with radiolabeled SCAP (*top panel*) or SREBP-2 (*bottom panel*) cDNA probes. Each restriction enzyme digest of CHO-7 and SRD-19 genomic DNA produced fragments of identical size that hybridized with the SCAP and SREBP-2 probes, but the intensities of SCAP-hybridizing fragments were markedly increased in the SRD-19 digests (*top and bottom panels, lanes 1-16*). The intensities of fragments hybridized to the SREBP-2 probe were similar in enzyme-digested genomic DNA from CHO-7 and SRD-19 cells (*bottom panel*). In Fig. 4-6D, various amounts of enzyme digested DNA from CHO-7 and SRD-19 cells were hybridized with radiolabeled SCAP and SREBP-2 cDNA probes. By densitometric scanning, we calculated about a 4-fold increase in the amount of hybridizable reductase DNA in SRD-19 cells as compared to CHO-7 cells.



These results indicate that the SCAP gene is amplified in SRD-19 cells, which likely accounts for the overproduction of SCAP mRNA and protein in the mutant cells.

When transfected cells overexpress SCAP, the Insig proteins become saturated, and 25-HC can no longer inhibit SREBP processing. Oxysterol-mediated inhibition can be restored by co-expression of either Insig-1 (Yang et al., 2002) or Insig-2 (Yabe et al., 2002a). If SCAP overexpression is the primary defect in SRD-19 cells, the regulatory effects of 25-HC should be restored by overexpressing Insig-1 or Insig-2. Thus, SRD-19 cells were transfected with pCMV-Insig-1-Myc or pCMV-Insig-2-Myc, expression plasmids encoding human Insig-1 and Insig-2, respectively, followed by six tandem copies of the c-Myc epitope. Clones that expressed equivalent levels of the Myc-tagged Insig proteins were isolated (Fig. 4-7, *bottom panel*) and analyzed further. As expected, SREBP-2 processing was sensitive to 25-HC in wild type CHO-7 cells (*top panel, lanes 1 and 2*), and resistant to sterol treatment in mock-transfected SRD-19 cells (*lanes 3 and 4*). Overexpression of Insig-1-Myc or Insig-2-Myc in SRD-19 cells restored a complete response to 25-HC (*lanes 5-8*). Overexpression of either Insig in SRD-19 cells also restored 25-HC-mediated suppression of SREBP-1 processing (data not shown).

**TABLE II. Incorporation of [ $^{14}\text{C}$ ] acetate into [ $^{14}\text{C}$ ] cholesterol and  $^{14}\text{C}$ -labeled fatty acids in parental cells and mutant cells resistant to 25-HC**

On day 0, monolayers of cells were set up for experiments at  $1 \times 10^5$  cells per 60-mm dish in medium A supplemented with 5% LPDS. On day 2, the cells were refed the identical medium containing 10  $\mu\text{Ci}/\text{dish}$  [ $^{14}\text{C}$ ] Acetate. After incubation at  $37^\circ\text{C}$  for 2 h, the cells were harvested for measurement of the cellular content of [ $^{14}\text{C}$ ] Cholesterol and  $^{14}\text{C}$ -fatty acids. A blank value, representing the amount of [ $^{14}\text{C}$ ] Acetate incorporated into [ $^{14}\text{C}$ ]-cholesterol (0.15 nmol/h/mg) and  $^{14}\text{C}$ -fatty acids (0.03 nmol/h/mg) in each cell line that was incubated for 2 h at  $4^\circ\text{C}$  was subtracted from each value. Each value is the mean of triplicate incubations.

Cell Lines	Incorporation of [ $^{14}\text{C}$ ] Acetate	
	[ $^{14}\text{C}$ ] Cholesterol	$^{14}\text{C}$ -Fatty Acids
	<i>nmol / h / mg protein</i>	
CHO-7	0.159	0.278
SRD-14	0.396	0.375
SRD-15	0.777	0.937
SRD-19	1.076	1.271

**FIGURE 4-1: Growth of parental and mutant cells in the absence and presence of 25-HC.**

CHO-7, SRD-14, SRD-15, SRD-19, and SRD-1 cells were set up in medium A supplemented with 5% LPDS. On day 1, the cells were washed with PBS and refed medium containing 5% LPDS and the indicated concentration of 25-HC. Cells were refed every 2 days. On day 10, the cells were stained with crystal violet.

FIGURE 4-1

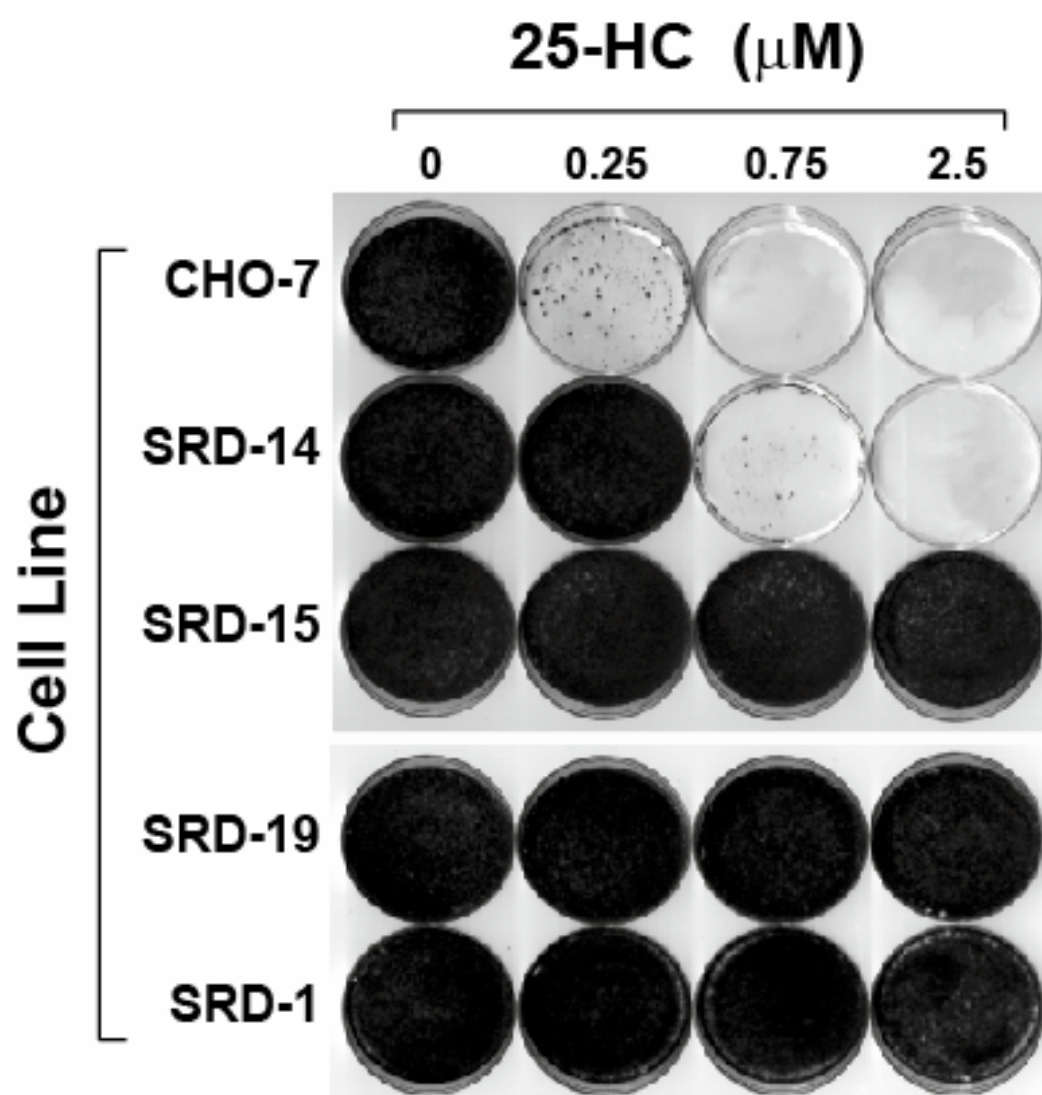
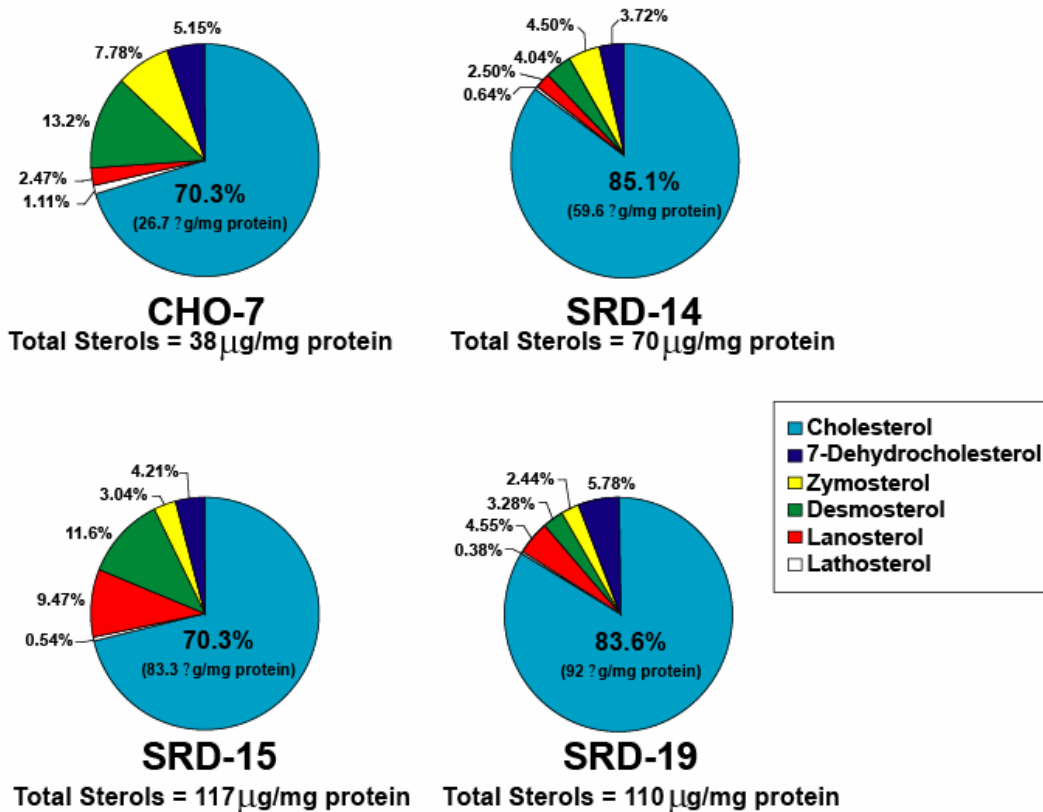


**FIGURE 4-2: Sterol content of wild type CHO-7 and mutant SRD-14, SRD-15, and SRD -19 cells.**

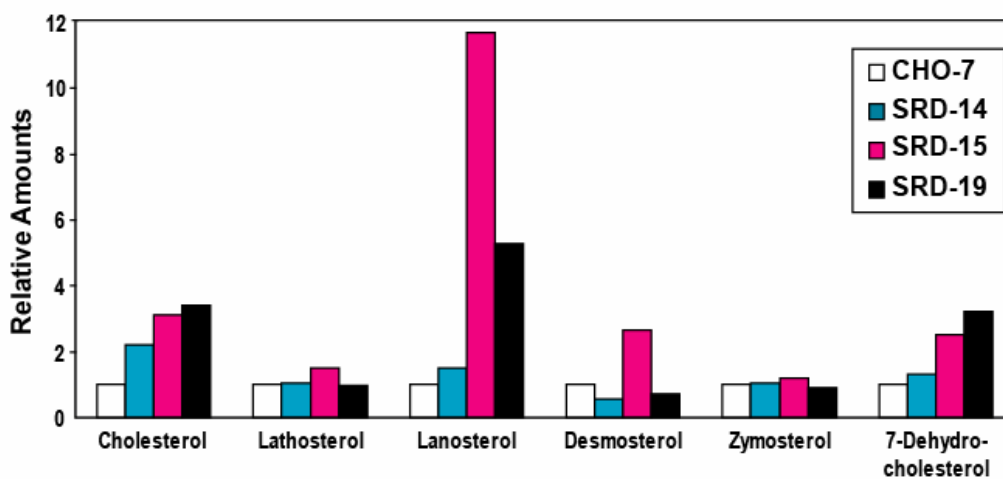
CHO-7, SRD-14, -15, and -19 cells were set up in medium A supplemented with 5% LPDS. On day 3, the cells were harvested, lysed and subjected to GC-MS analysis. In *A*, each sterol is reported as a percentage of total sterols in the various cell lines. In *B*, the values for each sterol are reported relative to those in parental CHO-7 cells, which are arbitrarily set at 1.

FIGURE 4-2

A

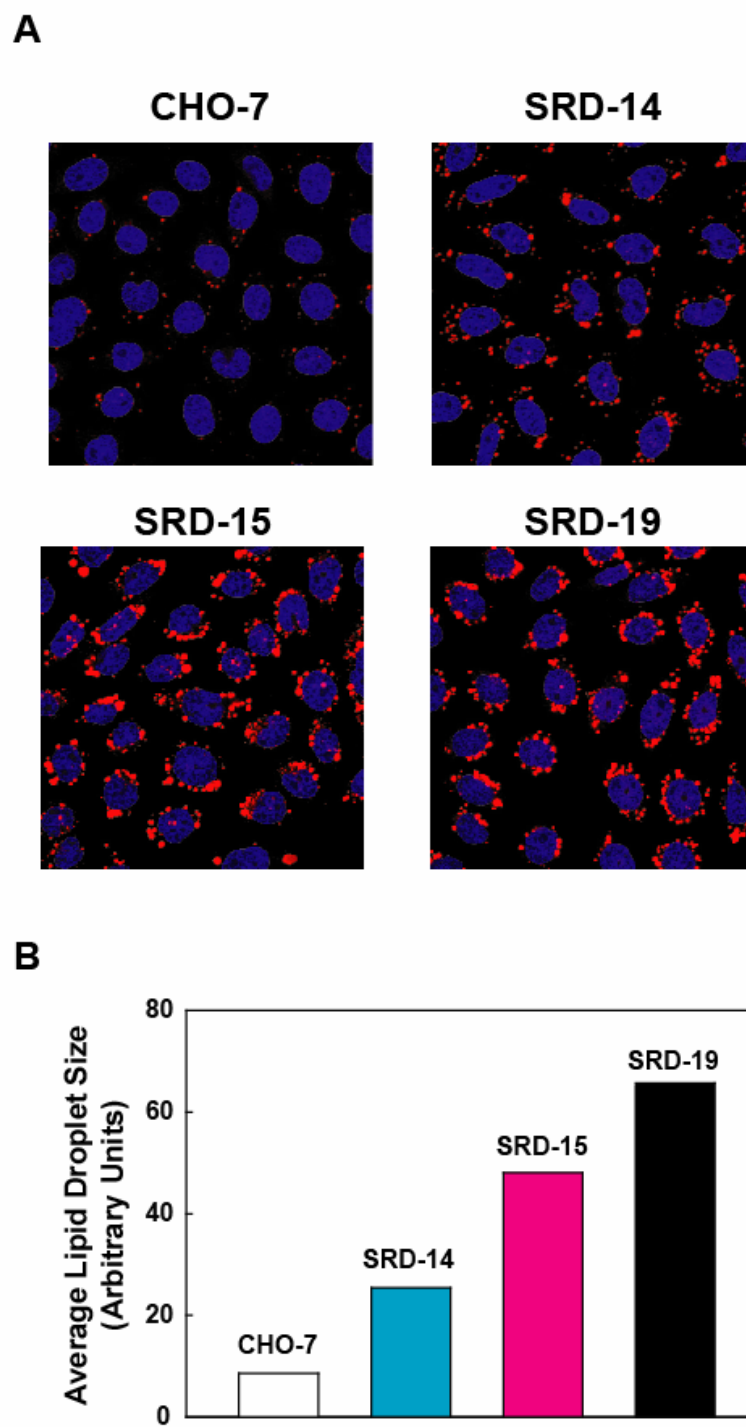


B



**FIGURE 4-3: Accumulation of neutral lipids in CHO-7, SRD-14, SRD-15, and SRD-19 cells as revealed by Oil Red O.**

*A*, on day 0, CHO-7, SRD-14, SRD-15, and SRD-19 cells were set up in medium A supplemented with 5% LPDS. On day 3, the cells were fixed and double stained with DAPI for nuclei (blue) and Oil red O for lipid droplets (red). *B*, images were analyzed using NIH IMAGE J software to determine the average size of lipid droplets in each cell line. Values were calculated by dividing the number particles (representing lipid droplets) by the total number of pixels (representing the total area of lipid droplets).

**FIGURE 4-3**



**FIGURE 4-4: Analysis of lipid isolated from parental CHO-7 and mutant SRD-14, SRD-15, and SRD-19 cells.**

*A*, on day 0, CHO-7, SRD-14, SRD-15, and SRD-19 cells were set up in medium A containing 5% FCS. On day 1, the cells were refed the identical medium containing 100  $\mu\text{Ci}$  [ $^{14}\text{C}$ ]acetate and incubated for an additional 2 day at 37 °C. The cells were subsequently harvested, lysed, and lipid droplet fractions were isolated and analyzed by thin layer chromatography. The percentage of [ $^{14}\text{C}$ ]acetate incorporated into the indicated lipids were determined by scintillation counting. *B*, on day 0, cells were set up at  $1 \times 10^5$  cells per 60-mm dish in medium A containing 5% LPDS. On day 2, the cells were switched to medium A containing 5% LPDS, 50  $\mu\text{M}$  sodium compactin, and 50  $\mu\text{M}$  sodium mevalonate. On day 2, the cells were refed the identical medium with either no addition or the indicated concentrations of LDL or 25-HC. After incubation for 5 h at 37 °C, cells were pulsed for 2 h with 0.2 mM [ $^{14}\text{C}$ ]oleate/albumin (10 dpm/nmol), after which the cells were harvested for measurement of their content of cholesteryl [ $^{14}\text{C}$ ]oleate and  $^{14}\text{C}$ -labeled triglycerides. Each value is the mean of triplicate incubations.

FIGURE 4-4

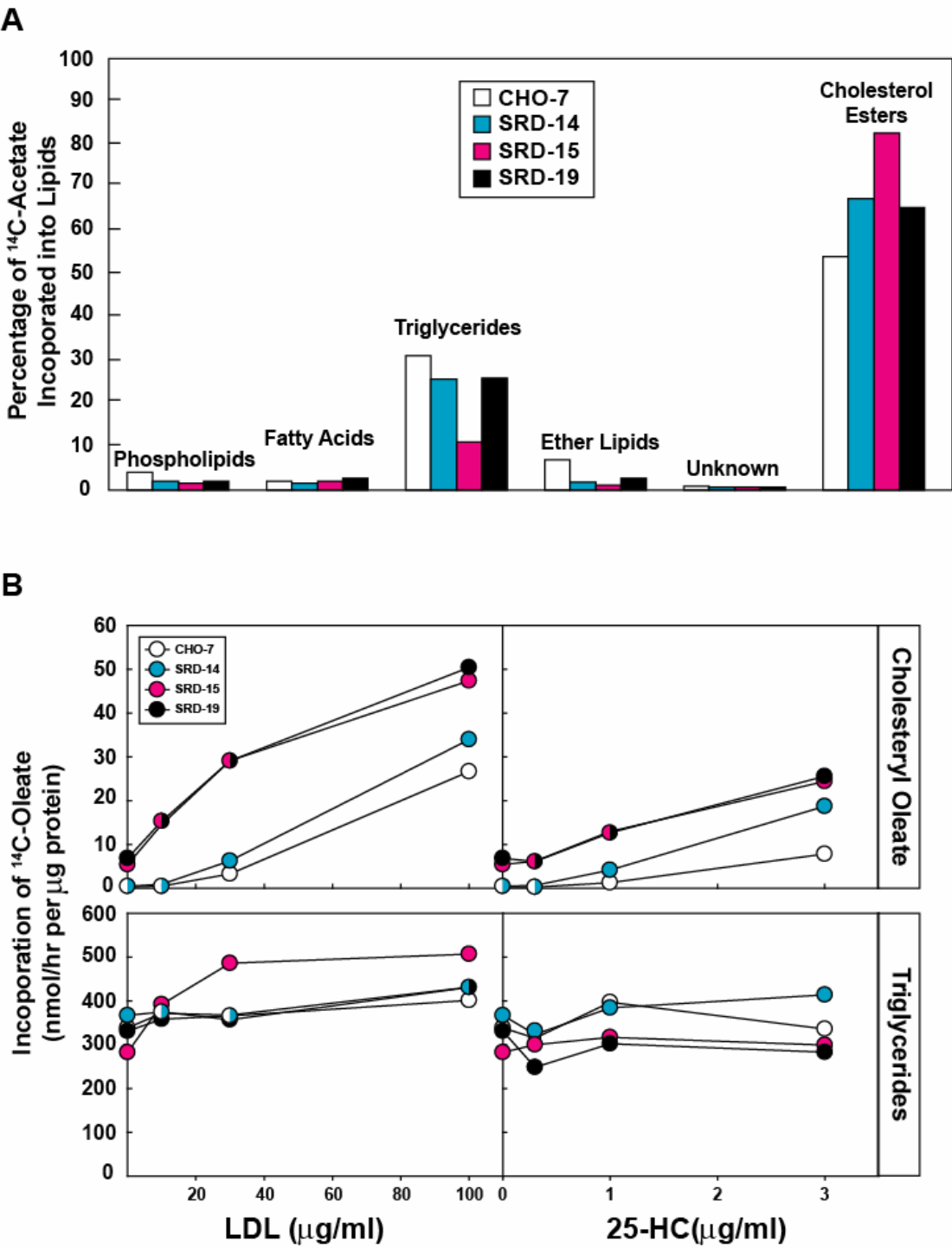


**FIGURE 4-5: Sterol regulation of SREBP processing in wild type and mutant cells.**

On day 0, CHO-7, SRD-14, SRD-15, SRD-19, and SRD-1 cells were set up in medium A supplemented with 5% LPDS. On day 2, the cells were switched to medium A containing 5% LPDS, 10  $\mu$ M compactin, and 50  $\mu$ M mevalonate in the absence or presence of 2.5  $\mu$ M 25-HC. After incubation for 16 hr at 37 °C, the cells were harvested and subjected to cell fractionation. Aliquots of membrane (27  $\mu$ g protein/lane) and nuclear extract (15  $\mu$ g protein/lane) fractions were subjected to SDS-PAGE and Immunoblot analysis with IgG-7D4 (SREBP-2), IgG-2179 (SREBP-1), and IgG-9D5 (SCAP).

FIGURE 4-5

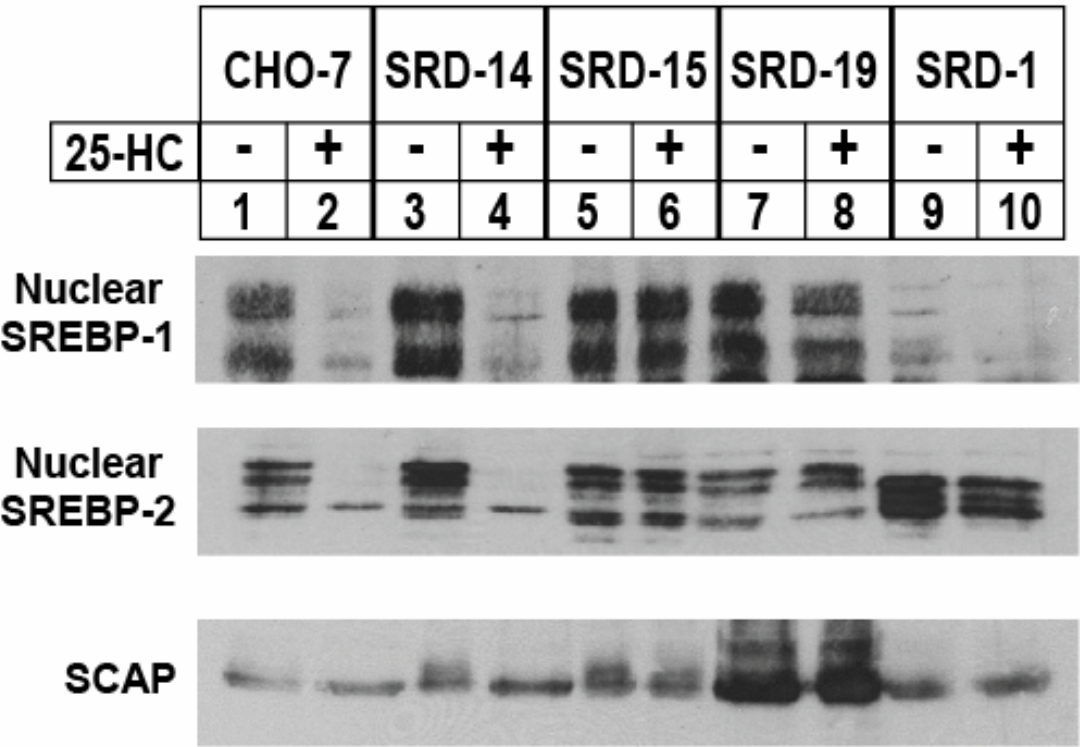


**FIGURE 4-6: Molecular characterization of SCAP mRNA and genomic DNA in parental CHO-7 and mutant SRD-19 cells.**

*A* and *B*, CHO-7, SRD-14, SRD-15, SRD-19, and SRD-13A cells were set up in medium A supplemented with 5% LPDS. On day 2, the cells were switched to medium A containing 10  $\mu$ M compactin and 50  $\mu$ M mevalonate in the absence or presence of 2.5  $\mu$ M 25-HC as indicated. After incubation for 16 hr at 37 °C, the cells were harvested for isolation of total RNA. *A*, aliquots of total RNA (20  $\mu$ g/lane) were subjected to electrophoresis in a denaturing (formaldehyde) gel and transferred to a nylon filter by capillary blotting. The filters were hybridized with the indicated  $^{32}$ P-labeled probe and exposed to film at -80 °C for 4 h (SCAP) and 24 h (GAPDH). *B*, total RNA was subjected to reverse transcription reactions, after which aliquots of the resulting first-strand cDNA was subjected to quantitative real time PCR using specific primers for the indicated genes. The relative amount of mRNA under each condition was normalized to an internal control gene (GAPDH). *C* and *D*, aliquots of genomic DNA (20  $\mu$ g/lane) in *C*; the indicated amount in *D*) from CHO-7 and SRD-19 cells were digested with the indicated restriction enzyme, subjected to electrophoresis on a 1.0% agarose gel, and transferred to nylon filters. Hybridizations were carried out with  $^{32}$ P-labeled cDNA probes corresponding to SCAP (nucleotides 1-697) or SREBP-2 (nucleotides 1-460). The filters were exposed to film at -80 °C for 24 hr (SCAP) and 48 hr (SREBP-2).

FIGURE 4-6

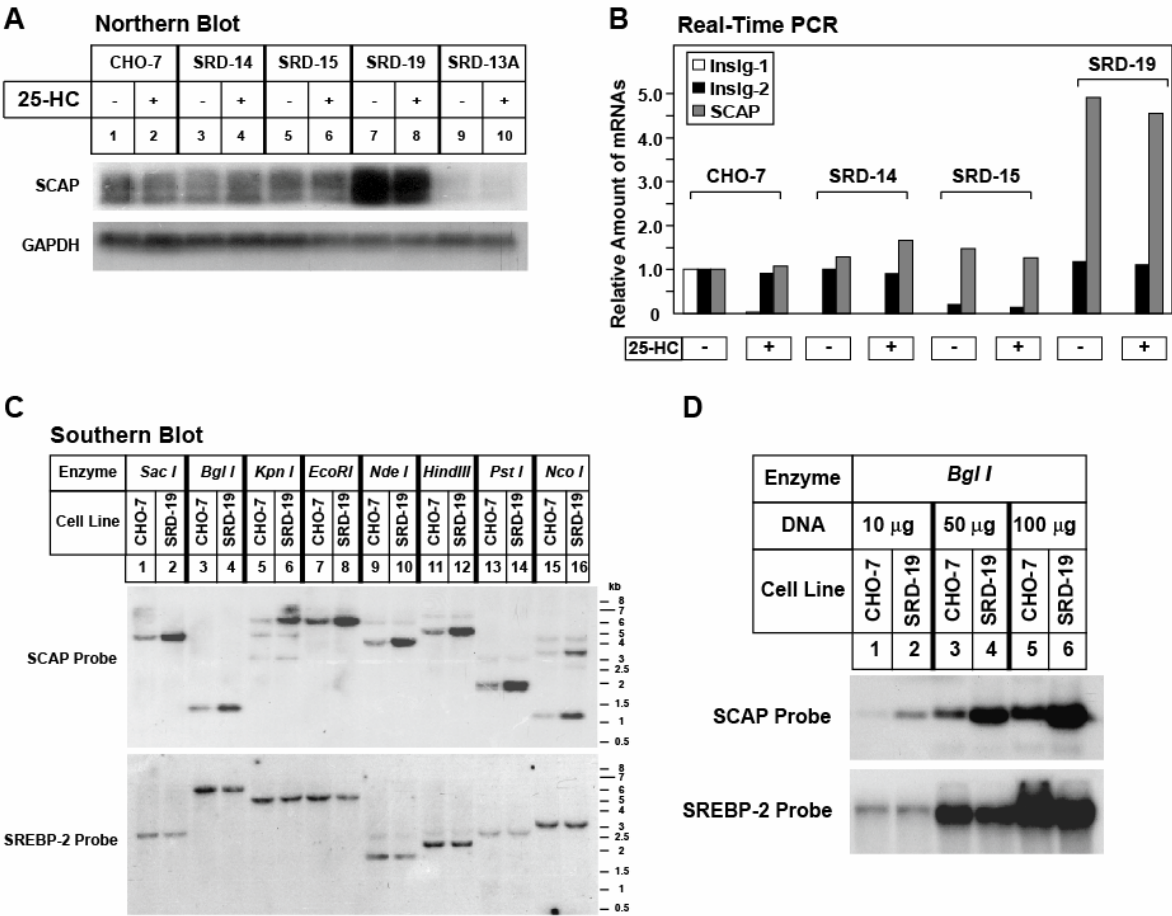
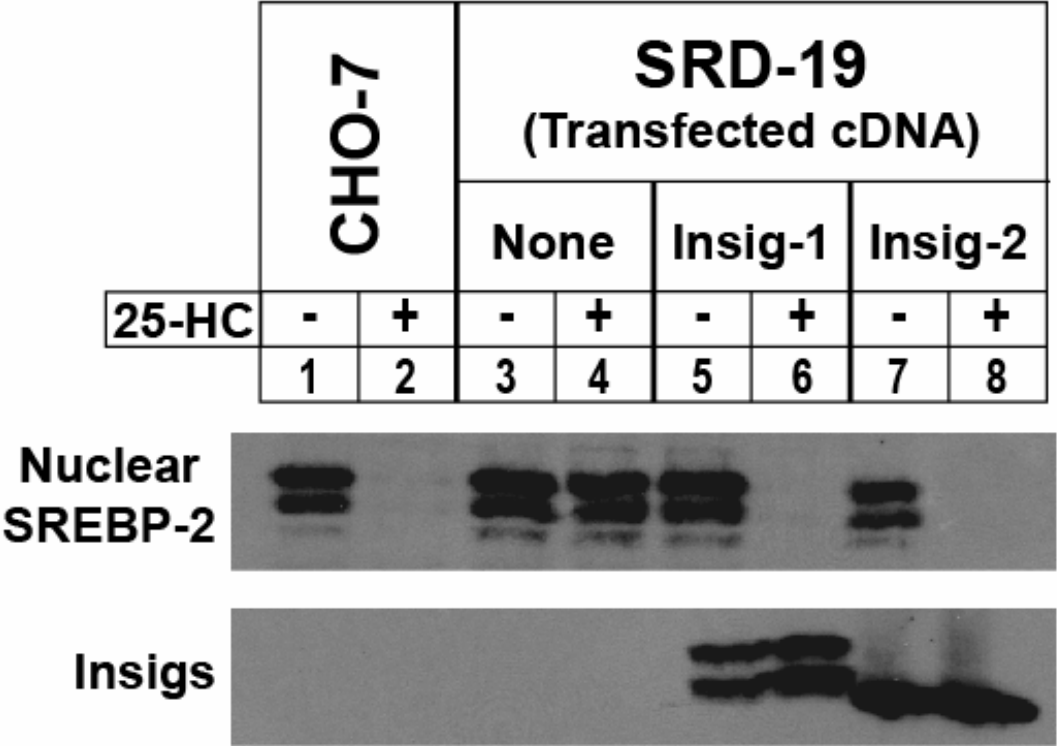


**FIGURE 4-7: Stable transfection of pCMV-Insig-1-Myc or pCMV-Insig-2-Myc restores sterol-mediated suppression of SREBP-2 processing in SRD-19 cells.**

Cells were set up in medium A supplemented with 5% LPDS. On day 2, the cells were switched to medium A containing 5% LPDS, 10  $\mu$ M compactin, and 50  $\mu$ M mevalonate in the absence or presence of 2.5  $\mu$ M 25-HC. After incubation for 16 h at 37 °C, the cells were harvested; membrane and nuclear extract fractions were prepared and subjected to immunoblot analysis with IgG-7D4 (SREBP-2) and IgG-9E10 (Insig-1 or Insig-2).

FIGURE 4-7





## DISCUSSION

The current data describe the characterization of SRD-19 cells, a line of mutant CHO cells that were produced by mutagenesis of Insig-1 deficient SRD-14 cells (Lee et al., 2005), followed by selection for growth in 25-HC (Fig. 4-1). Because of their resistance to 25-HC, SRD-19 cells fail to suppress proteolytic activation of SREBPs upon prolonged treatment with the sterol (Fig. 4-5). This resistance is accompanied by the amplification of the gene encoding *SCAP* (Fig. 4-6C and D), which leads to the overproduction of SCAP mRNA and protein (Fig. 4-5 and 4-6). Although the number of copies of the *SCAP* gene is apparently increased in SRD-19 cells, the gene does not appear to have undergone any gross structural rearrangements, at least at the level that is detectable by the cDNA probe used in the current study.

A reasonable explanation for resistance of SRD-19 cells to 25-HC is that excess SCAP saturates the remaining Insig-2 in the mutant cells. As a result, SREBPs continue to be processed and cholesterol synthesis is not inhibited, even in the presence of 25-HC. Accordingly, SRD-19 cells are resistant to chronic culture in the oxysterol. Evidence in support of this conclusion is provided by the experiment of Fig. 4-7, which shows that overexpression of cDNAs encoding either Insig-1 or Insig-2 restores normal sterol regulation of SREBP processing in SRD-19 cells. Our finding that SCAP overproduction causes resistance of SRD-19 cells to culture in 25-HC is analogous to the resistance of UT-1 cells to growth in the HMG CoA reductase inhibitor compactin. UT-1 cells, a line of mutant CHO cells isolated in 1982 (Chin et al., 1982), grow in the presence of compactin owing to the

>100-fold overproduction of reductase, which results from the amplification and enhanced transcription of the gene encoding the enzyme (Luskey et al., 1983).

Consistent with the partial (SRD-14) and complete (SRD-15 and SRD-19) resistance to 25-HC, rates of cholesterol and fatty acid synthesis were markedly elevated in the mutant cells (Table II). Moreover, an accumulation of total sterol (Fig. 4-2) and neutral lipid content (as determined by Oil Red O staining; Fig. 4-3) was observed in SRD-14, SRD-15, and SRD-19 cells in proportion to their resistance to 25-HC (Fig. 4-5). GC-MS analysis revealed that cholesterol was the most abundant sterol in CHO-7, SRD-14, SRD-15, and SRD-19 cells; levels of the sterol were elevated 2-4 fold in the mutant cells as compared to wild type cells (Fig. 4-2). Several intermediates in the cholesterol biosynthetic pathway were only elevated in SRD-15 and SRD-19 cells. Specifically, lanosterol, the first sterol intermediate in cholesterol synthesis, was elevated 11-fold in SRD-15 and 5-fold in SRD-19 cells. This is an interesting finding with regards to results from a previous study, which suggested that production of lanosterol is a key focal point of the sterol regulatory system (Song et al., 2005a). In normal cells, lanosterol triggers ubiquitination and rapid degradation of HMG CoA reductase, thereby reducing carbon flow through the cholesterol synthetic pathway. Inappropriate accumulation of lanosterol is prevented owing to its inability to block SREBP processing by inhibiting the activity of SCAP. Thus, mRNAs encoding enzymes that catalyze reactions subsequent to lanosterol remain elevated, and lanosterol is metabolized to cholesterol. The accumulation of cholesterol triggers the ER retention of SCAP-SREBP complexes, which leads to the inhibition of SREBP processing and ultimately shuts down the entire cholesterol synthetic pathway. In SRD-15 and SRD-19 cells, this feedback regulation

is lost and as a result, cholesterol and its sterol precursors accumulate inappropriately. It should be noted that C-14 demethylation, the initial step in conversion of lanosterol to cholesterol, has been implicated as a rate-limiting step in cholesterol synthesis. This might help to explain the selective increase in the level of lanosterol in SRD-15 and SRD-19 cells. Alternatively, Insigs (whose activities are reduced in SRD-15 and SRD-19 cells) may directly or indirectly participate in the demethylation of lanosterol. Future studies will be aimed toward resolving these issues.

Three types of mutant CHO cells have been classified as resistant to 25-HC owing to their failure to suppress cholesterol synthesis under conditions of sterol overload (Goldstein et al., 2002; Lee et al., 2005). Type 1 mutants express truncated forms of SREBP-2 that migrate to the nucleus and activate gene transcription regardless of sterol treatment. Type 2 mutants express forms of SCAP that harbor point mutation in the sterol-sensing domain that prevents binding to Insigs. These mutant forms of SCAP continue to transport SREBPs to the Golgi even when cells are overloaded with sterols. Type 3 mutants have deficiencies in Insig-1 and Insig-2 and as a result, both reductase and SCAP are refractory to sterol regulation. Data from the current study demonstrate that SRD-19 cells represent a fourth type of 25-HC-resistant cells. SRD-19 cells have exploited the stoichiometric relationship between Insigs and their targets (reductase and SCAP) by overproducing SCAP. The overexpressed SCAP saturates the remaining Insig-2 in SRD-19 cells, rendering them refractory to sterol regulation. The other 19 cell lines isolated in the same mutagenesis/selection experiment that yielded SRD-19 cells were deficient in Insig-1 and Insig-2. Considering that 1) the other 19 cell lines isolated in the same mutagenesis/selection experiment that yielded SRD-19 cells

were deficient in Insig-1 and Insig-2; and 2) the unbiased selection for 25-HC resistance in these experiments, it is likely that the spectrum of proteins participating in Insig-mediated regulation of sterol metabolism is known and our knowledge of mechanism underlying the process is near completion.

## CONCLUSION AND PERSPECTIVE

Somatic cell genetics has proven invaluable in illuminating the complex pathway for lipid homeostasis that is controlled by the SREBP pathway (Goldstein *et al.*, 2002). The identity and function of the following proteins has been in some way revealed by somatic cell genetics through studies using mutant Chinese hamster ovary cells; HMG CoA reductase, HMG CoA Synthesis, SCAP, SREBP, ACAT, S1P, S2P and others (Chang *et al.*, 1993a; Chin *et al.*, 1982; Hua *et al.*, 1996; Luskey *et al.*, 1983; Rawson *et al.*, 1999; Rawson *et al.*, 1997; Sakai *et al.*, 1998).

In the past, mutagenized CHO cells were selected by chronic treatment in the presence of 25-HC, a potent inhibitor of cholesterol synthesis because of its ability to accelerate degradation of reductase and block proteolytic activation of SREBPs (Brown and Goldstein, 1999; Nohturfft *et al.*, 2000; Wang *et al.*, 1994). The oxysterol is toxic to wild type cells because it cannot substitute for cholesterol as a structural membrane component, and cells die unless a source of cholesterol is supplied exogenously. Mutant cells survive chronic 25-HC treatment because they do not turn off cholesterol synthesis in the presence of oxysterols, forming the genetic basis for their isolation. However, the sterol-resistant mutants isolated to date either harbored point mutations in the sterol-sensing domain of SCAP or produced abnormal truncated versions of SREBP-2 that enter the nucleus without requiring proteolysis (Dawson *et al.*, 1991; Hua *et al.*, 1996; Yabe *et al.*, 2002b; Yang *et al.*, 1995; Yang *et al.*, 1994). Thus, to facilitate the isolation of mutant cells incapable of accelerating reductase degradation, selection of mutagenized cells was carried out with a reagent that replaces sterols to promote reductase degradation but not ER retention of SCAP. The hypocholesterolemic

activity of 1,1-bisphosphonate esters such as SR-12813, and its structurally related analog, Apomine, has been well documented (Berkhout et al., 1997; Berkhout et al., 1996; Roitelman et al., 2004). In cultured cells, these drugs decrease reductase activity by accelerating degradation of the enzyme, which triggers an increase in the expression of LDL receptors, thus explaining the hypocholesterolemic activity of the drugs when administered orally to animals. The effects of SR-12813 on reductase appear similar to those of oxysterols; however, unlike oxysterols, SR-12813 treatment does not reduce but rather enhances mRNAs for reductase and the LDL receptor. In the current studies, we evaluated the utility of SR-12813 as a selecting agent in mutagenesis experiments aimed toward isolating mutant cells incapable of accelerating reductase degradation but having normal regulation of SREBP processing.

In Chapter 1, SRD-14 cells were produced by  $\gamma$ -irradiation of CHO cells, followed by selection in medium supplemented with SR-12813. SRD-14 was found to harbor a partial deletion of the *INSIG-1* gene. SRD-14 cells cannot accelerate reductase degradation in response to sterols or SR-12813, and the rate of sterol-mediated suppression of SREBP processing in the cells is dramatically reduced. Resistance to SR-12813 and 25-HC was completely corrected by the overexpression of either Insig-1 or Insig-2. The experiments with the SRD-14 cells provide formal genetic proof of the essential role Insigs play in not only reductase degradation but also the ER retention of SCAP·SREBP. Although 25-HC did block SREBP processing, which effect required a longer exposure to the oxysterol in SRD-14 cells as compared with wild-type cells. Considering that in wild-type CHO cells Insig-1

accounts for ~90% of total Insigs, we proposed that the remaining Insig-2 was sufficient to maintain partial sterol regulation of SCAP-SREBP but not reductase.

In Chapter 2, I describe the generation, isolation, and characterization of mutagenized SRD-14 cells that are totally resistant to 25-HC. This cell line, designated SRD-15, was found to harbor a deletion of one allele of the *INSIG-2* gene, and Insig-2 mRNA expression was reduced to less than 20% of wild-type cells. As a result of their combined deficiencies in Insig-1 (100% deficiency) and Insig-2 (80% deficiency), SRD-15 cells were completely refractory to sterol-mediated actions on SREBP processing, as well as reductase degradation. The experiments with the SRD-15 cells provide genetic proof that cells require at least one Insig protein in order to exhibit normal feedback regulation of cholesterol metabolism. Twenty sterol-resistant cell lines were obtained through this procedure; 19 of them were deficient in Insig-2 and one was designated SRD-15. The remaining cell line, which produced normal levels of Insig-2, was not further characterized.

In Chapter 3, I describe the characterization of three mutant SR-12813-resistant CHO cell lines, in which reductase is resistant to ubiquitination and degradation mediated not only by SR-12813 but by sterols as well. In contrast, the mutant cells retain their sensitivity to the sterol-mediated suppression of SREBP processing. In all three mutant cell lines, resistance was traced to point mutations within the membrane domain of reductase that resulted in substitutions of aspartate for serine-60, arginine for glycine-87, and proline for alanine-333. Overexpression of the S60N, G87R, or A333P versions of reductase conferred the resistance of wild-type cells to chronic culture in SR-12813, demonstrating the dominant nature of each mutation. Moreover, all three mutant forms of reductase were refractory to sterol-mediated

ubiquitination and degradation, owing to decreased affinity for Insigs. These results highlight the importance of interactions between Insigs and the membrane domain of reductase in the feedback control of a rate-determining step in cholesterol synthesis.

In Chapter 4, I characterized the remaining 25-HC-resistant CHO cell line, derived from mutagenesis and selection of SRD-14 cells, which continue to produce Insig-2. This cell line, designated SRD-19, was found to have exploited the stoichiometric requirement of Insigs by overproducing SCAP. Indeed, the SCAP gene is amplified and the mRNA is overproduced 4-fold in SRD-19 cells.

These studies demonstrate 1) absolute requirement for Insig proteins in the regulatory system that mediates lipid homeostasis in animal cells; 2) the importance of interactions between Insigs and the membrane domain of reductase in feedback control of a rate-determining step in cholesterol synthesis; 3) SCAP-Insig ratios are key for normal regulated processing of SREBPS.

Until now, two types of mutant CHO cells have been classified as resistant to 25-HC in that they fail to suppress cholesterol synthesis under conditions of sterol overload and survive chronic oxysterol treatment (Goldstein *et al.*, 2002). Type 1 mutants occur in the SREBP-2 gene, producing truncated SREBP-2 that terminates before the first transmembrane segment and therefore constitutively travels to the nucleus. Type 2 mutants are point mutations, Y298C, L315F and D443N, which are in the sterol-sensing domain of SCAP. These mutations render mutant SCAP refractory to sterol regulation; therefore it escorts SREBPs from the ER to the Golgi even when the cells are overloaded with sterols. It should be noted that both Type 1 and Type 2 sterol-resistant mutants exhibit a dominant phenotype.



Data in the current studies demonstrate that the SRD-14 and SRD-15 cells represent a new type of mutant CHO cells designated as Type 3 sterol-resistant mutants. Type 3 sterol-resistant mutants have been traced to their deficiencies in either Insig-1 or both Insigs. However, unlike other sterol-resistant mutants, the phenotype of the Type 3 mutants is recessive due to their lack of both Insig-1 and Insig-2.

So far, recessive mutant cells have been difficult to characterize due to the lack of available compounds to carry out appropriage screens. One candidate compound is Amphotericin B, which is a polyene antibiotic that kills the cells by binding to cholesterol and forming pores in the plasma membrane (Cadigan et al., 1988). The cellular levels of cholesterol content in mutant cells that survive in 25-HC or SR-12813 are higher than in wild-type cells and rendered more sensitive to amphotericin B cytotoxicity. Cell fusion studies can determine the dominant or recessive phenotype. For instance, SR-128313 selected mutant cells stably transfected with *neo* can be fused to wild-type cells stably transfected with *zeo* and select with *neo*, *zeo* with or without SR-12813. Dominant cells can survive in the presence of SR-123813 while recessive cells cannot. Based on this strategy, recessive cells can be stably transfected with wild-type expression library and selected by amphotericin B treatment. However, this method has been limited because 1) chronic treatment also kills wild-type cells, 2) cells differ in kinetic response to amphotericin B, and 3) the difficulty of isolating the complementation gene.

Perhaps the use of retrovirus system such as the ROSA  $\beta$ -geo retroviral promoter trap (Friedrich and Soriano, 1991; Zambrowicz et al., 1997) can overcome the difficulty fo isolating the complementation gene. Gene traps are based on the integration of a reporter

gene,  $\beta$ -galactosidase ( $\beta$ -gal), lacking a promoter into the genome and its expression from a tagged endogenous promoter (Fig. 4). The vectors appear to be effective mutagens. Single gene mutation frequencies are 100–1000 fold higher in cells isolated after gene trap selection than in cells containing randomly integrated retroviruses (Chang et al., 1993b). When a gene trap vector integrates into expressed genes, insertional mutants can be easily selected by a selectable phenotype conferred by the gene trap vector. The fusion transcript also serves as the template for PCR-based cloning by 5'-RACE. To date, a number of mutant cells have been isolated with gene trap mutagenesis. For instance, OVCA1, a tumor suppressor gene, has been identified as a component of the biosynthetic pathway of diphthamide, which is a target of bacterial ADP-ribosylating toxins (Nobukuni et al., 2005). Also, another study demonstrated elongation factor 1A1-1 plays a critical role in oxidative and ER stress during fatty acids overload-induced death in cardiomyocytes (Borradaile et al., 2006). These studies encourage us to apply gene trap mutagenesis and selection with SR-12813 or 25-HC to identify additional regulatory proteins of the cholesterol biosynthetic pathway.

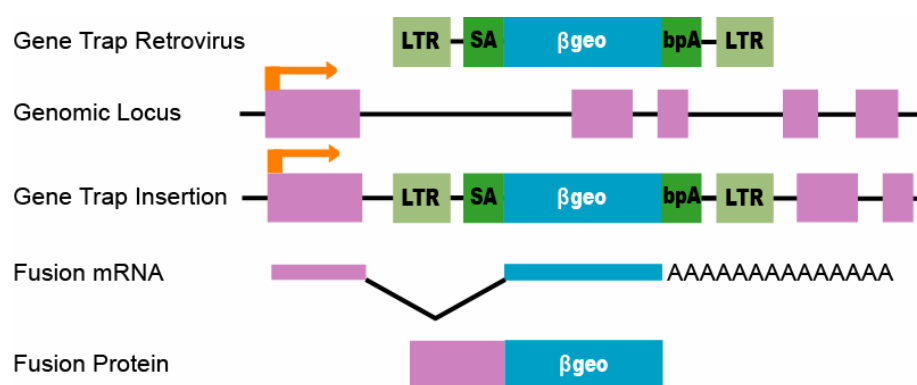


**FIGURE 4: Gene Trap Vector.**

Slice Acceptor (SA), Long Terminal Repeat (LTR),  $\beta$ geo (encodes a  $\beta$ galactosidase-neomycin phosphotransferase fusion protein), polyadenylation (bpA)

## BIBLIOGRAPHY

Adams, C. M., Reitz, J., De Brabander, J. K., Feramisco, J. D., Li, L., Brown, M. S., and Goldstein, J. L. (2004). Cholesterol and 25-Hydroxycholesterol Inhibit Activation of SREBPs by Different Mechanisms, Both Involving SCAP and Insigs. *J Biol Chem* 279, 52772-52780.

Berkhout, T. A., Simon, H. M., Jackson, B., Yates, J., Pearce, N., Groot, P. H. E., Bentzen, C., Niesor, E., Kerns, W. D., and Suckling, K. E. (1997). SR-12813 lowers plasma cholesterol in beagle dogs by decreasing cholesterol biosynthesis. *Atherosclerosis* 133, 203-212.

Berkhout, T. A., Simon, H. M., Patel, D. D., Bentzen, C., Niesor, E., Jackson, B., and Suckling, K. E. (1996). The Novel Cholesterol-lowering Drug SR-12813 Inhibits Cholesterol Synthesis via an Increased Degradation of 3-Hydroxy-3-methylglutaryl-coenzyme A Reductase. *J Biol Chem* 271, 14376-14382.

Borradaile, N. M., Buhman, K. K., Listenberger, L. L., Magee, C. J., Morimoto, E. T. A., Ory, D. S., and Schaffer, J. E. (2006). A Critical Role for Eukaryotic Elongation Factor 1A-1 in Lipotoxic Cell Death. *Mol Biol Cell* 17, 770-778.

Brown, M. S., Faust, J. R., and Goldstein, J. L. (1978). Induction of 3-hydroxy-3-methylglutaryl coenzyme A reductase activity in human fibroblasts incubated with compactin (ML-236B), a competitive inhibitor of the reductase. *J Biol Chem* 253, 1121-1128.

Brown, M. S., and Goldstein, J. L. (1980). Multivalent feedback regulation of HMG CoA reductase, a control mechanism coordinating isoprenoid synthesis and cell growth. *J Lipid Res* 21, 505-517.

Brown, M. S., and Goldstein, J. L. (1996). Heart Attacks: Gone with the Century? *Science* 272, 629-620.

Brown, M. S., and Goldstein, J. L. (1997). The SREBP Pathway: Regulation of Cholesterol Metabolism by Proteolysis of a Membrane-Bound Transcription Factor. *Cell* 89, 331-340.

Brown, M. S., and Goldstein, J. L. (1999). A proteolytic pathway that controls the cholesterol content of membranes, cells, and blood. *PNAS* 96, 11041-11048.

Cadigan, K. M., Heider, J. G., and Chang, T. Y. (1988). Isolation and characterization of Chinese hamster ovary cell mutants deficient in acyl-coenzyme A:cholesterol acyltransferase activity. *J Biol Chem* 263, 274-282.

Chang, C. C., Huh, H. Y., Cadigan, K. M., and Chang, T. Y. (1993a). Molecular cloning and functional expression of human acyl-coenzyme A:cholesterol acyltransferase cDNA in mutant Chinese hamster ovary cells. *J Biol Chem* 268, 20747-20755.

Chang, W., Hubbard, S. C., Friedel, C., and Ruley, H. E. (1993b). Enrichment of Insertional Mutants Following Retrovirus Gene Trap Selection. *Virology* 193, 737-747.

Chin, D. J., Luskey, K. L., Anderson, R. G. W., Faust, J. R., Goldstein, J. L., and Brown, M. S. (1982). Appearance of Crystalloid Endoplasmic Reticulum in Compactin-Resistant Chinese Hamster Cells with a 500-Fold Increase in 3-hydroxy-3-methylglutaryl-coenzyme A Reductase. *PNAS* 79, 1185-1189.

Dawson, P. A., Metherall, J. E., Ridgway, N. D., Brown, M. S., and Goldstein, J. L. (1991). Genetic distinction between sterol-mediated transcriptional and posttranscriptional control of 3-hydroxy-3-methylglutaryl-coenzyme A reductase. *J Biol Chem* 266, 9128-9134.

DeBose-Boyd, R. A., Brown, M. S., Li, W.-P., Nohturfft, A., Goldstein, J. L., and Espenshade, P. J. (1999). Transport-Dependent Proteolysis of SREBP: Relocation of Site-1 Protease from Golgi to ER Obviates the Need for SREBP Transport to Golgi. *Cell* 99, 703-712.

Engelking, L. J., Kuriyama, H., Hammer, R. E., Horton, J. D., Brown, M. S., Goldstein, J. L., and Liang, G. (2004). Overexpression of Insig-1 in the livers of transgenic mice inhibits SREBP processing and reduces insulin-stimulated lipogenesis. *J Clin Invest* 113, 1168-1175.

Fang, S., Ferrone, M., Yang, C., Jensen, J. P., Tiwari, S., and Weissman, A. M. (2001). The tumor autocrine motility factor receptor, gp78, is a ubiquitin protein ligase implicated in degradation from the endoplasmic reticulum. *PNAS* 98, 14422-14427.

Friedrich, G., and Soriano, P. (1991). Promoter traps in embryonic stem cells: a genetic screen to identify and mutate developmental genes in mice. *Genes Dev* 5, 1513-1523.

Gil, G., Faust, J. R., Chin, D. J., Goldstein, J. L., and Brown, M. S. (1985). Membrane-bound domain of HMG CoA reductase is required for sterol-enhanced degradation of the enzyme. *Cell* 41, 249-258.

Goldstein, J. L., Basu, S. K., and Brown, M. S. (1983). Receptor-mediated endocytosis of low-density lipoprotein in cultured cells. *Methods Enzymol* 98, 241-260.

Goldstein, J. L., and Brown, M. S. (1990). Regulation of the mevalonate pathway. *Nature* 343, 425-430.

Goldstein, J. L., DeBose-Boyd, R. A., and Brown, M. S. (2006). Protein Sensors for Membrane Sterols. *Cell* 124, 35-46.

Goldstein, J. L., Rawson, R. B., and Brown, M. S. (2002). Mutant Mammalian Cells as Tools to Delineate the Sterol Regulatory Element-Binding Protein Pathway for Feedback Regulation of Lipid Synthesis. *Archives of Biochemistry and Biophysics* 397, 139-148.

Horton, J. D., Goldstein, J. L., and Brown, M. S. (2002). SREBPs: activators of the complete program of cholesterol and fatty acid synthesis in the liver. *J Clin Invest* 109, 1125-1131.

Hua, X., Nohturfft, A., Goldstein, J. L., and Brown, M. S. (1996). Sterol Resistance in CHO Cells Traced to Point Mutation in SREBP Cleavage-Activating Protein. *Cell* 87, 415-426.

Ikonen, E. (2006). Mechanisms for Cellular Cholesterol Transport: Defects and Human Disease. *Physiol Rev* 86, 1237-1261.

Kita, T., Brown, M., and Goldstein, J. (1980). Feedback regulation of 3-hydroxy-3-methylglutaryl coenzyme A reductase in livers of mice treated with mevinolin, a competitive inhibitor of the reductase. *J Clin Invest* 66, 1094-1100.

Kuwabara, P. E., and Labouesse, M. (2002). The sterol-sensing domain: multiple families, a unique role? *Trends in Genetics* 18, 193-201.

Lee, J. N., Song, B., DeBose-Boyd, R. A., and Ye, J. (2006). Sterol-regulated Degradation of Insig-1 Mediated by the Membrane-bound Ubiquitin Ligase gp78. *J Biol Chem* 281, 39308-39315.

Lee, P. C. W., Nguyen, A. D., and DeBose-Boyd, R. A. (2007). Mutations within the membrane domain of HMG-CoA reductase confer resistance to sterol-accelerated degradation. *J Lipid Res* 48, 318-327.

Lee, P. C. W., Sever, N., and DeBose-Boyd, R. A. (2005). Isolation of Sterol-resistant Chinese Hamster Ovary Cells with Genetic Deficiencies in Both Insig-1 and Insig-2. *J Biol Chem* 280, 25242-25249.

Liang, G., Yang, J., Horton, J. D., Hammer, R. E., Goldstein, J. L., and Brown, M. S. (2002). Diminished Hepatic Response to Fasting/Refeeding and Liver X Receptor Agonists in Mice with Selective Deficiency of Sterol Regulatory Element-binding Protein-1c. *J Biol Chem* 277, 9520-9528.

Libby, P., Aikawa, M., and Schonbeck, U. (2000). Cholesterol and atherosclerosis. *Biochimica et Biophysica Acta (BBA) - Molecular and Cell Biology of Lipids* 1529, 299-309.

Liscum, L., Finer-Moore, J., Stroud, R. M., Luskey, K. L., Brown, M. S., and Goldstein, J. L. (1985). Domain structure of 3-hydroxy-3-methylglutaryl coenzyme A reductase, a glycoprotein of the endoplasmic reticulum. *J Biol Chem* 260, 522-530.

Liscum, L., Luskey, K. L., Chin, D. J., Ho, Y. K., Goldstein, J. L., and Brown, M. S. (1983). Regulation of 3-hydroxy-3-methylglutaryl coenzyme A reductase and its mRNA in rat liver as studied with a monoclonal antibody and a cDNA probe. *J Biol Chem* 258, 8450-8455.

Liu, P., Ying, Y., Zhao, Y., Mundy, D. I., Zhu, M., and Anderson, R. G. W. (2004). Chinese Hamster Ovary K2 Cell Lipid Droplets Appear to Be Metabolic Organelles Involved in Membrane Traffic. *J Biol Chem* 279, 3787-3792.

Luskey, K. L., Faust, J. R., Chin, D. J., Brown, M. S., and Goldstein, J. L. (1983). Amplification of the gene for 3-hydroxy-3-methylglutaryl coenzyme A reductase, but not for the 53-kDa protein, in UT-1 cells. *J Biol Chem* 258, 8462-8469.

Metherall, J. E., Goldstein, J. L., Luskey, K. L., and Brown, M. S. (1989). Loss of transcriptional repression of three sterol-regulated genes in mutant hamster cells. *J Biol Chem* 264, 15634-15641.

Nakanishi, M., Goldstein, J. L., and Brown, M. S. (1988). Multivalent control of 3-hydroxy-3-methylglutaryl coenzyme A reductase. Mevalonate-derived product inhibits translation of mRNA and accelerates degradation of enzyme. *J Biol Chem* 263, 8929-8937.

Nobukuni, Y., Kohno, K., and Miyagawa, K. (2005). Gene Trap Mutagenesis-based Forward Genetic Approach Reveals That the Tumor Suppressor OVCA1 Is a Component of the Biosynthetic Pathway of Diphthamide on Elongation Factor 2. *J Biol Chem* 280, 10572-10577.

Nohturfft, A., Brown, M. S., and Goldstein, J. L. (1998). Topology of SREBP Cleavage-activating Protein, a Polytopic Membrane Protein with a Sterol-sensing Domain. *J Biol Chem* 273, 17243-17250.

Nohturfft, A., Yabe, D., Goldstein, J. L., Brown, M. S., and Espenshade, P. J. (2000). Regulated Step in Cholesterol Feedback Localized to Budding of SCAP from ER Membranes. *Cell* 102, 315-323.

Ponting, C. P. (2000). Proteins of the endoplasmic-reticulum-associated degradation pathway: domain detection and function prediction. *Biochem J* 351, 527-535.

Rawson, R. B., Cheng, D., Brown, M. S., and Goldstein, J. L. (1998). Isolation of Cholesterol-requiring Mutant Chinese Hamster Ovary Cells with Defects in Cleavage of Sterol Regulatory Element-binding Proteins at Site 1. *J Biol Chem* 273, 28261-28269.



Rawson, R. B., DeBose-Boyd, R., Goldstein, J. L., and Brown, M. S. (1999). Failure to Cleave Sterol Regulatory Element-binding Proteins (SREBPs) Causes Cholesterol Auxotrophy in Chinese Hamster Ovary Cells with Genetic Absence of SREBP Cleavage-activating Protein. *J Biol Chem* 274, 28549-28556.

Rawson, R. B., Zelenski, N. G., Nijhawan, D., Ye, J., Sakai, J., Hasan, M. T., Chang, T. Y., Brown, M. S., and Goldstein, J. L. (1997). Complementation Cloning of S2P, a Gene Encoding a Putative Metalloprotease Required for Intramembrane Cleavage of SREBPs. *Molecular Cell* 1, 47-57.

Roitelman, J., Masson, D., Avner, R., Ammon-Zufferey, C., Perez, A., Guyon-Gellin, Y., Bentzen, C. L., and Niesor, E. J. (2004). Apomine, a Novel Hypocholesterolemic Agent, Accelerates Degradation of 3-Hydroxy-3-methylglutaryl-coenzyme A Reductase and Stimulates Low Density Lipoprotein Receptor Activity. *J Biol Chem* 279, 6465-6473.

Roitelman, J., Olender, E. H., Bar-Nun, S., Dunn, W. A., Jr., and Simoni, R. D. (1992). Immunological evidence for eight spans in the membrane domain of 3- hydroxy-3-methylglutaryl coenzyme A reductase: implications for enzyme degradation in the endoplasmic reticulum. *J Cell Biol* 117, 959-973.

Roitelman, J., and Simoni, R. D. (1992). Distinct sterol and nonsterol signals for the regulated degradation of 3-hydroxy-3-methylglutaryl-CoA reductase. *J Biol Chem* 267, 25264-25273.

Russell, D. W. (1999). Nuclear Orphan Receptors Control Cholesterol Catabolism. *Cell* 97, 539-542.

Sakai, J., Nohturfft, A., Cheng, D., Ho, Y. K., Brown, M. S., and Goldstein, J. L. (1997). Identification of Complexes between the COOH-terminal Domains of Sterol Regulatory

Element-binding Proteins (SREBPs) and SREBP Cleavage-Activating Protein. *J Biol Chem* 272, 20213-20221.

Sakai, J., Rawson, R. B., Espenshade, P. J., Cheng, D., Seegmiller, A. C., Goldstein, J. L., and Brown, M. S. (1998). Molecular Identification of the Sterol-Regulated Luminal Protease that Cleaves SREBPs and Controls Lipid Composition of Animal Cells. *Molecular Cell* 2, 505-514.

Sato, R., Goldstein, J. L., and Brown, M. S. (1993). Replacement of Serine-871 of Hamster 3-Hydroxy-3-Methylglutaryl-CoA Reductase Prevents Phosphorylation by AMP-Activated Kinase and Blocks Inhibition of Sterol Synthesis Induced by ATP Depletion. *PNAS* 90, 9261-9265.

Sever, N., Lee, P. C. W., Song, B.-L., Rawson, R. B., and DeBose-Boyd, R. A. (2004). Isolation of Mutant Cells Lacking Insig-1 through Selection with SR-12813, an Agent That Stimulates Degradation of 3-Hydroxy-3-methylglutaryl-Coenzyme A Reductase. *J Biol Chem* 279, 43136-43147.

Sever, N., Song, B.-L., Yabe, D., Goldstein, J. L., Brown, M. S., and DeBose-Boyd, R. A. (2003a). Insig-dependent Ubiquitination and Degradation of Mammalian 3-Hydroxy-3-methylglutaryl-CoA Reductase Stimulated by Sterols and Geranylgeraniol. *J Biol Chem* 278, 52479-52490.

Sever, N., Yang, T., Brown, M. S., Goldstein, J. L., and DeBose-Boyd, R. A. (2003b). Accelerated Degradation of HMG CoA Reductase Mediated by Binding of Insig-1 to Its Sterol-Sensing Domain. *Molecular Cell* 11, 25-33.

Shimizua, b. K., Tania, M., Watanabec, H., Nagamachia, Y., Niinakad, Y., Shiroishie, T., Ohwadab, S., Razd, A., and Yokotaa, J. (1999). The autocrine motility factor receptor gene

encodes a novel type of seven transmembrane protein<sup>11</sup>The nucleotide sequence data reported in the paper will appear in the GenBank/EMBL/DDBJ database with the accession numbers AF124144 and AF124145. *FEBS Letters* 456, 295-300.

Skalnik, D. G., Narita, H., Kent, C., and Simoni, R. D. (1988). The membrane domain of 3-hydroxy-3-methylglutaryl-coenzyme A reductase confers endoplasmic reticulum localization and sterol-regulated degradation onto beta-galactosidase. *J Biol Chem* 263, 6836-6841.

Song, B.-L., Javitt, N. B., and DeBose-Boyd, R. A. (2005a). Insig-mediated degradation of HMG CoA reductase stimulated by lanosterol, an intermediate in the synthesis of cholesterol. *Cell Metabolism* 1, 179-189.

Song, B.-L., Sever, N., and DeBose-Boyd, R. A. (2005b). Gp78, a Membrane-Anchored Ubiquitin Ligase, Associates with Insig-1 and Couples Sterol-Regulated Ubiquitination to Degradation of HMG CoA Reductase. *Molecular Cell* 19, 829-840.

Sun, L.-P., Li, L., Goldstein, J. L., and Brown, M. S. (2005). Insig Required for Sterol-mediated Inhibition of Scap/SREBP Binding to COPII Proteins in Vitro. *J Biol Chem* 280, 26483-26490.

Thorpe, J. L., Doitsidou, M., Ho, S.-Y., Raz, E., and Farber, S. A. (2004). Germ Cell Migration in Zebrafish Is Dependent on HMGC<sub>o</sub>A Reductase Activity and Prenylation. *Developmental Cell* 6, 295-302.

Wang, X., Briggs, M. R., Hua, X., Yokoyama, C., Goldstein, J. L., and Brown, M. S. (1993). Nuclear protein that binds sterol regulatory element of low density lipoprotein receptor promoter. II. Purification and characterization. *J Biol Chem* 268, 14497-14504.

Wang, X., Sato, R., Brown, M. S., Hua, X., and Goldstein, J. L. (1994). SREBP-1, a membrane-bound transcription factor released by sterol-regulated proteolysis. *Cell* 77, 53-62.

Yabe, D., Brown, M. S., and Goldstein, J. L. (2002a). Insig-2, a second endoplasmic reticulum protein that binds SCAP and blocks export of sterol regulatory element-binding proteins. *PNAS* 99, 12753-12758.

Yabe, D., Xia, Z.-P., Adams, C. M., and Rawson, R. B. (2002b). Three mutations in sterol-sensing domain of SCAP block interaction with insig and render SREBP cleavage insensitive to sterols. *PNAS* 99, 16672-16677.

Yamamoto, T., Davis, C. G., Brown, M. S., Schneider, W. J., Casey, M. L., Goldstein, J. L., and Russell, D. W. (1984). The human LDL receptor: A cysteine-rich protein with multiple Alu sequences in its mRNA. *Cell* 39, 27-38.

Yang, J., Brown, M. S., Ho, Y. K., and Goldstein, J. L. (1995). Three Different Rearrangements in a Single Intron Truncate Sterol Regulatory Element Binding Protein-2 and Produce Sterol-resistant Phenotype in Three Cell Lines. *J Biol Chem* 270, 12152-12161.

Yang, J., Sato, R., Goldstein, J., and Brown, M. (1994). Sterol-resistant transcription in CHO cells caused by gene rearrangement that truncates SREBP-2. *Genes Dev* 8, 1910-1919.

Yang, T., Espenshade, P. J., Wright, M. E., Yabe, D., Gong, Y., Aebersold, R., Goldstein, J. L., and Brown, M. S. (2002). Crucial Step in Cholesterol Homeostasis: Sterols Promote Binding of SCAP to INSIG-1, a Membrane Protein that Facilitates Retention of SREBPs in ER. *Cell* 110, 489-500.

Zambrowicz, B. P., Imamoto, A., Fiering, S., Herzenberg, L. A., Kerr, W. G., and Soriano, P. (1997). Disruption of overlapping transcripts in the ROSA beta geo 26 gene trap strain leads

to widespread expression of beta -galactosidase in mouse embryos and hematopoietic cells. PNAS 94, 3789-3794.

Zhong, X., Shen, Y., Ballar, P., Apostolou, A., Agami, R., and Fang, S. (2004). AAA ATPase p97/Valosin-containing Protein Interacts with gp78, a Ubiquitin Ligase for Endoplasmic Reticulum-associated Degradation. J Biol Chem 279, 45676-45684.

## **VITAE**

Peter Lee was born in New York, USA, on December 22, 1974, the son of Kyung-Shik Lee and Hyea Ja Park. After completing his work at Sang Moon High School, Seoul, Korea in 1993, he entered Seoul National University at Seoul, Korea where he received the degree of Bachelor of Science (1998) with a major in Animal Science and Technology. In 1998 he began his thesis work with Dr. Youn-Jaie Choi at the same University and received the degree of Master of Science (2000) with a major in Agricultural Biotechnology. The following three years, he served Military Service in Hyupsung HISCO and Choongang Biotechnology a special case company as a Technical Research Personnel. In August, 2003 he entered the graduate program at The University of Texas Southwestern Medical Center at Dallas where he joined the laboratory of Dr. Russell DeBose-Boyd in Molecular Genetics. He and his wife Ji Yeon were married in 2003. Their son Joseph Kyu-Chan Lee was born on December 13, 2006, in Dallas, Texas. He graduated with a Ph.D. degree in April 2007.

Permanent Address: 6-1006 Mujigae APT, Secho-2-dong, Secho-gu, Seoul, Korea, 137-771

This dissertation was typed by Peter Lee